

学位論文

Development of Real-time Monitoring Method for Heterogeneous Reactions Using DART-MS
(不均一系有機反応の解析を目的とした質量分析による迅速反応モニタリング手法の開発)

平成 26 年 12 月博士（理学）申請

指導教官：小林 修

東京大学大学院理学系研究科
化学専攻

増田光一郎

Table of Contents

1. General introduction	5
1-1. Chemical kinetics and heterogeneous reactions.....	5
1-2. Mass Spectrometry	8
1-2-1. A brief history of mass spectrometry	8
1-2-2. Soft ionization techniques.....	8
1-2-3. Ambient ionization	10
1-2-4. Direct analysis in real-time	10
1-3. Isotopic indicators.....	11
2. General aspects of quantitative monitoring using DART-MS	12
2-1. Hypothesis for quantitative reaction monitoring	12
2-2. Monitoring system with auto-sampler and its evaluation	14
3. Monitoring study of chemical reaction under micellar conditions.....	20
3-1. Introduction.....	20
3-2. Direct-type catalytic asymmetric hydroxymethylation reactions in water.....	23
3-2-1. Synthesis of internal standard	23
3-2-2. Monitoring trial and condition optimizations	23
3-2-3. Reaction kinetics of direct-type hydroxymethylation reaction	30
3-2-4. Feedback of kinetic analysis to organic synthesis.....	33
3-3. Mukaiyama-type catalytic asymmetric hydroxymethylation reactions in water	34
3-3-1. Monitoring trial and detection of intermediate	34
3-3-2. Reaction kinetics.....	40
3-4. Mechanistic considerations	43
3-4-1. Mechanistic considerations of direct-type aldol reactions	43
3-4-2. Mechanistic considerations of Mukaiyama aldol reactions	45
3-5. Conclusion	46
4. Monitoring study of liquid-liquid heterogeneous reactions: 1,4-addition/ enantioselective protonation reactions in water.....	47
4-1. Introduction.....	47

4-2.	Initial trials	48
4-3.	Substrate scope for good detection	50
4-4.	Condition optimizations for reproducibility	55
4-5.	Reaction profiles and pH measurement	61
4-6.	Conclusion	63
5.	Monitoring study of liquid-liquid-solid tri-phasic heterogeneous reactions: Indium(0) catalyzed allylation reactions in water	64
5-1.	Introduction.....	64
5-2.	Initial trials.....	67
5-3.	Reagent scope for detection conditions	70
5-4.	Conclusion	74
6.	Organosuperbase-catalyzed 1,4-addition reactions of sulfonylimidates	75
6-1.	Introduction.....	75
6-2.	1,4-Addition reactions of sulfonylimidates with acrylates and analogues.....	77
6-3.	1,4-Addition reactions of sulfonylimidates with crotonates and analogues.....	77
6-4.	Substrate scope	80
6-5.	Further conversions of sulfonylimidate 1,4-adducts	81
6-6.	Determination of stereochemistry.....	82
6-7.	Conclusion	82
7.	Summary and perspectives	83
8.	Experimental.....	86
9.	References.....	120
	Acknowledgement.....	124

Abbreviations

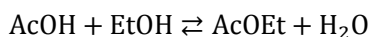
APCI	Atmospheric Pressure Chemical Ionization
ASAP	Atmospheric-pressure Solid Analysis Probe
Boc	<i>tert</i> -Butoxycarbonyl
BTPP	<i>tert</i> -butylimino-tri(pyrrolidino)phosphorane
CI	Chemical Ionization
DART	Direct Analysis in Real Time
DBDI	Dielectric Barrier Discharge Ionization
DBU	1,8-diazabicyclo[5.4.0]undec-7-ene
DCM	Dichloromethane
DEAD	Diethyl azodicarboxylate
DMF	Dimethylformamide
DMSO	Dimethylsulfoxide
EASI	Easy Ambient Sonic-spray Ionization
EESI	Extractive Electrospray Ionization
EI	Electron Ionization
ESI	Electrospray Ionization
GC	Gas Chromatography
HPLC	High Performance Liquid Chromatography
<i>i</i> Bu-PAP	<i>N,N',N''</i> -triisobutyl-2,5,8,9-tetraaza-1-phosphabicyclo[3.3.3]undecane
ICP-AES	Inductively Coupled Plasma Atomic Emission Spectroscopy
LAH	Lithium Aluminum Hydride
LASC	Lewis-Acid Surfactant Combined
LASER	Light Amplification by Stimulated Emission of Radiation
LTP	Low-Temperature Probe
MALDI	Matrix-Assisted LASER desorption ionization
MS 4A	Molecular Sieves 4A
NMR	Nuclear Magnetic Resonance
P ₂ -Et	1-Ethyl-2,2,4,4,4-pentakis(dimethylamino)-2λ5,4λ5- catenadi(phosphazene)
RSD	Relative Standard Deviation
SIC	Selected Ion Current
TfOH	Trifluoromethanesulfonic acid
THF	Tetrahydrofuran
TIC	Total Ion Current
TLC	Thin-Layer Chromatography

1. General introduction

1-1. Chemical kinetics and heterogeneous reactions

In the synthesis of organic molecules, various analytical techniques play important roles. A compound is weighed on a balance, an amount of solvent is measured by a syringe, a reaction temperature is controlled, a crude mixture is analyzed by NMR spectrometry, a molecular weight is determined by mass spectrometry, and a full spectroscopic information of an isolated compound is collected. Moreover, analytical studies including chemical kinetics and detection of intermediates are indispensable for modern organic chemistry.

The history of chemical kinetics goes back to the study of the inversion rate of sucrose by Wilhelmy in 1850.¹ His pioneering work was the first quantitative approach toward reaction rates. In 1862 Berthelot and Saint-Gilles reported the study toward the reaction between ethanol and acetic acid to give ethyl acetate. They were mainly focused on the equilibrium,² whose experiment is nowadays common for students with educational purpose.



Guldberg and Waage's investigation³ in late 1860s is important for the understandings of quantitative relationships between a reaction rate and an equilibrium, which is currently known as *the law of mass action* (Scheme 1-1). Guldberg was a mathematician while Waage was a chemist, and they carried out investigations in a collaborative way. At the same time of Guldberg and Waage, independently, Harcourt and Esson investigated the reactions of hydrogen peroxide with hydrogen iodide and of potassium permanganate with oxalic acid in details.^{4,5} They were also the combination of a chemist and a mathematician.

Scheme 1-1. The law of mass action.

If a chemical reaction ($a\text{A} + b\text{B} + \cdots \rightleftharpoons c\text{C} + d\text{D} + \cdots$) is under equilibrium,

$$\text{a value } K = \frac{[\text{A}]^a \cdot [\text{B}]^b \cdots}{[\text{C}]^c \cdot [\text{D}]^d \cdots} \text{ is a constant.}$$

Later in 1889, Arrhenius proposed that an equilibrium existed between reactive state and unreactive state of a molecule in a reaction system to lead the famous equation ($k = A e^{-\frac{E}{RT}}$), which is known as Arrhenius equation today.⁶ Thanks to the great advance in physical and analytical chemistry, especially in spectrometry, chemical kinetics had a great progress at this age. Contributions are also noted of van't Hoff in the relation between a rate constant and an equilibrium constant,⁷ of Ostwald in the interpretation of catalysis by the velocity of reactions.⁸

In early 20th century, statistical mechanics and quantum physics provided theoretical approaches toward chemical kinetics from two opposite viewpoints. From a macroscopic viewpoint, a chemical reaction is interpreted by statistical mechanics to lead Transition State Theory.^{9,10} Quantum Mechanics, a microscopic approach toward a chemical reaction, explained the diagrams of potential surfaces versus reaction coordinates.¹¹

Laidler pointed out the significance of chemical kinetics with its relevancy in branches of science (Table 1-1).¹² The basis of chemical kinetics, statistical mechanics and quantum mechanics, is very fundamental in wide fields of science.

Table 1-1. Some branches of science to which kinetics is relevant (quoted from *Chemical Kinetics*)¹²

Branch	Applications of kinetics
Biology	Physiological processes (e.g., digestion and metabolism), bacterial growth
Chemical engineering	Reactor design
Electrochemistry	Electrode processes
Geology	Flow processes
Inorganic chemistry	Reaction mechanisms
Mechanical engineering	Physical metallurgy, crystal dislocation mobility
Organic chemistry	Reaction mechanisms
Pharmacology	Drug action
Physics	Viscosity, diffusion, nuclear processes
Psychology	Subjective time, memory

For experimental investigations of chemical kinetics, a number of analytical techniques have been developed. Most rate measurements by determining the mass changes over time are based on the assumption that the reaction system is in thermal equilibrium. Such a measurement is considered to be a “bulk” experiment to determine *macroscopic* kinetics. On the contrary, the study of the behavior of molecules at a local region can be referred as *microscopic* kinetics. Molecular dynamics like first-principle calculations are good examples of such an approach. For heterogeneous reactions, both *macroscopic* and *microscopic* viewpoints are very important toward further understandings of reaction mechanisms (Figure 1-1).

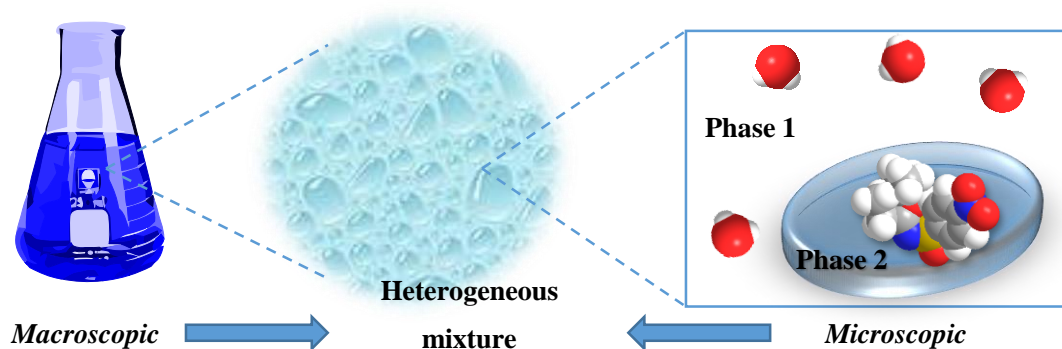


Figure 1-1. Analytical study of heterogeneous reactions

Heterogeneous reactions are classified in two manners; phases the reaction contains, a place where the reaction is proceeding. A number of combinations of phases are possible; the three state of the matter, solid, liquid or gas, are combined each other to form a heterogeneous mixture. Two or more liquids with different properties, like water and oil, form a heterogeneous system. A combination of solids also forms a heterogeneous system in a similar way. On the other hand, the classification by a reaction environment is rather simple. Heterogeneous reactions are allocated into three types:

- **One-phase (heterogeneous) reactions**

All the reagent/reactant exist in one phase, and the other phase works as “supporting” phase (e.g., removal of heat, relaxation of viscosity)

- **Interfacial reactions**

Reagent/reactant exist in different phases, and a reaction proceeds on the surface of phases

- **Extractive reactions**

Reagent/reactant exist in different phases, and one of the reagent/reactant is extracted into the other phase to proceed the reaction

Among many types of heterogeneous reactions, a reaction on solid surface have been extensively studied for many years. After the definition of *catalyst* by Berzelius in 1836,^{13–15} a number of chemical reactions on solid catalyst have been developed. Heterogeneous reactions on solid catalysts are essential especially in industrial fields such as Haber-Bosch process to produce ammonia, ammonia oxidation to nitric acid, reforming of naphtha, sulfuric acid process and so on. Nowadays Ca. 80% of industrial catalytic processes are under heterogeneous conditions. Reaction mechanism of surficial catalysis in gas phase is explained by an adsorption of molecules and bond dissociation-reorganization. An adsorption of a gas molecule follows Langmuir isotherm, and simple gas-phase reactions with solid catalysts are described by Lindemann-Hinshelwood mechanism^{16–18} or Eley-Redeal mechanism.¹⁹

Despite those extensive studies of heterogeneous reactions of gas phase, however, heterogeneous systems in other particular systems have not been investigated so much from a *macroscopic* viewpoint due to technical difficulties. For example, a liquid-liquid heterogeneous mixture has some difficulty in separation of its phases, and optical spectroscopic analysis does not work well because of strong light scattering by heterogeneity. Instead, an aliquot sample analysis is often employed to elucidate the degree of reaction progress;^{20,21} however, due to the large deviations of material ratio in a heterogeneous sample, a large number (or amount) of a sample is required to treat the data statistically.

In order to address the heterogeneous issue, quite recently, some interesting approaches have been demonstrated from a *microscopic* viewpoint. Enami *et al.* investigated Fenton chemistry at aqueous interfaces using mass spectrometry to have found high-valent ferryl ($\text{Fe}^{\text{IV}}=\text{O}$) species generated on a surface of microdroplet.²² Fita applied the surface second harmonic generation to a surface of phase transfer catalysis system to monitor the concentration of thymolphthalein on a surface of organic/aqueous boundary.²³

As heterogeneous reactions are a subject of great interest to chemists, there are big motivations to develop new methodology to address the reaction mechanism under heterogeneous conditions especially from *macroscopic* viewpoint. Many scientists, including the author of this thesis, are interested in this problem.

1-2. Mass Spectrometry

1-2-1. A brief history of mass spectrometry

Mass spectrometry is a technique to determine mass to charge ratio of a certain cation or anion. An original idea came from Wien's experiment of kanalstrahlen (canal ray, or an anode ray) changing its direction by strong electric or magnetic fields.²⁴ Thomson observed bent kanalstrahlen of neon showed one strong spot and the other weak spot on photographic plate.²⁵ It was the first isolation of isotopes, ^{20}Ne and ^{22}Ne , following their mass-to-charge ratio. Based on these discoveries, Aston and Dempster established modern techniques of mass spectrometry.²⁶⁻²⁹

The mechanisms of mass spectrometry are discussed separately into two steps; a detection and an ionization. A number of techniques have been developed until today for both steps. A molecule is turned into charged particle under ionization conditions, and an ion is separated in order of their mass to charge ratio by electric or magnetic field under vacuum conditions. For example of separation/detection techniques, sector instruments,³⁰ time-of-flight,³¹ quadrupole,³² Penning ion trap,³³ orbitrap³⁴ and Fourier transform ion cyclotron resonance³⁵ are famous nowadays. The detail of each detection techniques are not described in this article; see references for details. The other step, ionization, is rather essential to determine the property of mass spectrometry. For example, original experiment in Crookes tube is regarded as glow discharge ionization.³⁶ Glow discharge is generated at low pressure gas to give very high energy to gas molecules.

An ionization of an organic molecule, whose atoms are connected together by covalent bonds, have been a great task after the invention of mass spectrometry. Some of the early ionization techniques, such as EI or CI, are regarded as hard ionization. Due to the high energy given to the molecule, a covalent bond of an organic molecule is easily scissored to give fragmented particles. This fragmentation is quite unique to a functional group on a molecule, and fragmentation pattern has been used for the structural elucidation/characterization of a molecule.^{37,38} However, such a fragmented pattern is rather problematic in the analysis of mixed samples. Another problem of hard ionization is applicability to large molecules.

1-2-2. Soft ionization techniques

There are two important methods of soft ionization on the history of mass spectrometry. ESI, an electron spray ionization (Figure 1-2) have been developed by Fenn and Yamashita in 1984,³⁹ ionizes the molecule by a "Coulomb explosion" of a charged droplet containing analyte molecules. ESI is recognized as a very efficient and soft ionization suitable for a molecule with relatively high polarity. An application of ESI demonstrated with biomolecules met a great surprise and praise.⁴⁰

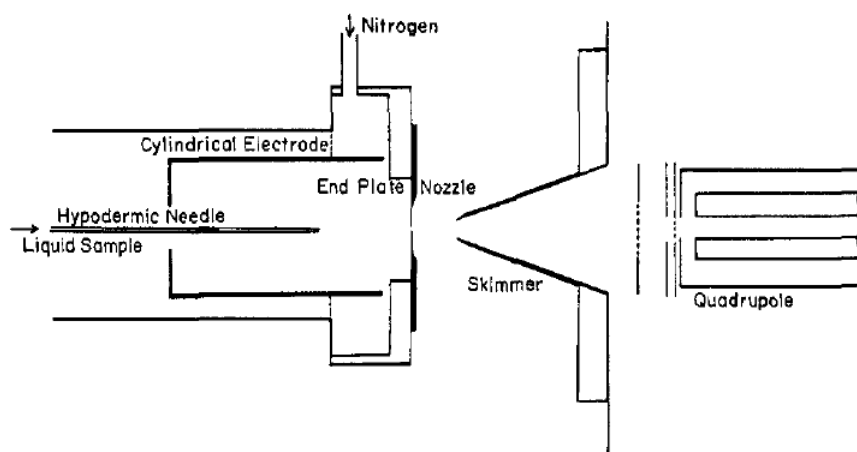


Figure 1-2. Original image of electrospray ionization (reprinted from Fenn and Yamashita³⁹)

MALDI, a matrix-assisted LASER desorption ionization (Figure 1-3), have been invented by Karas, Hillenkamp and coworkers in 1983.⁴¹ A LASER-absorbing molecule is desorbed and ionized firstly to assist an ionization of other non-LASER-absorbing molecules. The breakthrough for large molecules came in 1988 by Tanaka of Shimadzu Co.⁴² They prepared a sample by the “ultra fine metal and liquid matrix method” to successfully show the detection of molecules up to 100 kDa.

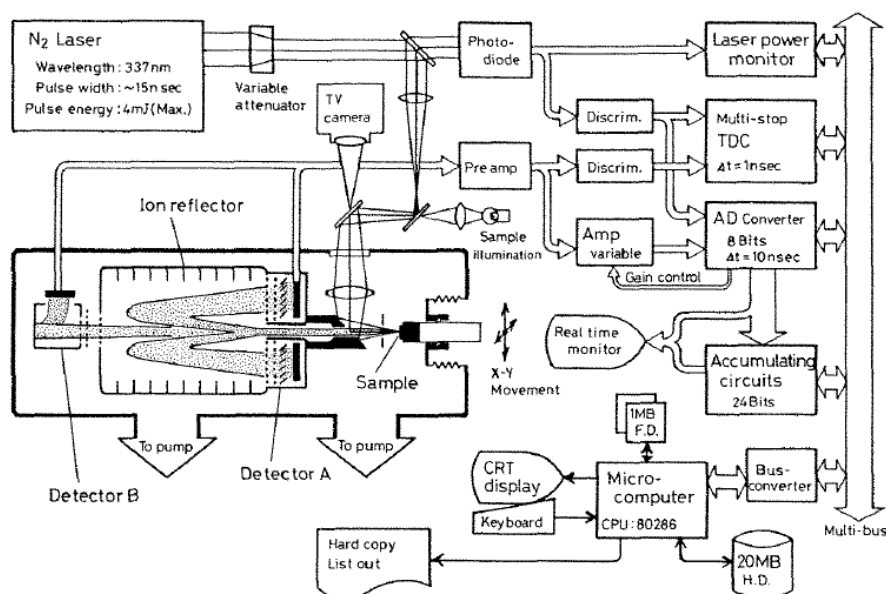


Figure 1-3. Original image of matrix-assisted LASER desorption ionization (reprinted from Tanaka *et al.*⁴²)

1-2-3. Ambient ionization

For the discussion of the development of ionization technologies, an “ambient ionization” is also an important concept.⁴³ An analysis of a sensitive sample sometimes prefers less sample preparation. A heterogeneous mixed sample have some difficulties to apply to the conventional ionization techniques. For example, an analysis by ESI requires liquid sample diluted in polar and volatile solvent such as methanol or acetonitrile. An ionization under MALDI requires sample preparation mixing with a matrix material. In recent years, a number of application method is reported based on ESI technique or APCI (atmospheric pressure chemical ionization) technique.⁴⁴

ESI based alternatives employ various desorption techniques and an ESI ionization in a combination. An extractive electrospray ionization (EESI) reported by Cooks employs dual solution nebulizer, one of which sprays a charged droplet for ionization, while the other nebulizes non-charged sample solution.⁴⁵ Separation of ionization spray and sample nebulizer allowed to apply highly concentrated samples or heterogeneous mixtures like raw urine or milk. Eberlin developed easy ambient sonic-spray ionization (EASI) employing no voltage, no discharge, no light irradiation or no high temperature.⁴⁶ Solvent spray at ultrasonic speed attacks on a sample surface to ionize the molecules. Electrospray-assisted LASER desorption ionization developed by Shiea is suitable technique to analyze a sample on solid surface.⁴⁷ A sample is desorbed by LASER absorption, and small particle of sample is extracted into ESI droplet and then ionized.

Some improved methods of APCI are also noted. ASAP, an atmospheric-pressure solid analysis probe developed by McEwen of DuPont Co. in 2005, employs hot nitrogen gas stream with discharge to ionize a sample on a melting point capillary as a sampling rod.⁴⁸ Solid or some viscous liquid sample are applicable without any special sample treatment. DBDI, a dielectric barrier discharge ionization was first demonstrated by Zhang *et al.* in 2007.⁴⁹ Dielectric current between a needle electrode flowing helium or other gases and a glass sample plate as the discharge barrier on plate electrode generates stable plasma to ionize a sample on a glass plate. LTP, a low-temperature plasma probe by Cooks, Zheng *et al.* is more sophisticated ionization method generating plasma separately from a sample ionization area.⁵⁰ LTP do not expose any discharge or heat on sample, therefore the fragmentation tendency during ionization is sufficiently low.

1-2-4. Direct analysis in real-time

Direct analysis in real-time, called DART, is one of the most successful ambient and soft ion source developed by Cody *et al.* of JEOL USA Co.⁵¹ DART is regarded as an APCI technique. Helium (or other gas) is activated by glow discharge to generate metastable species, and this metastable gas molecule activate a water molecule in air to form water-cluster cation as a soft protonation source. A sample is analyzed under ambient conditions; open to air, no voltage, and no discharge. DART ion source is commercially available from ionsense® Inc. and is possible to attach various MS analyzers.

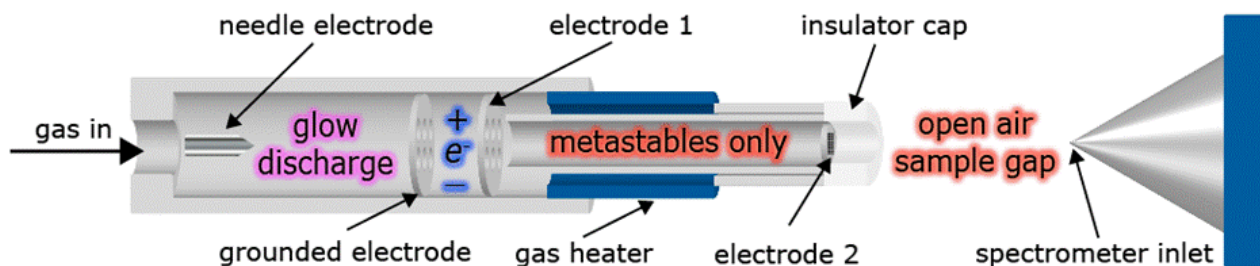
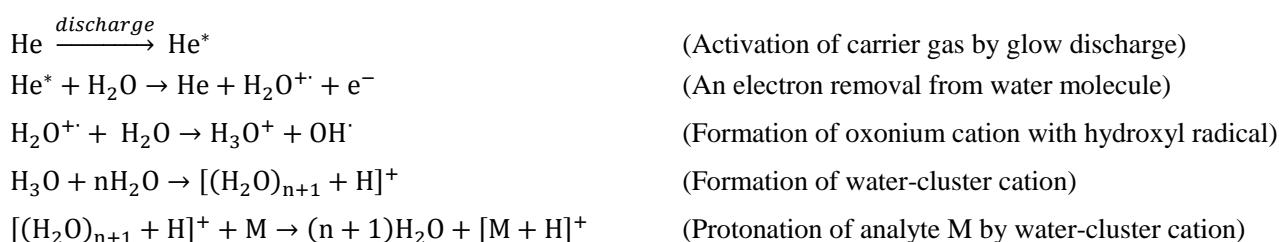


Figure 1-4. A schematic image of DART ionization system (reprinted from <http://www.jeolusa.com>)

An ionization process is considered as follows;



1-3. Isotopic indicators

Isotopes, variants of an element which have different number of neutrons, have played important roles in analytical chemistry. Radioactive isotopes such as ^{14}C , ^3H , ^{32}P or ^{35}S are easily detectable due to their high energy radiation on their decay. George de Hevesy and Melvin Calvin have been awarded Nobel Prize for their contributions to disclose mechanisms of chemical/biochemical reactions, “For his work on the use of isotopes as tracers in the study of chemical processes” (Hevesy, 1943) and “For his research on the carbon dioxide assimilation in plants” (Calvin, 1961). Such a use of isotopes as tracers are not limited to radioactive ones. Stable isotopes are detectable by mass spectrometry, an analytical technique based on physical properties, while their chemical properties are almost identical. Isotope-labelled internal standard is widely used to conduct quantitative analysis of wide variety of samples.⁵²⁻⁵⁶ In order to prepare an isotope-labelled internal standard for such an analysis of organic/bioorganic molecules, a reliable synthetic methodology is necessary. Deuterium⁵⁷ (^2H) or ^{13}C are often used for this purpose due to their availability. Abundance ratio of deuterium is only 0.015%, however, due to the large mass difference to its isotope hydrogen, deuterium is easily separated by centrifugation. ^{13}C is relatively abundant on the earth; its abundance is about 1.1%. Some books^{58,59} or journals⁶⁰ are available for this purpose.

2. General aspects of quantitative monitoring using DART-MS

2-1. Hypothesis for quantitative reaction monitoring

The use of an isotopic indicator as an internal standard will lead good quantitativity on mass spectrometry (Figure 2-1). The amount of “artificial” labeled internal standard is static during the reaction, while that of “natural” non-labeled reaction product increases. In order to conduct the analysis under heterogeneous conditions, there are several requirements exist:

- (1) No reverse reaction / no decomposition of product

If a chemical reaction has a reverse pathway or a decomposition pathway of a product, an internal standard could decompose as it is the same chemical as the reaction product. In the monitoring study of a target reaction, the pathway must not exist, or at least must be ignorably slow.

- (2) Fast matter exchange between phases

A reaction proceeds in limited area of a reaction mixture such as interface. A matter exchange between phases is faster than a reaction to keep the ratio of isotopes uniform.

- (3) No reaction on ionization process

Any further reaction after sampling must be avoided to maintain isotope ratio of a product. An ionization process on mass spectrometry applies large energy to ionize a molecule, and this large energy sometimes induces unexpected chemical reactions. An ionization method must be chosen carefully to keep an isotopic ratio during ionization on mass spectrometry.

- (4) Fast analysis without sample preparation

In order to monitor a chemical reaction in real-time, a number of data points are required within small time lag. Each analysis must be conducted as quickly as possible. Time-taking sample pretreatment must be avoided; in other word, direct analysis is highly desirable of a crude sample from a heterogeneous reaction mixture without any sample pretreatment. An ionization method must be robust enough to analyze a heterogeneous mixture of solid, liquid and gas samples.

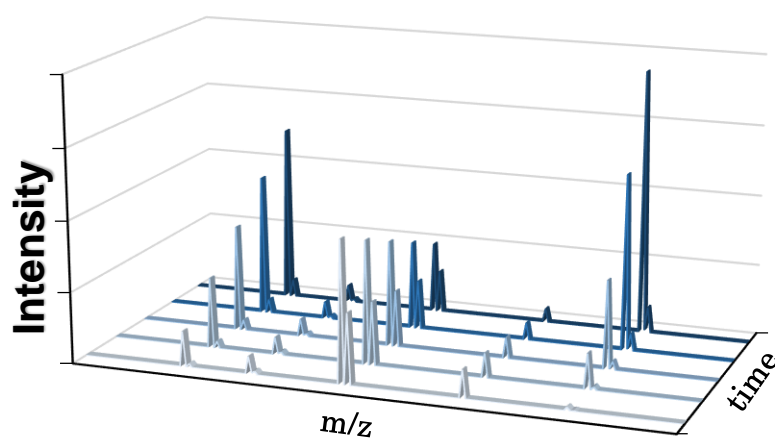


Figure 2-1. Hypothesis for quantitative monitoring using isotopic indicator

Based on those requirements, DART-MS was chosen as the most appropriate ionization method for its soft and robust ionization. In order to monitor an organic chemical reactions, an auto-sampler machine for DART-MS has been developed in our laboratory.

2-2. Monitoring system with auto-sampler and its evaluation

On the sampling study using ambient ionization techniques of mass spectrometry, an accurate control over sample treatment is crucial for a stable detection of a peak with adequate intensity and reproducibility. An ionization area of DART-MS is open to the air, and there is very high flexibility in holding a sample onto the area. The use of mechanically controlled sampling-ionization sequences can address the issue to detect a sample with good reproducibility. A semi-quantitative sampling/ionization have been demonstrated by using a robot arm auto-sampler with a glass rod for samples such as drugs in biological matrixes,⁶¹ allium chemistry,⁶² and additives in food packaging.⁶³ An inexpensive auto-ionization system has been demonstrated with cotton buds attached on a N-scale model railroad.⁶⁴⁻⁶⁸ Surface contaminants,⁶⁵ airborne-dispersed chemicals,⁶⁶ or batch slurry reaction mixture⁶⁸ were absorbed into a cotton bud head on a model train and was horizontally passed through an ionization area of DART-MS at a steady speed.

In our laboratory a new auto-sampler system was designed for the monitoring study of fine organic synthesis. A reaction vessel with precise condition control, and a robot arm auto-sampler were combined together. A simplified image of an auto-sampler system is shown in Figure 2-2. Pictures are shown in Figure 2-3 and Figure 2-4. A reaction is conducted in a glass vessel up to 15 mL scale under a positive flow of nitrogen. A reaction temperature and a stirring speed are controlled accurately ($-20 \sim +80$ °C, 0 ~ 1500 rpm). An auto-sampler takes a small aliquot sample from a vessel by the robot arm with a sample rod to send to an ionization area of DART-MS.

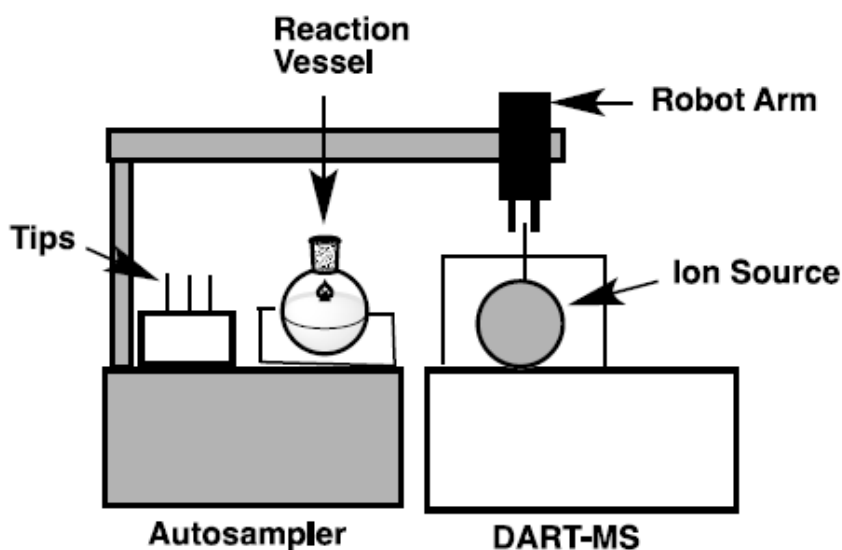


Figure 2-2. A simplified image of an auto-sampler for DART-MS reaction monitoring system

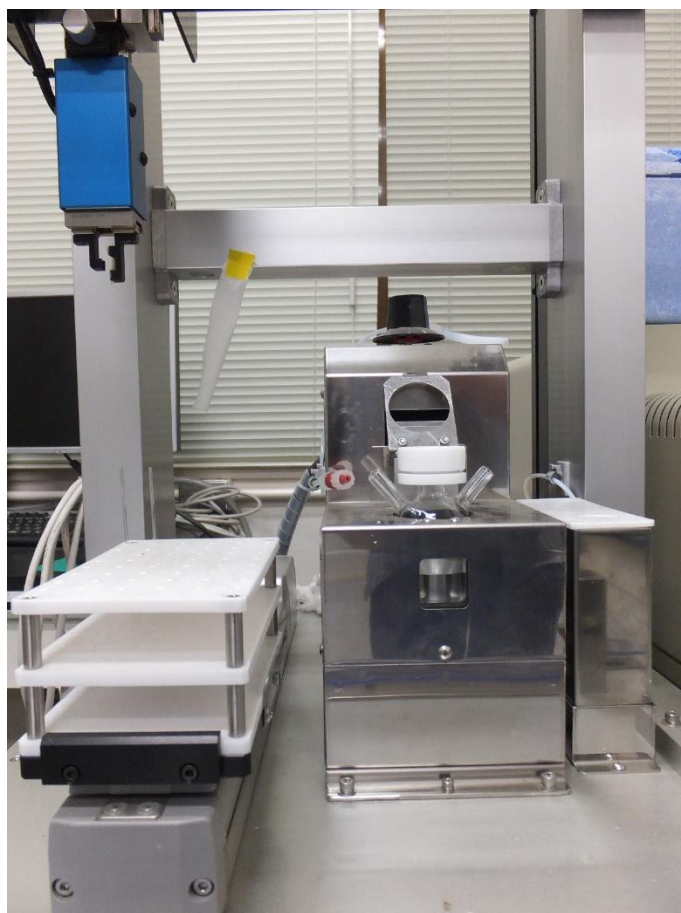


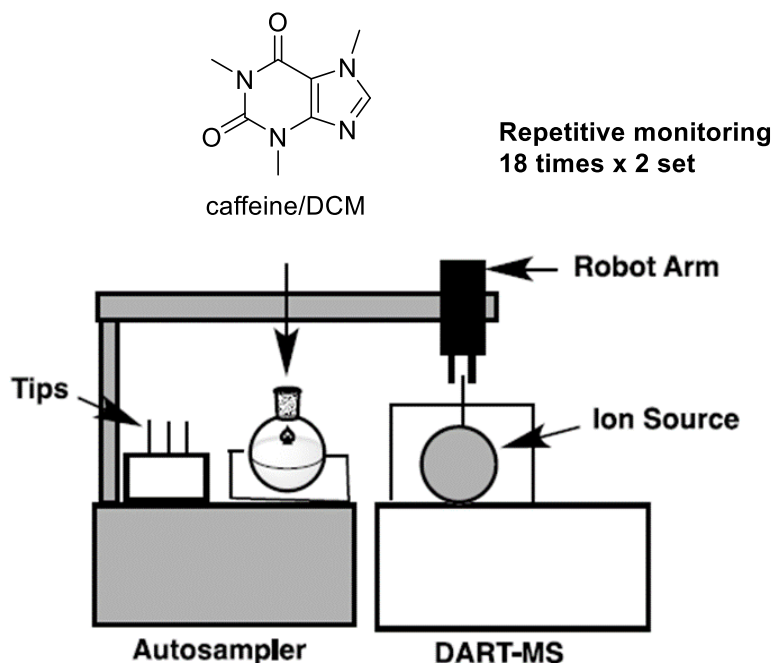
Figure 2-3. Auto-sampler system



Figure 2-4. Ionization by DART-MS with auto-sampler

In order to evaluate an auto-sampler system for its sampling ability, a standard solution of caffeine (400 ppm) in dichloromethane was analyzed repeatedly (Experiment 2-1, see experimental section for details).

Experiment 2-1. Repetitive ionization experiment of caffeine using auto-sampler system



The caffeine solution was analyzed 18 times in one measurement with approximately 1 minute intervals, and two sets of the measurement was conducted (Figure 2-5 and Figure 2-6). Each peak intensities were quite excellent showing up to 7500 S/N ratio. An integration of a peak area was obtained after the baseline correction following Sonneveld-Visser method.⁶⁹ As a result, distributions of a peak area in repetitive measurements were relatively large. Relative standard deviations of two sets were 19.2% and 17.6% each.

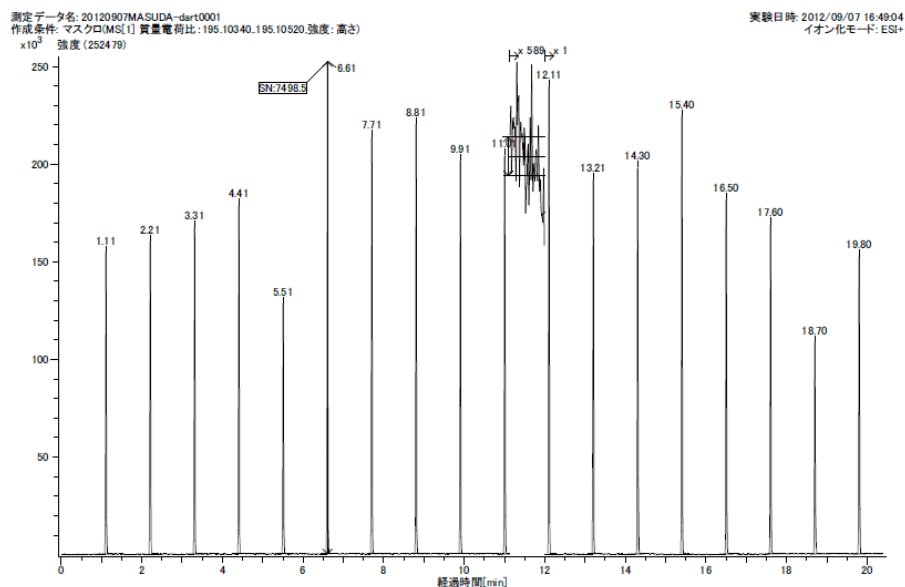


Figure 2-5. Selected ion chromatogram ($m/z = 195.00-195.50$) of experiment 3-1 (1)

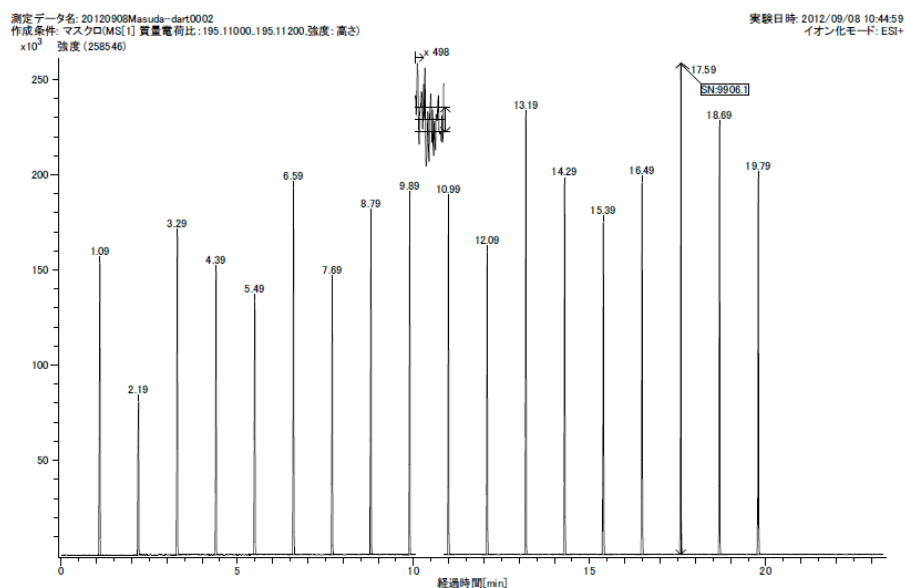
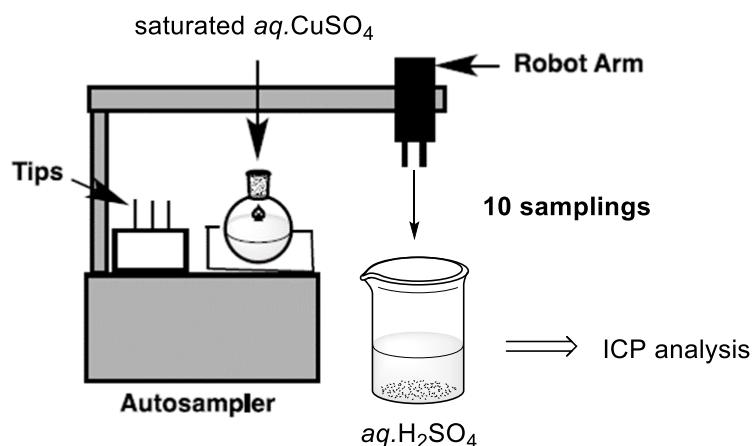


Figure 2-6. Selected ion chromatogram ($m/z = 195.00-195.50$) of experiment 3-1 (2)

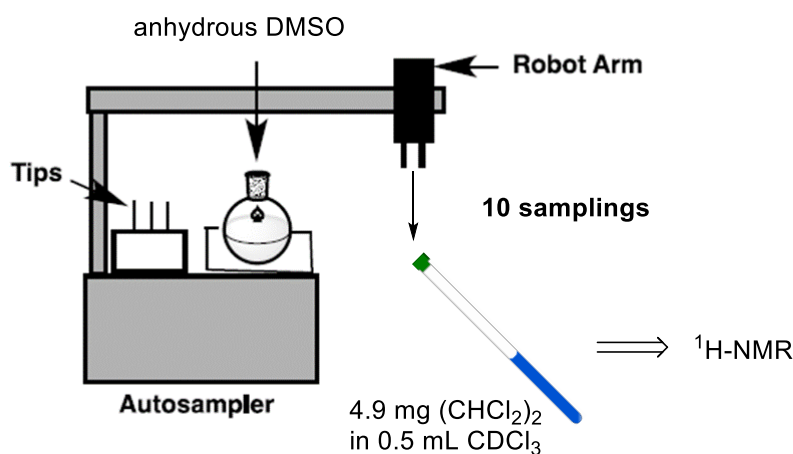
An ionization on DART-MS with the auto-sampler system included relatively large random error. The error was attributed to two steps; a sampling and an ionization. Firstly a sampling step of an auto-sampler was evaluated by the ICP-AES and NMR spectrometry analyses (Experiment 2-2 and Experiment 2-3).

Experiment 2-2. Calibration of auto-sampler by ICP-AES



A saturated CuSO₄ aqueous solution was placed in a reaction vessel and an aliquot sample was taken by an auto-sampler with a closed-end melting point tube ($\phi = 1.8$ mm) as a sampling rod. The sample taken was dipped into 100 mL of an aqueous sulfuric acid (2%), and the solution was analyzed by ICP-AES. The analysis was repeated for 10 times. As a result, an average amount of Cu²⁺ in the solution was determined as 0.182 ppm with 53.8% relative standard deviation for 10 repetitive measurements. This large distribution is supposedly due to a high surface tension of an aqueous sample ($\gamma = 72.8$ mN/m, pure water).⁷⁰

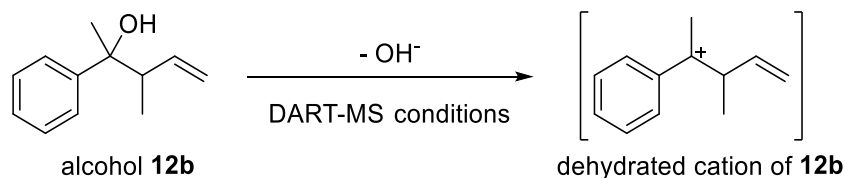
Experiment 2-3. Calibration of auto-sampler by NMR



Anhydrous DMSO was chosen as an analyte of a calibration experiment using NMR spectrometry for its low volatility. Surface tension of DMSO ($\gamma = 42.9$ mN/m) is more similar to that of dichloromethane ($\gamma = 27.9$ mN/m) than that of water.⁷⁰ DMSO was placed in a reaction vessel and an aliquot sample was taken by an auto-sampler with a closed-end melting point tube ($\phi = 1.8$ mm) as a sampling rod. The sample taken was dipped into 0.5 mL CDCl₃ containing 4.9 mg tetrachloroethane as an internal standard, and the amount of DMSO was determined by ¹H-NMR analysis. 10 times of repetitive measurements revealed an average of the DMSO taken by melting point tube was 0.35 mg with 22.2% relative standard deviation.

These two independent sampling experiments using ICP-AES and NMR spectrometry indicated that the amount of sample taken by an auto-sampler has already distributed largely. An ionization experiment was conducted again with homoallyl alcohol **12b** using auto-sampler DART-MS system for large number ($N = 47$) of repetitive measurement to show a structure of a distribution in a histogram (Experiment 2-4).

Experiment 2-4. Ionization experiment with readily sample-soaking materials



A solution of tertiary alcohol **12b** in DCM (2.8 mg in 4 mL) was used as an ionization sample for the evaluation of a structure of a distribution. The alcohol **12b** easily loses its hydroxyl group to give a dehydrated cation during ionization under DART-MS conditions. For the measurement this dehydrated peak on $m/z = 159$ was chosen. A sample was taken by an auto-sampler with closed-end melting point tube ($\phi = 1.8$ mm) as a sampling rod, and ionized by DART-MS (He as carrier gas, 200 °C). A histogram of the result is shown in Figure 2-7.

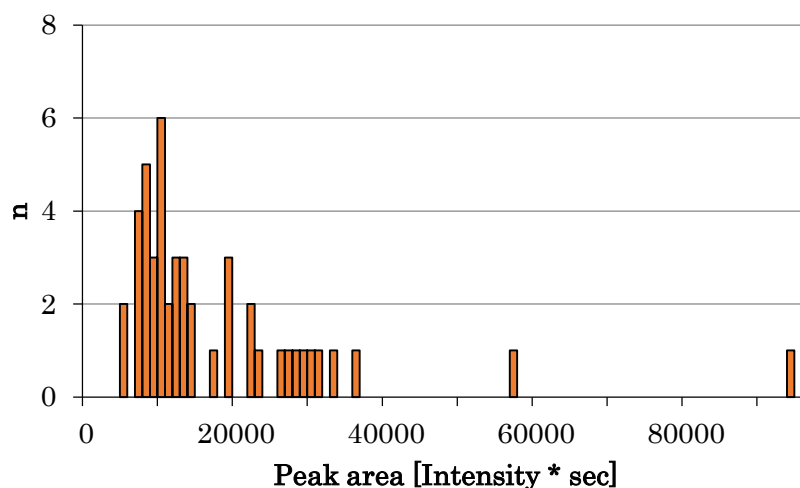


Figure 2-7. A histogram for ionizations of alcohol 12b ($N = 47$)

Obviously a Poisson distribution was observed with large a distribution width. Judging from these experiments, direct quantification requires a number of a repetitive measurement with such a largely distributing auto-sampler system. To conduct a quantitative analysis of a certain chemical species, the use of an internal standard is necessary for an auto-sampler DART-MS system.

3. Monitoring study of chemical reaction under micellar conditions

3-1. Introduction

Organic materials are often immiscible with water, and the organic chemical reactions in water are heterogeneous. In the presence of a surfactant, organic materials form colloidal dispersion called micelle. The boundary of organic materials and water are greatly extended, and surficial reactions are enhanced. Kobayashi and coworkers have discovered that the combination of a water-stable Lewis acid and a surfactant moiety works as an efficient catalyst in water.^{71–73} Transition metal catalyzed novel bond-forming reactions in water with functional surfactants are also noted.^{74,75}

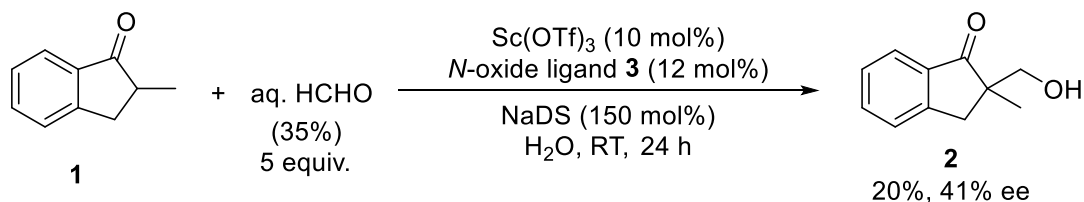
The reactions in micellar conditions are regarded as heterogeneous; conventional analytical method such as transmission spectrometry (NMR, IR) are highly problematic, and aliquot sampling study requires relatively large volume of a sample or repetitive sampling. Therefore, a new and practical reaction monitoring method is highly desired. As is already described in the previous section, the use of an isotopic indicator allows us to quantify a chemical species quite accurately even under heterogeneous conditions. The principle of an isotopic indicator is general to any kind of mass spectrometry.

The aldol reaction, that is a nucleophilic addition of an enol/enolate to a ketone or an aldehyde, is a highly useful carbon-carbon bond forming reaction.^{76–80} A number of nucleophiles can be employed in this reaction including synthetic equivalents of carbonyl compounds such as silicon enolates^{81–84} or boron enolates.^{85–87} These pre-formed enolate species made it possible to control the reaction in high chemo-, diastereo- and enantioselective way. The reaction of silicon enolates with aldehydes are nowadays called Mukaiyama aldol reaction named from its pioneer. However, those enolate species or Lewis acids employed as activators are often sensitive toward water and it was difficult to conduct the reaction under aqueous conditions. Even with relatively stable silicon enolates, although the reactions were reported to be enhanced under aqueous conditions,^{88,89} enantioselective reactions were considered to be problematic. The use of water-stable Lewis acid was a major breakthrough of this problem. Kobayashi et al. discovered that lanthanide trifluoromethanesulfonates were water-compatible Lewis acids and accelerated the Mukaiyama aldol reactions in aqueous media (water/organic solvents).⁹⁰ One great challenge to Mukaiyama aldol reactions was to conduct the reaction in 100% water system. The possible approach was to enhance hydrophobicity of reaction environments to suppress hydrolysis of enolate species. Catalytic amount of anionic or non-ionic surfactants led significant rate enhancement of the reactions.⁹¹ And more, Lewis-Acid-Surfactant Combined catalysts (LASC), in which counter-anions of Lewis acids were replaced with surfactants, were found to be more efficient catalysts forming hydrophobic environments tightly surrounded by Lewis acid moieties.⁹² LASC catalysts effectively worked in pure water to catalyze Mannich-type reactions,⁹³ Mukaiyama aldol reactions,⁷¹ Diels-Alder reactions⁷¹ and Michael addition reactions.⁹⁴ enantioselective Mukaiyama aldol reactions in water were achieved by combination of chiral ligands and Lewis acids of LASC catalysts in 2008.⁹⁵ Later in 2010, it was found that combination of LASC and chiral ligands could catalyze enantioselective direct-type aldol reactions in water.⁹⁶ Direct-type aldol reactions and Mukaiyama aldol reactions started from different substrates to yield the same products. Representative two examples employed similar scandium/*N*-oxide ligand **3** complexes as catalysts, but their reaction

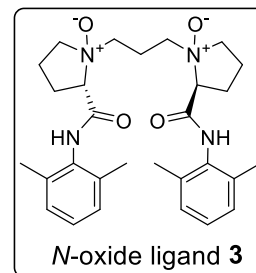
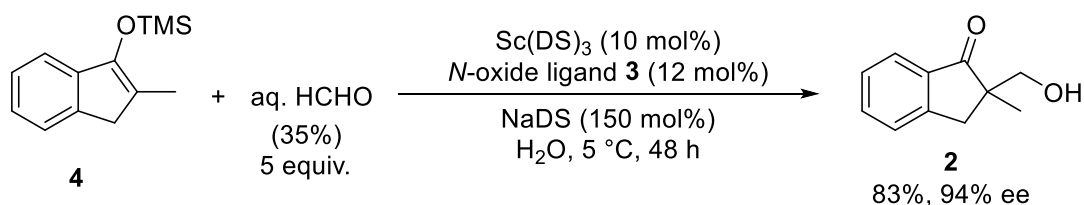
outcome was different (Scheme 3-1, DS = DodecylSulfate). The report showed that it was necessary to employ a catalytic amount of base to enhance the yield and the selectivity of the direct-type reactions with *N*-oxide ligand.⁹⁶

Scheme 3-1. Comparison of direct-type/Mukaiyama aldol reactions

Direct-type aldol reaction



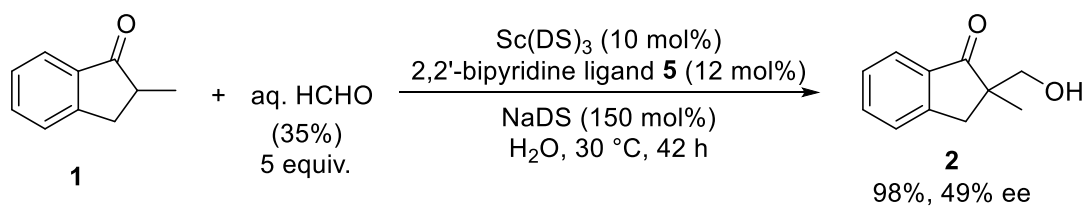
Mukaiyama aldol reaction



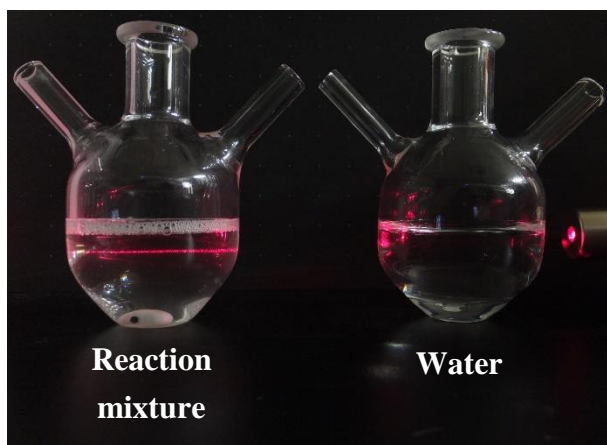
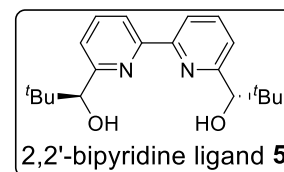
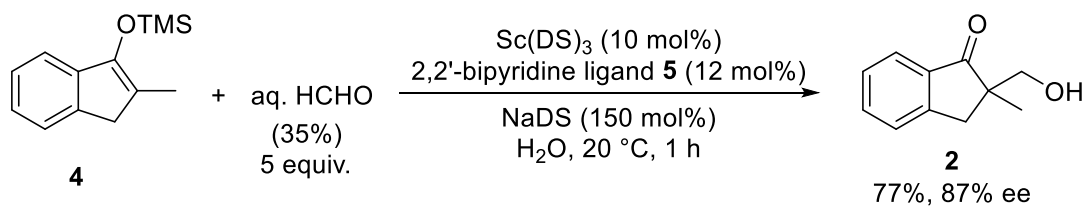
On the other hand, 2,2'-bipyridine ligand^{97,98} could promote the direct-type aldol reactions without additional use of base. Mukaiyama aldol reactions were also catalyzed by scandium/2,2'-bipyridine ligand **5** complex to furnish the product in good yield with slightly diminished enantioselectivity (Scheme 3-2). These slightly modified conditions were selected for the monitoring study of target reactions due to their high comparability. Under these conditions 1.5 equivalents of surfactant assisted the formation of small particles of organic materials (See picture in Scheme 3-2; light scattering was observed). Due to the formation of good dispersion, high reproducibility of reaction rate was expected.

Scheme 3-2. Modified reaction conditions for direct-type/Mukaiyama aldol reactions

Direct-type aldol reaction



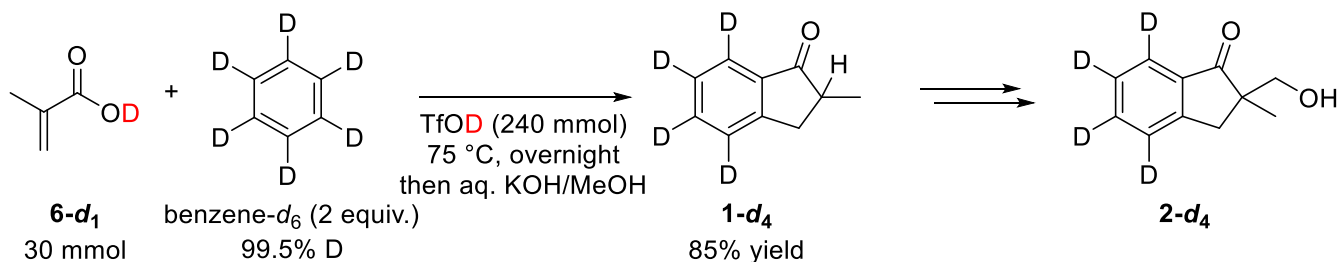
Mukaiyama aldol reaction



3-2. Direct-type catalytic asymmetric hydroxymethylation reactions in water

3-2-1. Synthesis of internal standard

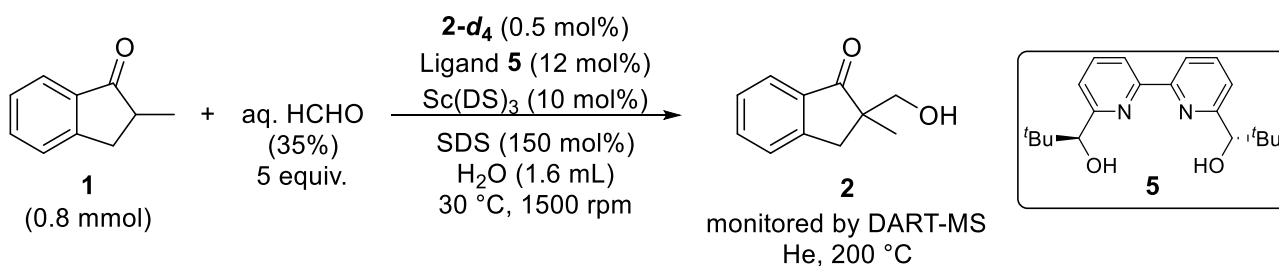
Scheme 3-3. Synthesis of deuterium-labeled product **2-*d*₄**



An isotope-labeled internal standard material **2-*d*₄** was synthesized following reported a synthetic method of non-labeled 2-methylindanone **1**.⁹⁹ Unfortunately at the initial trial, the D-H exchanged compound **1** was obtained with TfOH as a solvent because the reaction condition was acidic enough to protonate the aromatic rings. In order to prepare a fully deuterated compound, the reaction was conducted with the deuterated acid **6-*d*₁** and TfOD. The desired **1-*d*₄** was obtained in 85% yield and was converted into internal standard **2-*d*₄** under standard conditions of direct-type aldol reactions (Scheme 3-2).

3-2-2. Monitoring trial and condition optimizations

Scheme 3-4. Initial monitoring trial

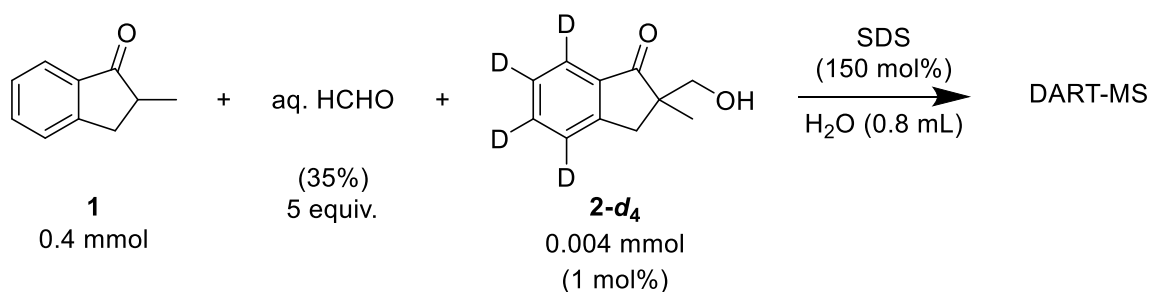


The reaction monitoring trial of a direct-type aldol reaction was conducted in the presence of isotope labeled compound **2-*d*₄** (Scheme 3-4). The reaction was conducted under the conditions indicated in Scheme 3-4 using a 10 mL vessel of auto-sampler machine. Small amount of samples were taken from a reaction mixture by the auto-sampler with closed end of a φ 1.8 mm melting point tube to send to ionization area of DART-MS. As an initial condition of DART, helium gas at 200 °C was selected as the carrier gas. As a result, however, no peak was observed with enough intensity at *m/z* = 177 or 181 (protonated cations of **2** and **2-*d*₄**, respectively) while strong peaks were observed at *m/z* = 147 (substrate **1**) and 329 (ligand **5**). By increasing gas temperature to 400 °C, some peaks were

observed at $m/z = 177$, though its S/N ratio was not enough to check the quantitativity from the ratio of isotopes. During the monitoring, the peak at $m/z = 147$ (substrate **1-d₀**) was quite strong, but no signal was detected at 151 (decomposed internal standard **1-d₄**). This indicates that the internal standard **2-d₄** was not decomposed into **1-d₄** under reaction or ionization conditions. The retro aldol reaction commonly occurs but these control reactions show that it proceeds at such a slow rate, which is probably due to the reactivity of the formaldehyde. Its overall effect to the decomposition of internal standard **2-d₄** is negligible.

In order to detect compound **2** from the reaction mixture using DART-MS, optimization of detection conditions was conducted by analysis of a mixture without Sc(DS)₃. In the presence of SDS, a 100/1 ratio of substrate **1** and internal standard **2-d₄** were well dispersed and 5 equivalent of formaldehyde was added. The mixture was analyzed under various DART conditions as shown in Scheme 3-5.

Scheme 3-5. Optimization of monitoring conditions

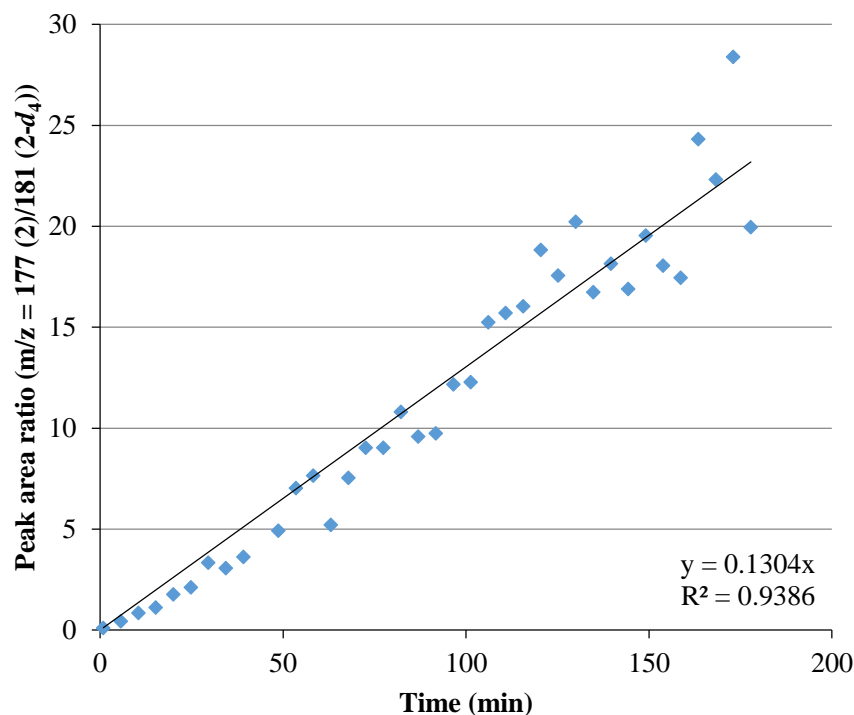


Entry	Gas	Gas temp. (°C)	2 (intensity)	2-d₄ (intensity)	S/N of 2-d₄ peak
1	He	200	3222	7592	19
2	N ₂	200	ND	1210	88
3	N ₂	400	707	3889	140
4	N ₂	100	ND	887	45.5

In the absence of the catalyst, desired peaks of **2** were observed at $m/z = 177$, 181 by using helium as a carrier gas (entry 1). Absolute intensities of the peaks were strong, however, S/N ratio was very poor due to the strong background noise. It is generally considered that helium is much more suitable carrier gas than nitrogen, but surprisingly, the S/N ratio of the peak for **2-d₄** was increased fourfold by using nitrogen gas at 200 °C (entry 2). Further improvement was observed for S/N ratio at 400 °C (entry 3). However, **2-d₀** was also detected at this temperature, which indicates heat-induced hydroxymethylation reaction of **1-d₀** proceeded during ionization. Finally the optimized ionization temperature was determined as 200 °C.

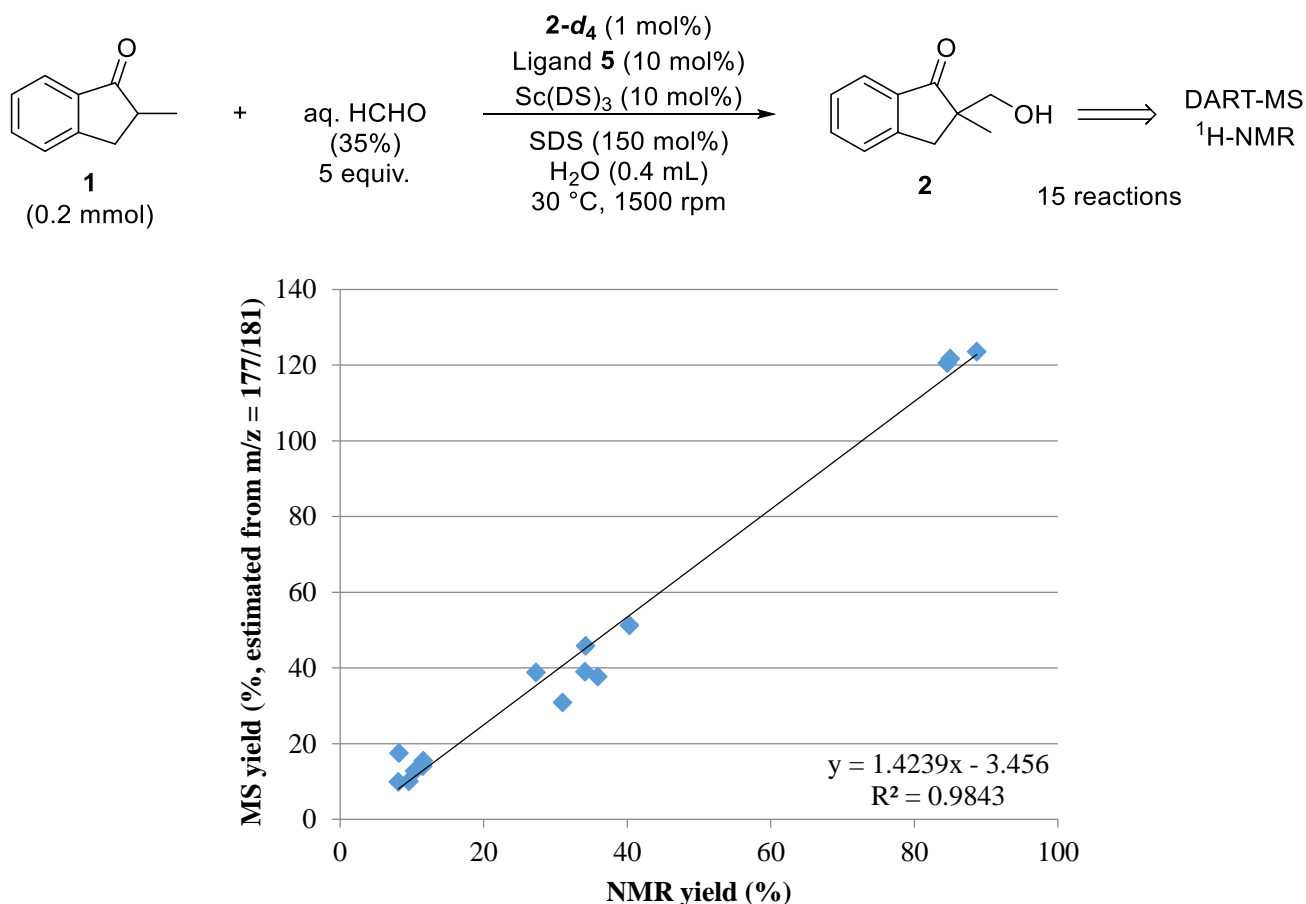
Then the reaction monitoring was conducted with the optimized conditions from Scheme 3-2 and with modified DART-MS conditions (N₂, 200 °C). As expected, peaks were observed at $m/z = 177$ and 181 successfully with the high S/N ratio. The corresponding MS yield calculated from the ratio of those peak areas showed good linear reaction profile (Figure 3-1).

Figure 3-1. Monitoring trial of direct-type aldol reactions. Raw SICs are in experimental section.



In order to verify the result obtained by mass spectrometry, comparative experiments were conducted with NMR spectrometry. Although direct monitoring by NMR spectrometry is not possible due to the heterogeneity, the yield of the product **2** can be easily determined from crude ¹H-NMR analysis after quenching the reaction mixture. The reactions were conducted in the presence of internal standard **2-d₄** at small scale. Crude NMR yields were determined by using 1,1,2,2-tetrachloroethane as an internal standard and MS yields were determined from the isotope ratio of product **2**. The reactions were conducted in several different reaction times to compare NMR yield and MS yield in wide range (Scheme 3-6).

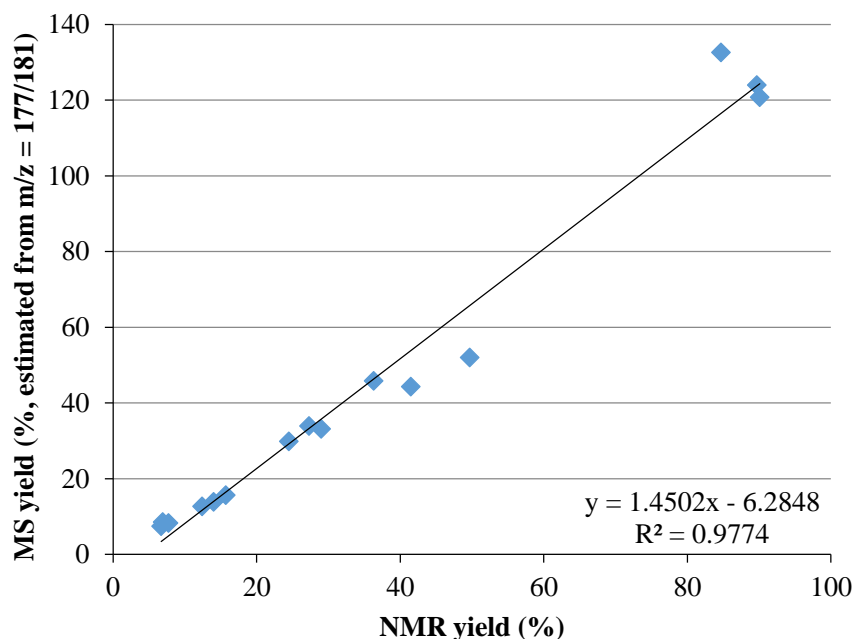
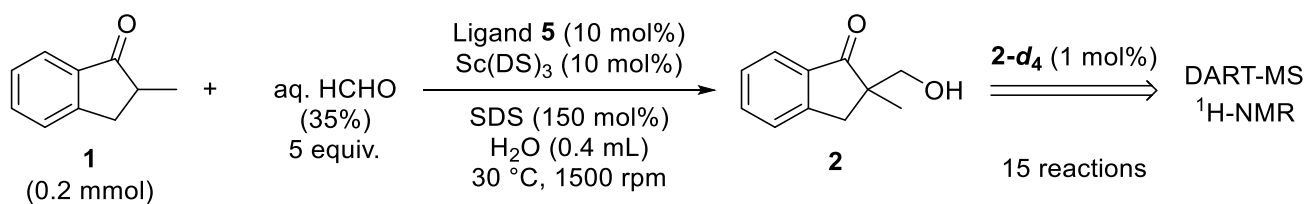
Scheme 3-6. Comparative experiments between MS and NMR (1)



The results showed good relationships between MS and NMR, however, the relationship was not in 1:1 ratio (Scheme 3-6, detailed data are given in experimental section). In some reactions the product **2** was isolated by preparative TLC and isolated yields were more corresponding to NMR yields than MS yields. If internal standard **2- d_4** were to decompose during the reaction, the yield calculated from isotope ratio would appear larger than true value. Fortunately, no peak of **1- d_4** ($m/z = 151$) was detected during crude DART-MS analysis of any experiment, which means there were no retro aldol process to decompose **2- d_4** . In order to disprove some other decomposition pathways of the internal standard, another set of experiment was conducted with a modified procedure avoiding an internal standard being compromised during the reaction conditions.

The reactions were conducted in the *absence* of internal standard **2- d_4** and quenched following the standard reaction procedure. After quenching internal standard **2- d_4** was added and then DART-MS and ¹H-NMR analyses were conducted as previous set of experiments. The results are shown in Scheme 3-7.

Scheme 3-7. Comparative experiments between MS and NMR (2): Late-stage addition of internal standard

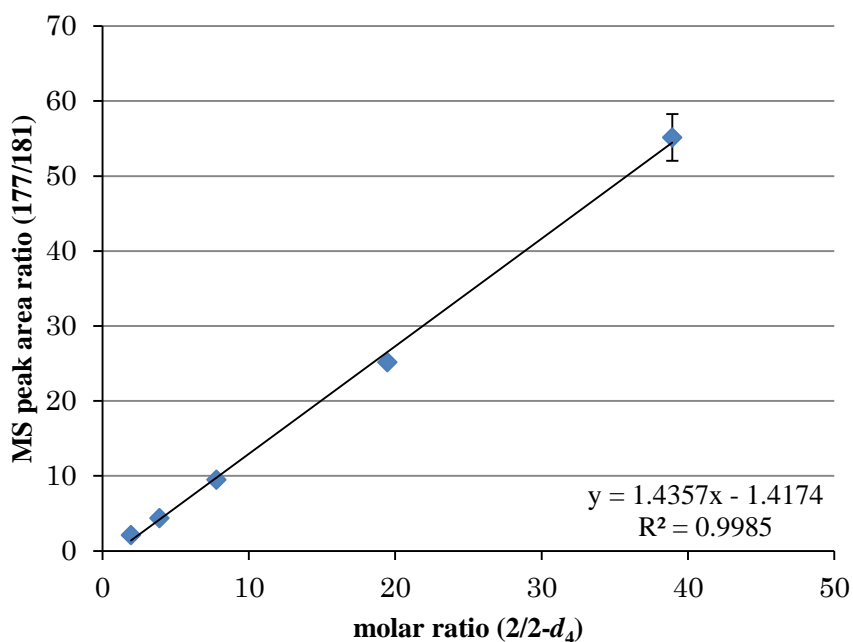


As a result, linear relationships between NMR and MS were observed with similar slope to previous experiment. The slopes 1.42 and 1.45 were in good agreement; Student t-test¹⁰⁰ of two dataset resulted $t = 0.125$, which is much smaller than the limit value of 99% confidence interval, 2.92. These statistics suggested these two experiment set showed the same result. It is concluded that there were no decomposition of internal standard during the reaction.

No decomposition of 2-d_4 during reaction means that the compound can be used as internal standard, and disagreement of yields calculated by MS and NMR were to be reasoned for some other issues. There are two possible hypothesis for MS/NMR deviation: Natural isotope distributions (especially carbon), contamination of proton during the synthesis of internal standard 2-d_4 . Probably this disagreement are caused by multiplex reasons, but the quantification would be practically possible with calibration between MS and NMR yield.

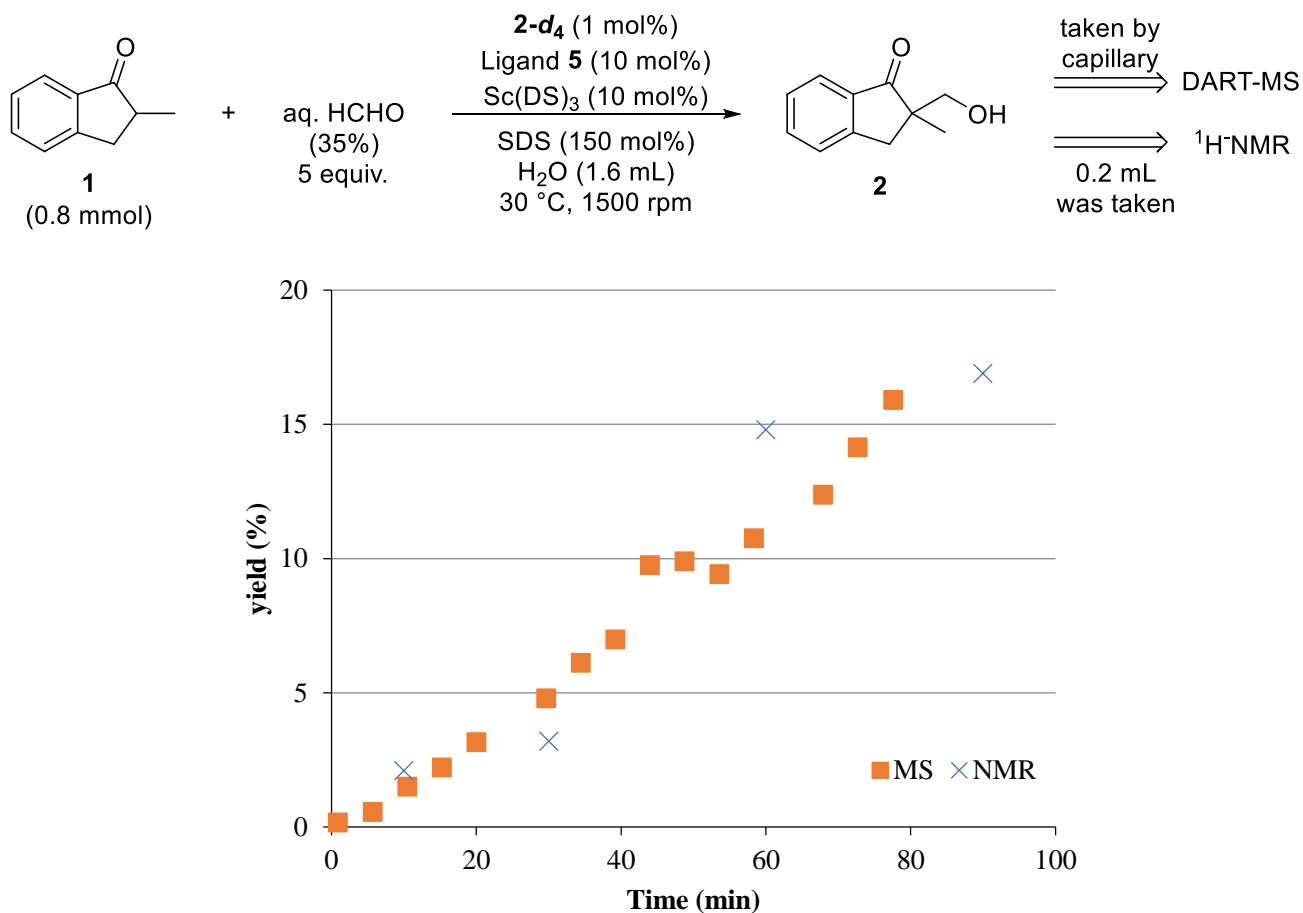
A calibration experiment was conducted by mixing compounds **2** and 2-d_4 in several different ratios. Aqueous solutions of compound 2-d_4 (5.055 g/L, 72.0 μL , 2.02 μmol as content) and 0.500, 1.00, 2.00, 5.00 and 10.00 mL of compound **2** solution in water (1.384 g/L) were mixed and analyzed by DART-MS. Each solutions were analyzed 6 times and averages were taken for the calibration curve.

Figure 3-2. A calibration curve of the yield derived from isotope ratio



In order to confirm the advantage of this method, the reaction was then directly monitored by DART-MS and by aliquot NMR analysis simultaneously (Scheme 3-8). The reaction was conducted in a large scale (0.8 mmol, total 1.6 mL reaction mixture), then the analytical sample was taken by an auto-sampler with capillary for DART-MS analysis, and 0.20 mL of aliquot was taken by syringe for NMR analysis. MS yield was determined by the isotope ratio of compound **2** with calibration given from Figure 3-2, NMR yield was determined by the ratio of starting material **1** and product **2**.

Scheme 3-8. Direct comparison of MS reaction profile and NMR profile

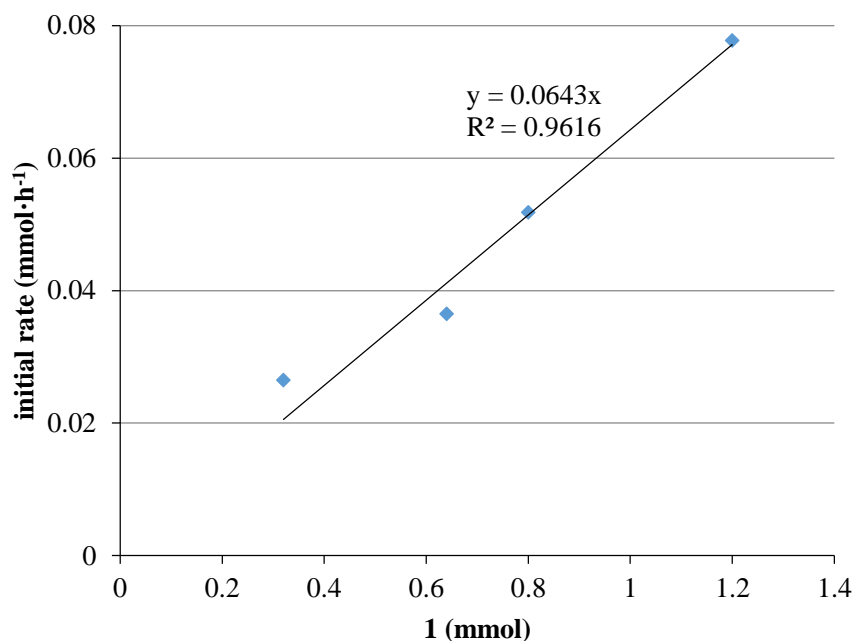
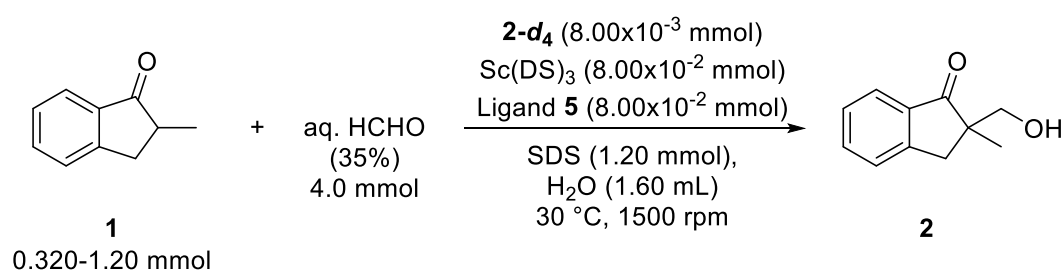


As a result, reaction profile by MS showed much better linearity than NMR. As mentioned above, an aliquot sample taken from the heterogeneous mixture do not reflect original molar ratio. Therefore, the result of NMR had some difficulties for quantitativity. Excellent linearity clearly demonstrated the advantage of MS monitoring method using isotope labelled internal standard.

3-2-3. Reaction kinetics of direct-type hydroxymethylation reaction

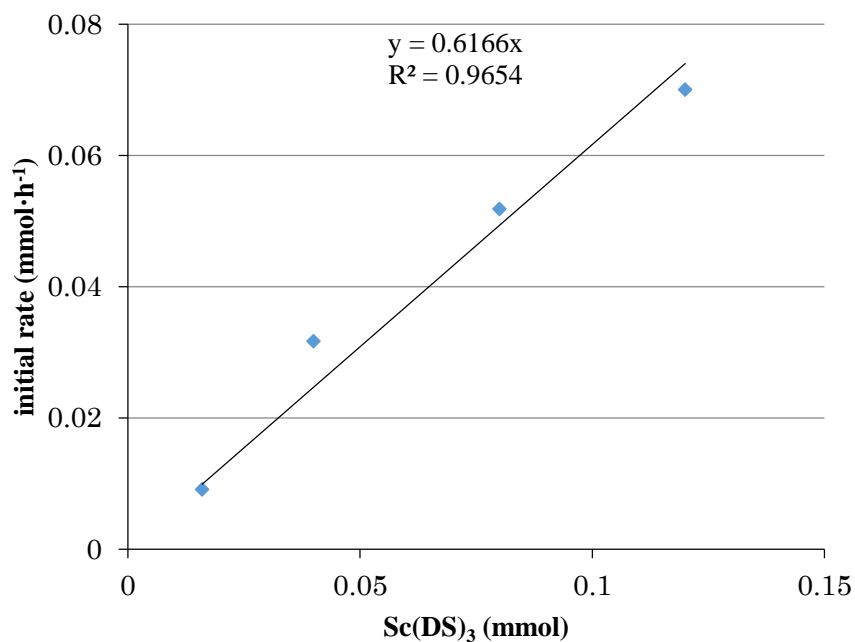
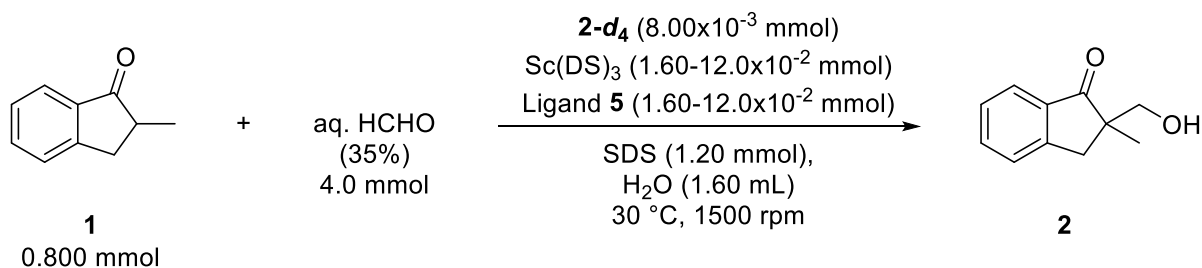
Kinetic analysis of the enantioselective hydroxymethylation reaction was then conducted based on this established method using DART-MS with internal standard. Following the standard procedure, initial velocity assays were conducted by changing the concentrations of each component. Initially dependency of the formation rate of product **2** on substrate **1** was investigated. The loading of **1** was changed from 0.320 to 1.20 mmol while those of catalyst complex and formaldehyde were kept constant. As a result, first order dependency was observed on the substrate **1** loading (Scheme 3-9).

Scheme 3-9. Kinetic study on indanone 1



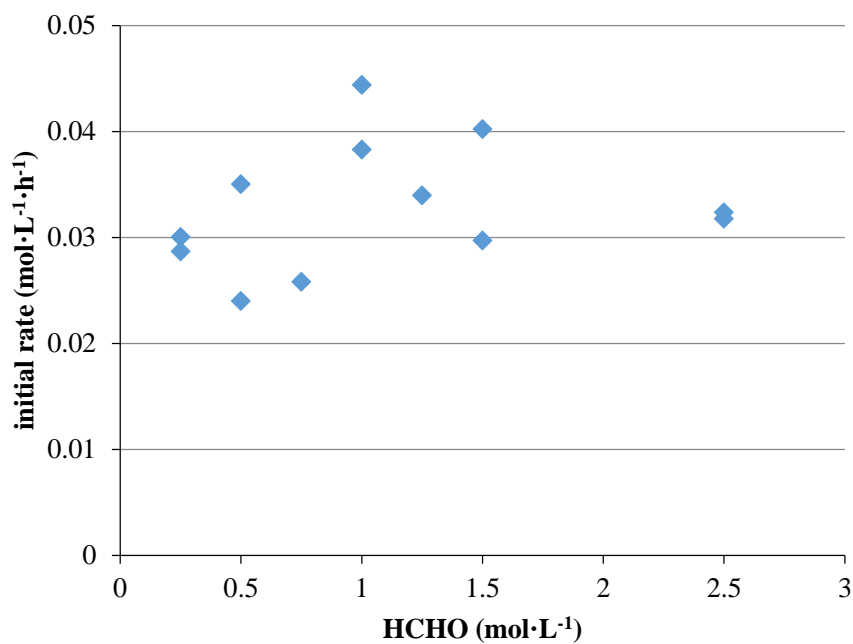
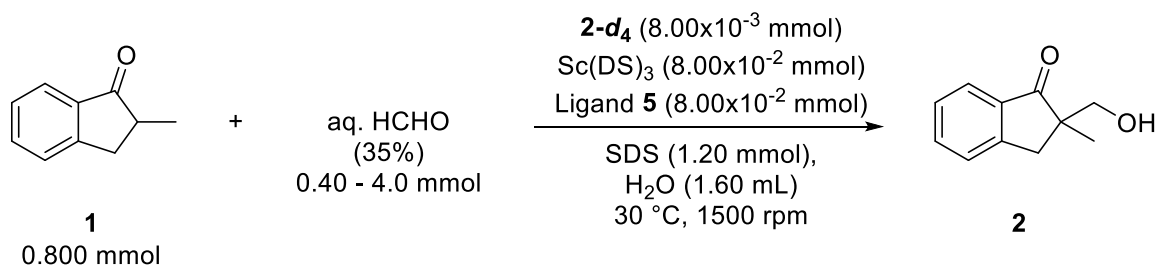
Then the dependency on the chiral Sc catalyst complex was investigated. The loading of $\text{Sc}(\text{DS})_3$ and 2,2'-bipyridine ligand **4** was varied from 0.0160 to 0.120 mmol while those of the substrate and formaldehyde were kept constant. The initial rate showed first-order dependency on the catalyst complex (Scheme 3-10).

Scheme 3-10. Kinetic study on scandium complex



On the other hand, an investigation toward formaldehyde revealed a different tendency. Concentration of formaldehyde was varied from 0.250 to 2.5 mol/L while those of substrate and catalysts remained constant, and as a result each experiments showed almost similar reaction profiles in moderate reproducibility (Scheme 3-11). Therefore, the rate dependency was regarded as 0th order on formaldehyde. No dependency on formaldehyde for reaction rate indicated that formaldehyde molecule was not concerning to the rate determining step of this reaction.

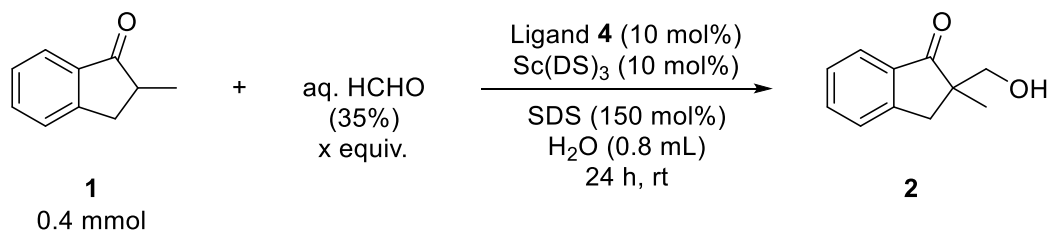
Scheme 3-11. Kinetic study on formaldehyde



3-2-4. Feedback of kinetic analysis to organic synthesis

The 0th order dependency on formaldehyde suggests the possibility that the amount of formaldehyde could be reduced. A simple control experiment showed it possible.

Scheme 3-12. Trial to decrease the amount of formaldehyde



Entry	x (equiv.)	yield (%)
1	5.0	90
2	1.5	85
3	1.2	82
4	1.2 (paraformaldehyde)	64

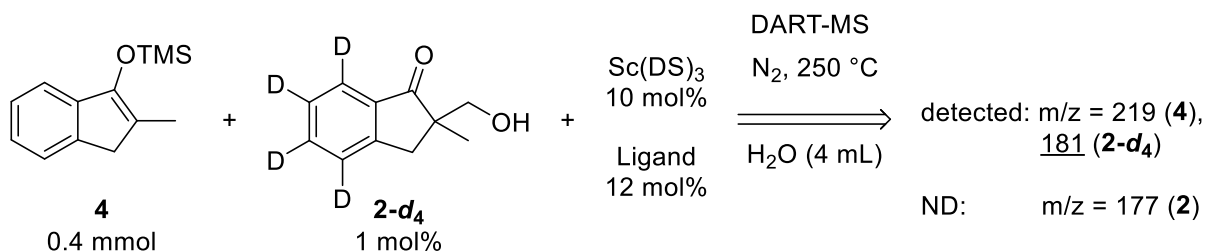
As a result, 1.5 equivalents of formaldehyde gave the desired product in high yield (entry 2). Furthermore, 1.2 equivalents of formaldehyde proved to be enough to promote the reaction in 82% yield (entry 3). The product was obtained in relatively high yield (62%) with 1.2 equivalents of paraformaldehyde as an alternate source of formaldehyde (entry 4).

3-3. Mukaiyama-type catalytic asymmetric hydroxymethylation reactions in water

3-3-1. Monitoring trial and detection of intermediate

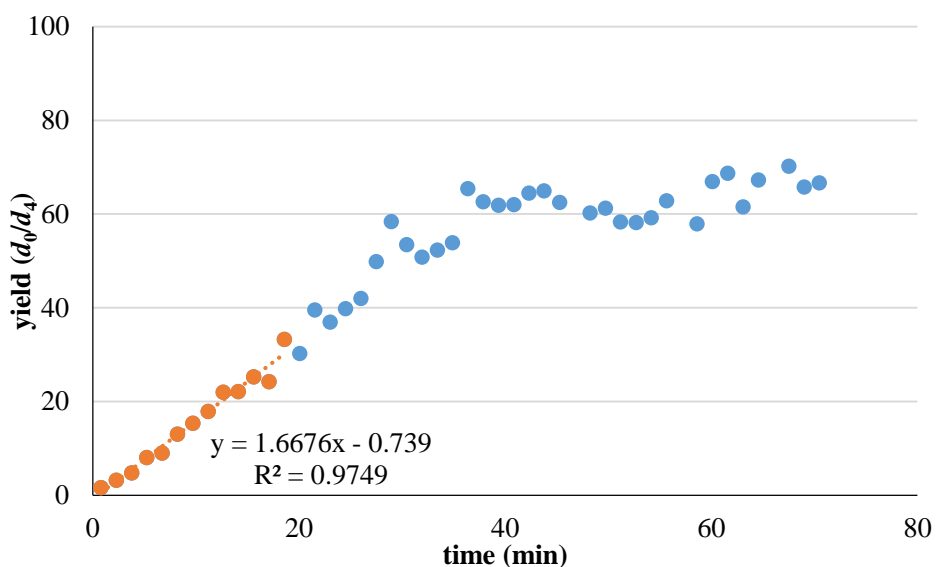
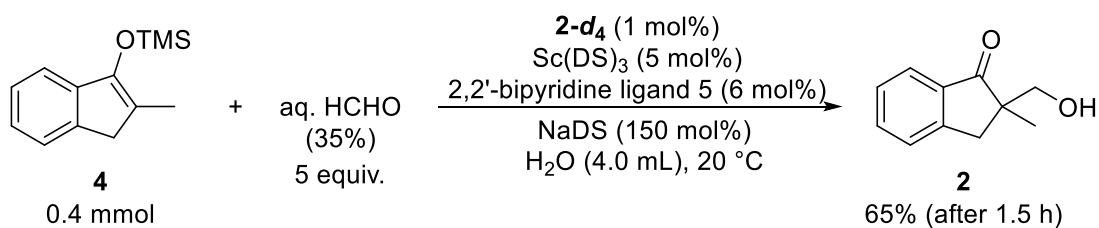
In order to confirm that the monitoring principle would work or not for the Mukaiyama aldol reaction, a detection check experiment was conducted for a reaction under modified conditions (Scheme 3-2). An analytical mixture was prepared following a standard reaction procedure in the absence of formaldehyde to avoid the formation of **2**, and a deuterium labelled reaction product **2-d₄** was added (Scheme 3-13). The mixture was analyzed under the optimized monitoring conditions of DART-MS for a direct-type aldol reaction (N₂ as carrier gas, 250 °C) to successfully detect a desired peak of an internal standard **2-d₄** at $m/z = 181$. No peak was observed at $m/z = 177$, corresponding to a non-deuterated reaction product **2**.

Scheme 3-13. A detection check for Mukaiyama aldol reactions



Based on the success of the detection check experiment, a monitoring trial was conducted for Mukaiyama aldol reactions (Scheme 3-14). In the presence of internal standard **2-d₄** the reaction was conducted, and was monitored by an auto-sampler DART-MS system using a glass capillary as a sampling rod. Gratifyingly, an isotope ratio of **2/2-d₄** showed the good reaction profile with a small dispersion of data. The reaction profile (calibrated by Figure 3-2. A calibration curve of the yield derived from isotope ratio) showed that the reaction have stopped at around 40 minutes with approximately 60 to 70% yield, which was corresponding to 65% isolated yield of the product **2** after the monitoring study.

Scheme 3-14. Reaction monitoring trial of Mukaiyama-type aldol reactions



A careful data mining of the obtained mass spectra found that new peaks appeared on $m/z = 249$ and 253 during the reaction monitoring. Both of them are assigned as the silylated reaction product **6** and **6-d₄**, respectively (Scheme 3-15). Those SICs are shown in Figure 3-3 and Figure 3-4. There are three possibilities to generate **6**; (1) from **4** and formaldehyde as an intermediate of silyl migration pathway *under reaction conditions*, (2) from product **2** with some silyl source as a side product *under reaction conditions*, and (3) from product **2** with some silyl source *during ionization* (Scheme 3-16).

Scheme 3-15. A possible structure of silylated reaction product 6

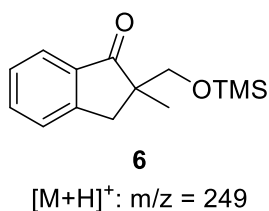


Figure 3-3. Selected ion chromatogram of $m/z = 249 - 249.5$

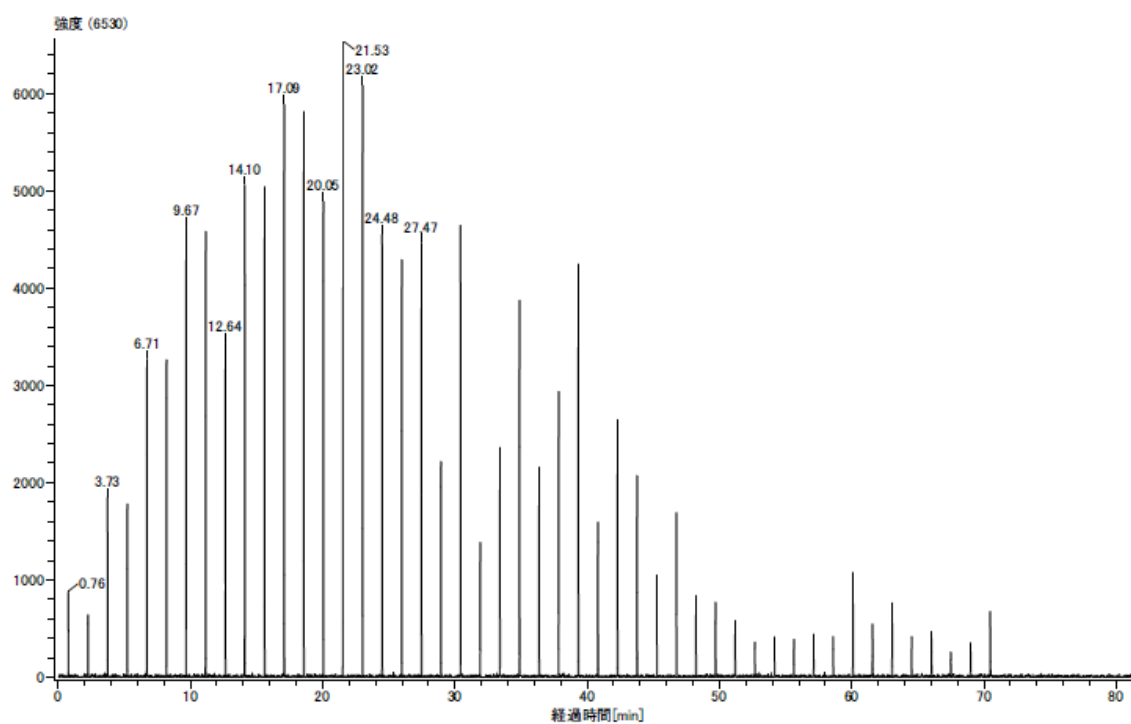
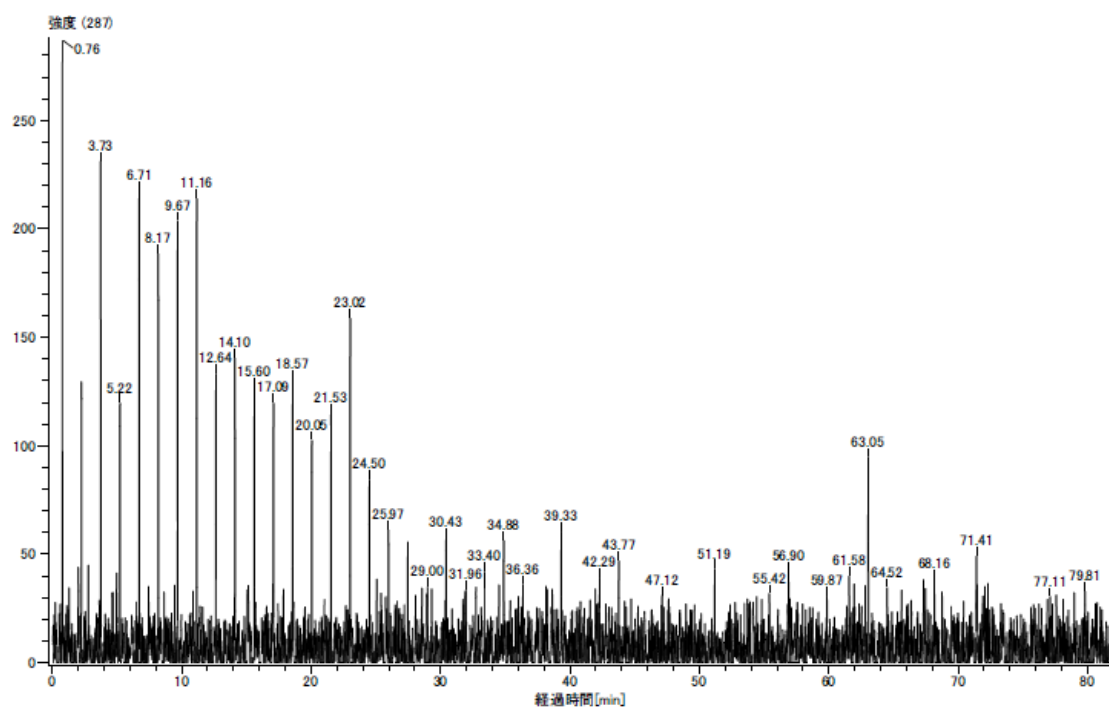
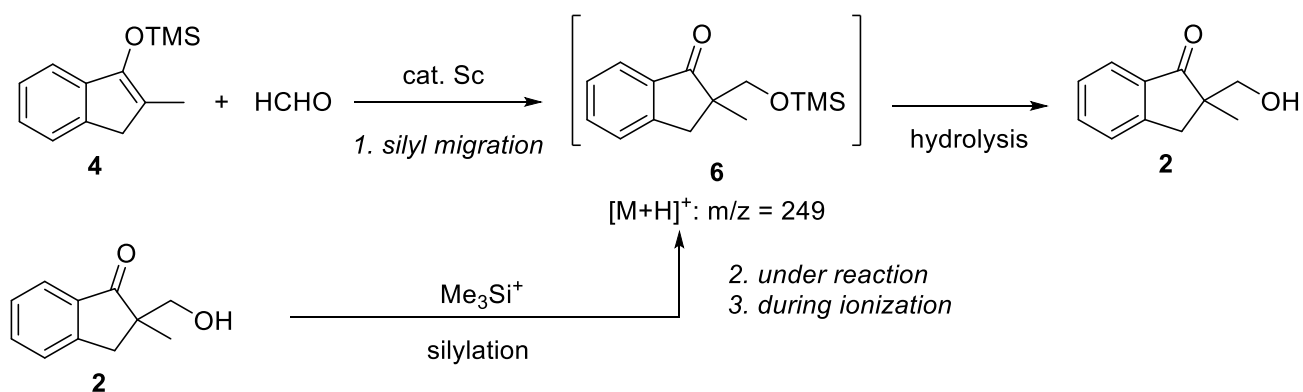


Figure 3-4. Selected ion chromatogram of $m/z = 253 - 253.5$



Scheme 3-16. Possibility of the reaction intermediate



From TIC (Total Ion Current) of Scheme 3-14, SICs of product **2**, substrate **4** and silylated product **6** were extracted. The standardized peak intensities of substrate **4** at $m/z = 219$ and silylated compound **6** at $m/z = 249$ were plotted as bar graphs versus time over the reaction profile of **2** obtained in Scheme 3-14 (Figure 3-5). 3-Point moving averages of **4** and **6** are given as dotted lines with each corresponding color.

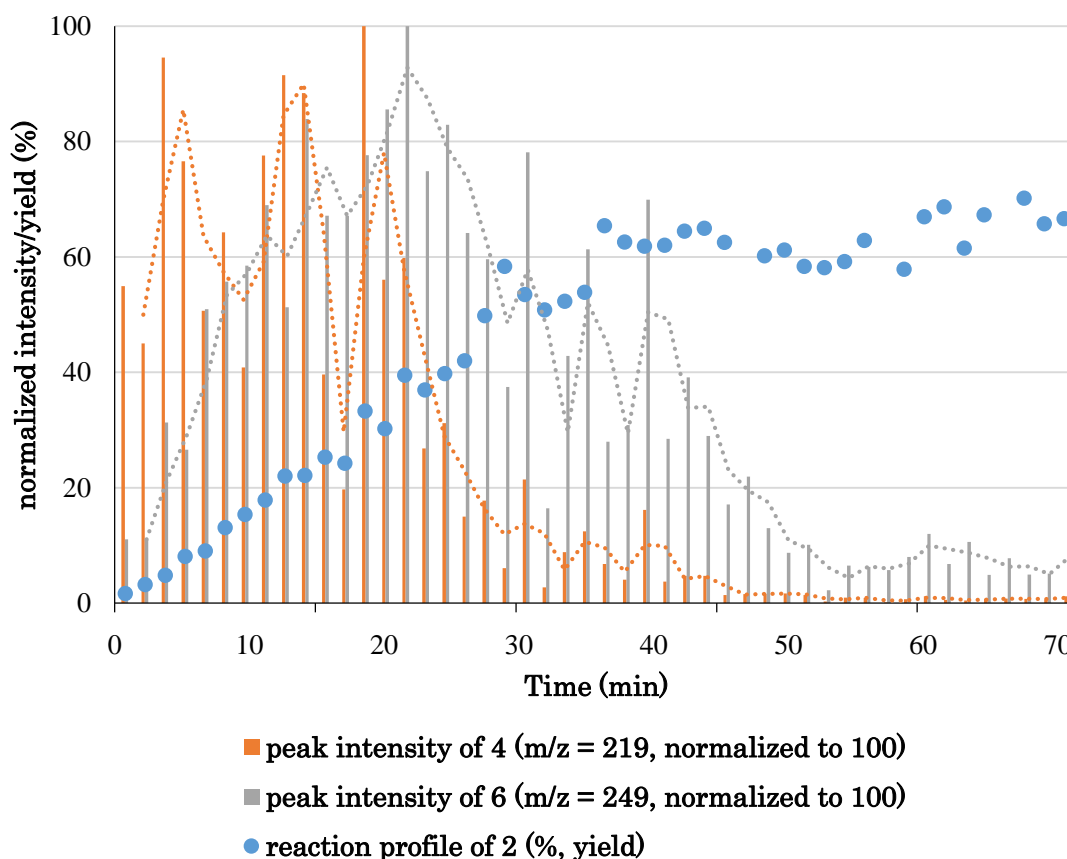
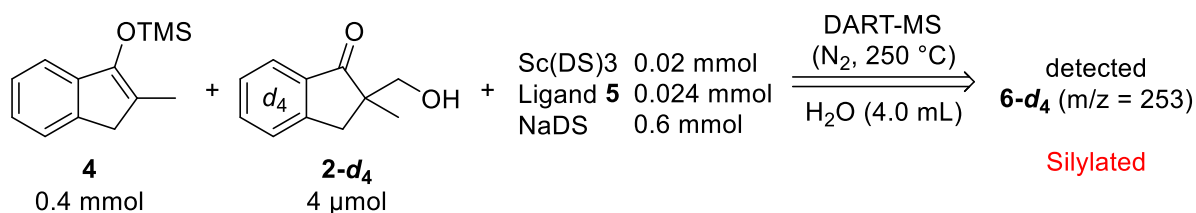


Figure 3-5. Intensity – time plot of substrate **4, silylated reaction product **6** and reaction profile of product **2****

A linearly increasing feature of the reaction product **2** and a decreasing feature of starting material **4** were in a good agreement. The peak intensity of **6** was first increased and then showed decreasing feature. From such a tendency it is easy to jump into a hasty conclusion that **6** is an intermediate of this Mukaiyama aldol reaction. However, this match is a coincidence and does not deny the possibility that **6** was generated from **2** during ionization on DART-MS. If **6** were to be generated under reaction conditions, the observed reaction rate of **2** would contain hydrolysis rate of **6** (Scheme 3-16). In the other case, an observed reaction rate of **2** is probably the “real” rate of catalytic reactions.

Under anhydrous conditions, Mukaiyama aldol reactions are generally considered to yield a silylated alcohols as products.^{101–104} However, a trimethylsilyl ether of a simple primary hydrocarbon is easily hydrolyzed under slightly acidic reaction conditions.¹⁰⁵ Some articles indicate that under aqueous conditions Mukaiyama aldol reactions proceed a desilylative activation of a silyl enol ether, and a silylated alcohol do not exist as an intermediate during the catalytic pathway.^{106–108} Indeed, no silylated product **6** was isolated from reaction mixtures of any stage of its progress by column chromatography. In order to elucidate the source of the peaks of **6** and **6-d₄** on $m/z = 249$ (and 253), several control experiments were conducted (Scheme 3-17, Scheme 3-18).

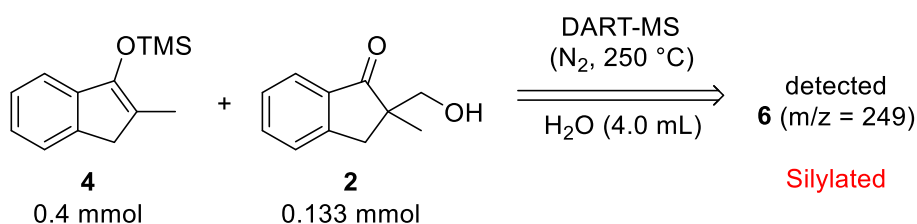
Scheme 3-17. Control experiment 1: Reaction condition without HCHO



A mixture of silyl enol ether **4** (0.4 mmol), internal standard **2-d₄** (4 μmol), scandium dodecylsulfate (20 μmol), 2,2'-bipyridine ligand **5** (24 μmol) and sodium dodecylsulfate (NaDS, 0.6 mmol) in water (4 mL) was prepared. The composition of the mixture is similar to the standard reaction condition but formaldehyde, so any non-deuterated compound **2** or **6** is generated from **4**. As a result of the DART-MS analysis under standard conditions (N₂ as carrier gas, 250 °C), a new peak was observed at $m/z = 253$, which is corresponding to the silylated internal standard **6-d₄**. This result, silylation of an internal standard **2-d₄**, indicates that the reaction product **2** can also be silylated under a reaction conditions or an ionization conditions.

In the next experiment, catalysts and a surfactant were removed from a mixture and an ionization was conducted under standard ionization conditions (N₂ as carrier gas, 250 °C, Scheme 3-18).

Scheme 3-18. Control experiment 2: Silylation reaction under DART conditions



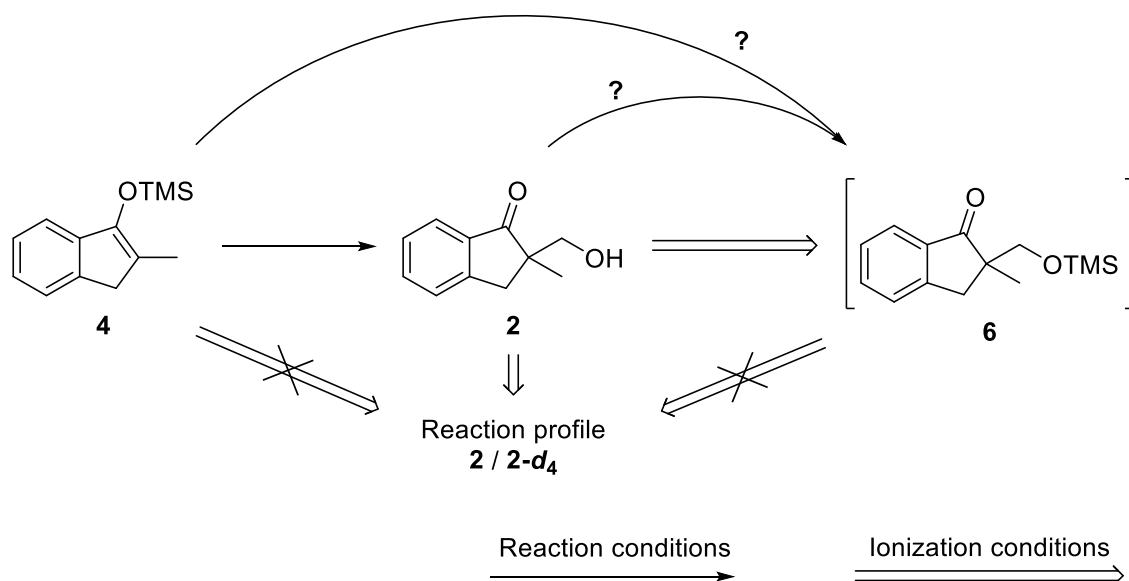
A mixture of silyl enol ether **4** (0.4 mmol) and non-deuterated reaction product **2** (0.133 mmol) were vigorously

mixed in water (4.0 mL). The mixture was analyzed by DART-MS to detect the peak of **6** on $m/z = 249$.

In the absence of Lewis acid, no silyl transfer from silyl enol ether **4** to alcohol **2** would proceed *under reaction conditions*. Therefore, in this control experiment a peak of **6** observed on DART-MS analysis was originated from **2** and **4** *during ionization*.

At this stage there were no direct evidence to deny the formation of **6** under catalytic reaction conditions, but the possibility is low. No disturbance on the reaction profile of **2** determined from its isotope ratio suggests the peak of **2** on MS is generated only from **2** in reaction. The rate of the formation of **2** includes not only catalytic reactions but also hydrolysis of **6**, if silyl ether **6** were to exist as an intermediate.

Scheme 3-19. A possible generation pathway of silyl ether **6**

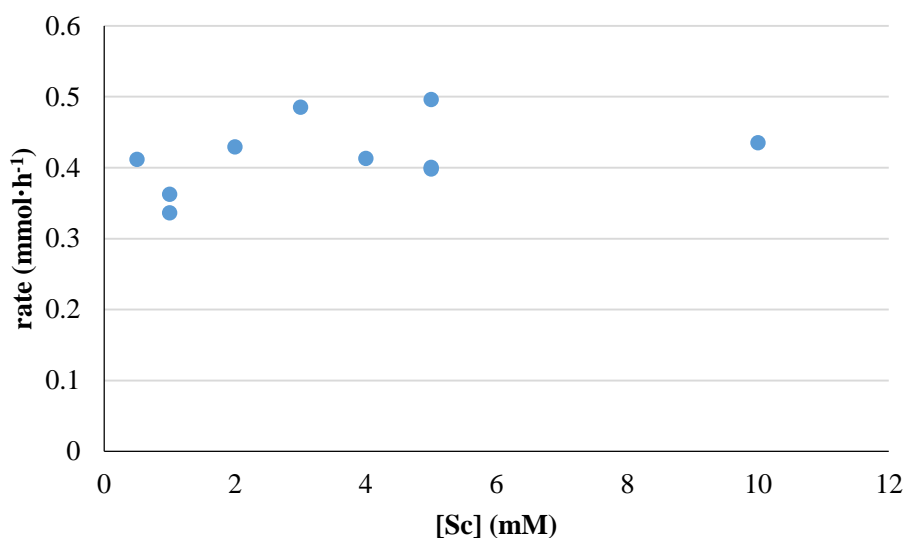
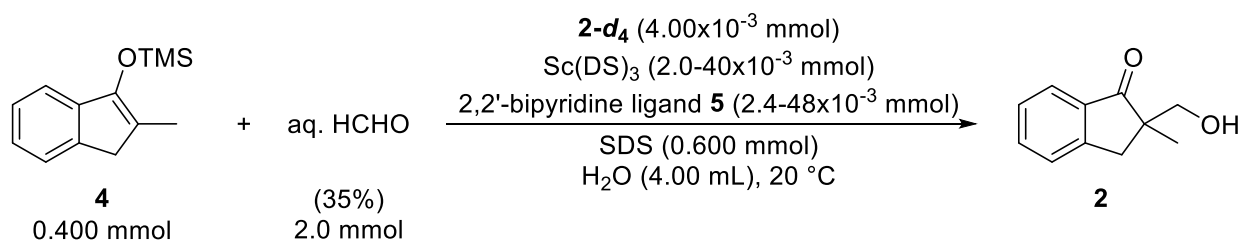


3-3-2. Reaction kinetics

Based on the established monitoring conditions, the kinetics experiments of Mukaiyama aldol reaction in water were conducted. Following the standard procedure, initial velocity assays were conducted by changing the concentration of each component.

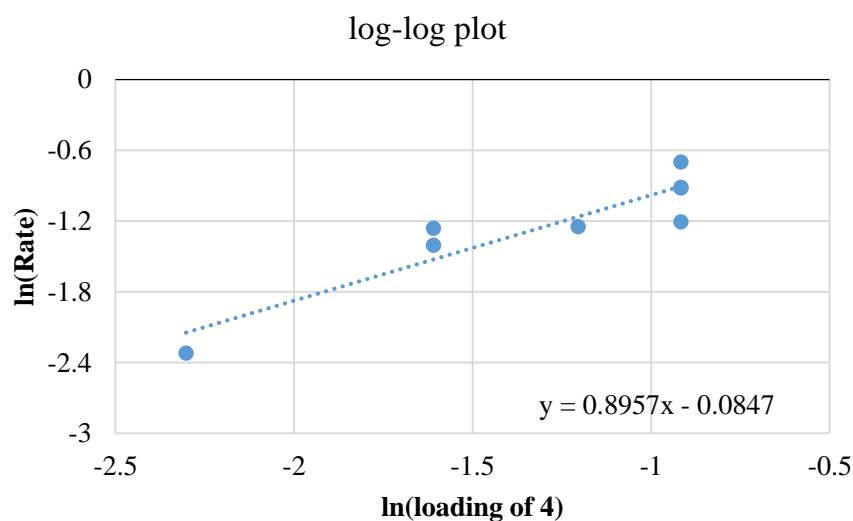
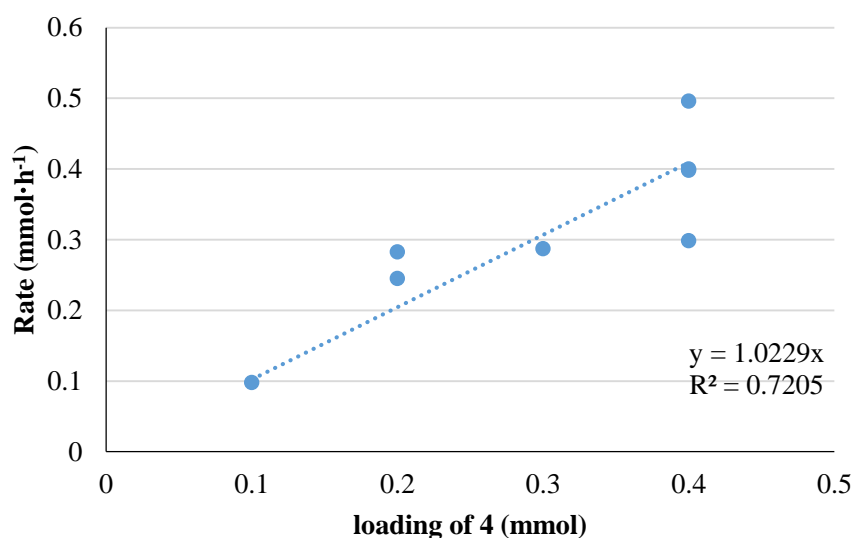
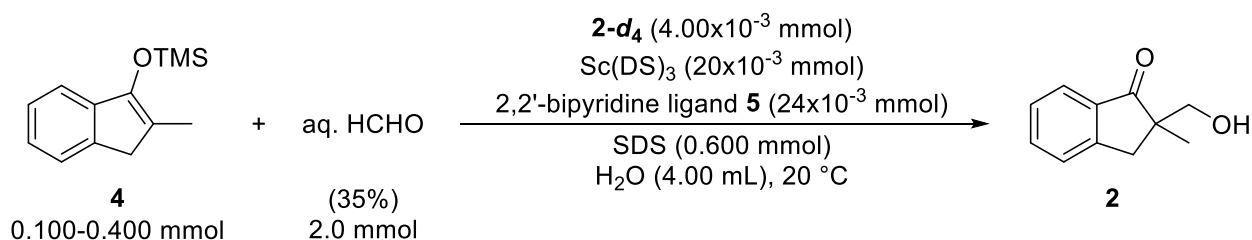
Firstly a dependency of the formation rate of product **2** on chiral scandium catalyst was investigated. A loading of scandium tris(dodecylsulfate) was changed from 0.0020 to 0.040 mmol and 2,2'-bipyridine ligand **5** were changed from 0.0024 to 0.048 while those of substrate **4** and formaldehyde were kept constant. Interestingly, an initial velocity assay revealed 0th order dependency of this reaction onto catalyst even though this is catalytic reaction (Scheme 3-20).

Scheme 3-20. Kinetic study on catalyst



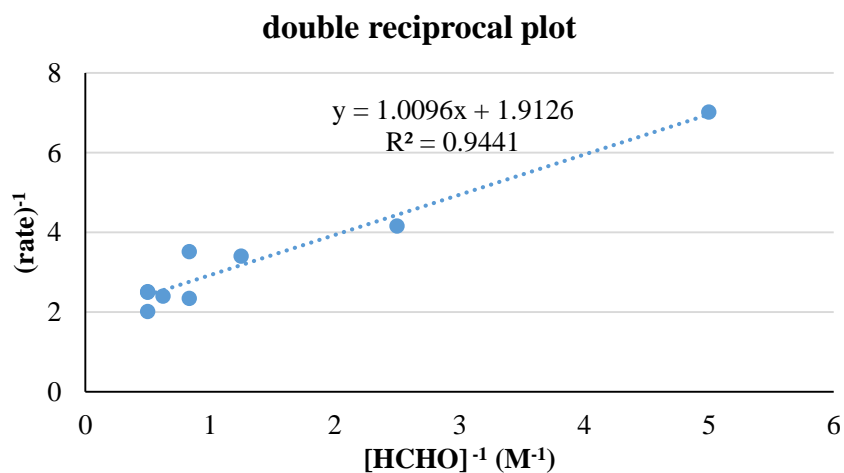
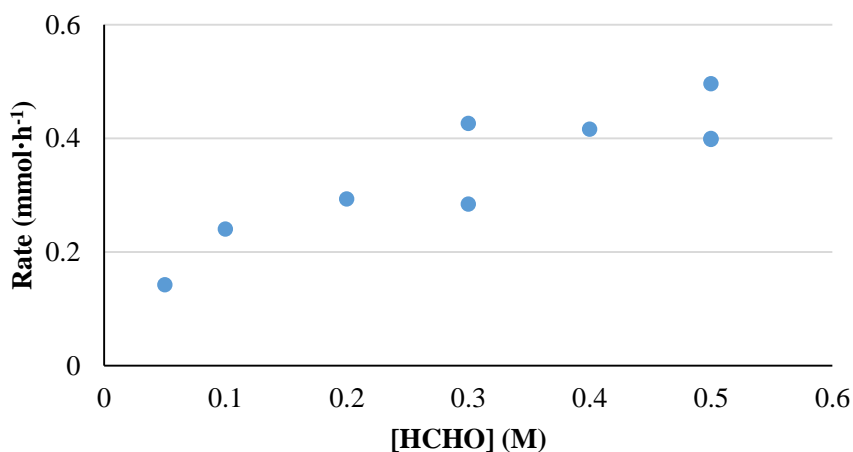
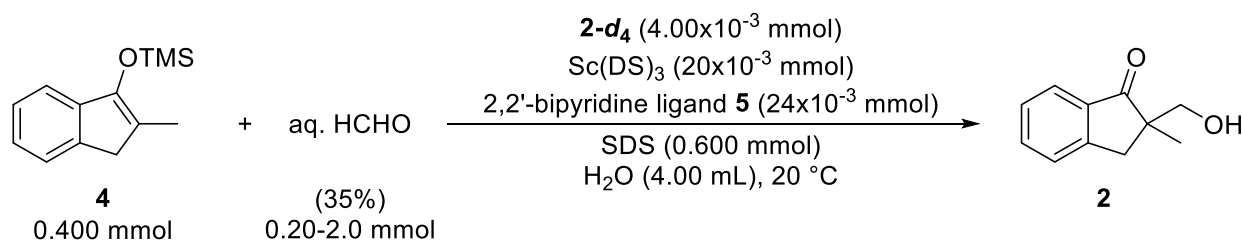
Next, an initial velocity assay on loading of substrate **4** was then conducted. Although the data distribution was relatively wide, positive correlation was apparently observed between reaction rate and loading of substrate **4**. With an assumption of Gaussian distribution, slope of log-log plot was determined as 0.9 ± 0.26 in 95% confidence interval.

Scheme 3-21. Kinetic experiment on silyl enol ether **4**



On the other hand, the reaction showed interesting kinetics on the concentration of formaldehyde. An initial velocity assay on formaldehyde was conducted by changing the concentration of formaldehyde from 0.050 to 0.50 M. The plot was not linear, rather was showing curved structure with saturation (Scheme 3-22). This obtained kinetics had some similarity to enzymatic ones, so the obtained data was plotted again in double reciprocal manner. As a result, excellent linear relationships were observed between the inverse of formaldehyde concentration and the inverse of the reaction rate.

Scheme 3-22. Kinetic experiment on formaldehyde



3-4. Mechanistic considerations

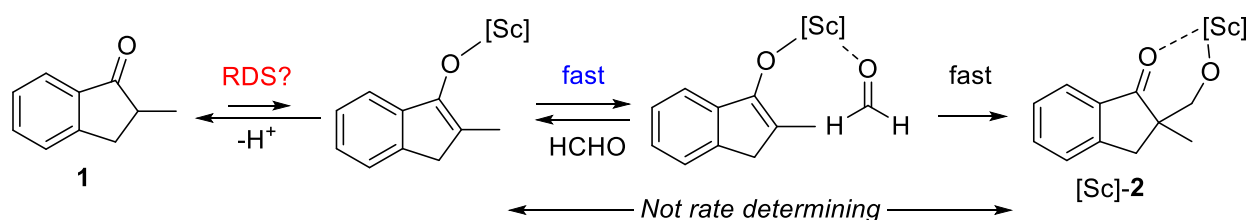
3-4-1. Mechanistic considerations of direct-type aldol reactions

A revealed first-order rate dependency of indanone **1** and chiral Sc catalyst complex while a 0th order dependency on formaldehyde represents an overall experimental rate-law of:

$$\text{Initial Reaction Rate} = k[\mathbf{1}]_0^1 [\text{Sc}]_0^1 [\text{HCHO}]_0^0$$

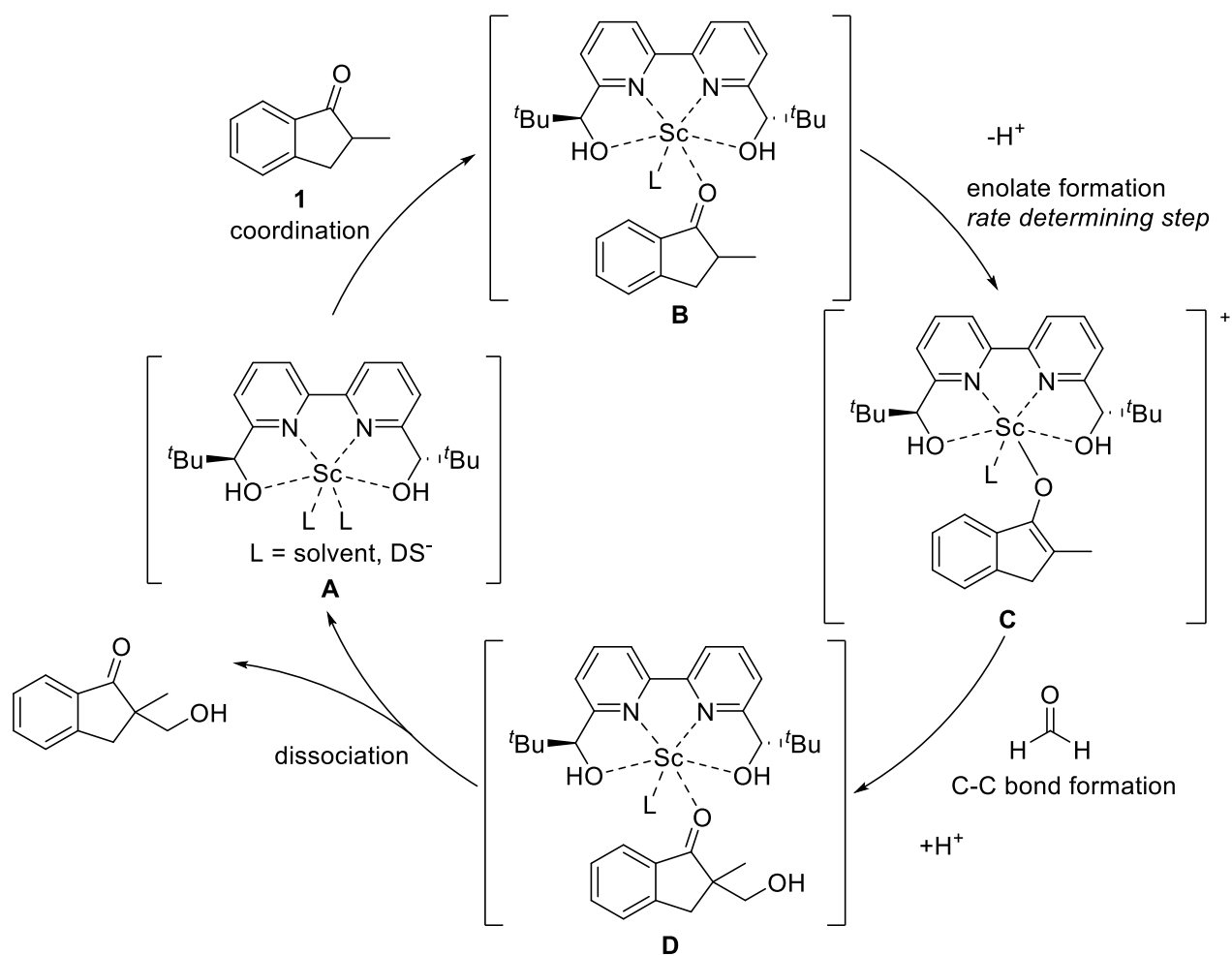
During the course of the reaction, scandium catalyst and two carbonyl species (indanone **1**, formaldehyde) are expected to form an intermediate complex. Judging from 0th order dependency of formaldehyde, however, the complex that contains formaldehyde is not the species at the rate determining step. A possible rate determining step other than carbon-carbon bond formation is the enolate formation step with deprotonation. After coordination of the scandium species, the scandium enolate will be formed with water or dodecylsulfate anion as a proton scavenger. The basicity of those species is not high, so the rate of enolate formation step could be slow enough to limit whole reaction rate.

Scheme 3-23. Considerable rate determining step



With these considerations and our previous studies,¹⁰⁹ here the reaction mechanism is assumed as follows. To a catalyst complex **A**, indanone **1** is coordinated and make intermediate complex **B**. Following slow deprotonation from **B** leads to active complex **C** and this species interacts with formaldehyde and following deprotonation gives product complex **D**. (Scheme 3-24)

Scheme 3-24. Assumed catalytic cycle



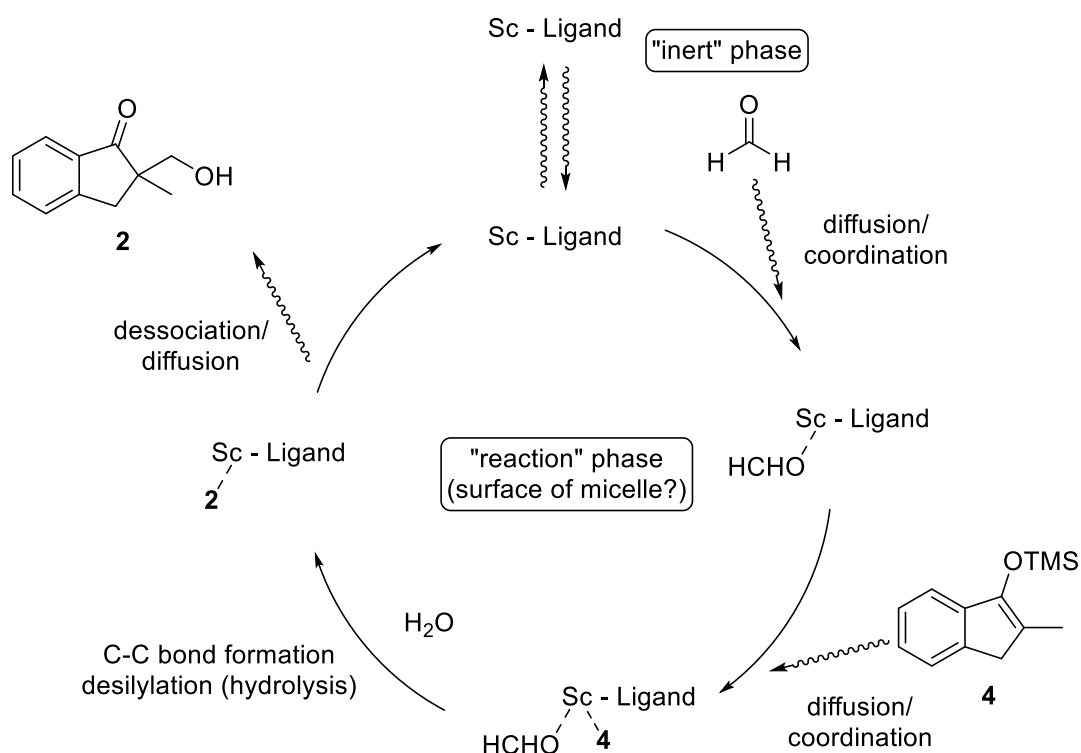
3-4-2. Mechanistic considerations of Mukaiyama aldol reactions

Obtained data indicated following results; 0th order on catalyst, 0.9th (or probably 1st) order on enolate, and Michaelis-Menten type kinetics on formaldehyde. An overall experimental rate-law is described as:

$$\text{Initial Reaction Rate} = k_1[\mathbf{4}]_0^{0.9}[\text{Sc}]_0^0 \frac{[\text{HCHO}]_0}{k_2[\text{HCHO}]_0 - k_3}$$

The reaction condition is employing micellar system, which is surely heterogeneous. Moreover, an initial rate of Mukaiyama aldol reactions is nearly 10 times faster than that of direct-type aldol reactions. For such a rapid reactions under heterogeneous conditions, it is required to consider not only “chemical” rates of reactions but also “physical” rates such as a diffusion or a permeation through the surfactant layer. Whole reaction system including diffusion step is assumed in Scheme 3-25.

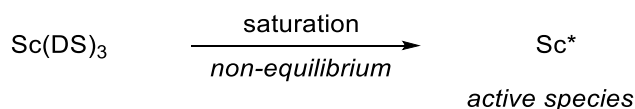
Scheme 3-25. Assumed reaction pathway including diffusion of substrate on micelle



The reaction probably takes place on the surface of micelle, as an enolate **4** exists in micelle and population of formaldehyde is considered to be greater in an aqueous phase. The surface of micelle is covered by surfactant molecules, and hydrophilic molecules such as formaldehyde have some difficulties to permeate through. Therefore, permeation of formaldehyde is possibly ignored, rather of enolate is to be considered.

On the other hand, zero-order rate law on catalyst could not be explained from estimated reaction rate equation containing catalyst concentration as a factor. It is possible that an amount of actual “active” scandium species is not proportional to corresponding catalyst loading. In other word, active species are saturated and limited amount of scandium are working as a catalyst (Scheme 3-26).

Scheme 3-26. Saturation of real active catalyst species



3-5. Conclusion

In Chapter 3, the direct reaction monitoring of heterogeneous reactions under micellar conditions was achieved using DART-MS with an isotope-labelled internal standard. An internal standard **2-d4** was successfully designed for the monitoring of direct-type aldol reactions of ketone **1** with formaldehyde catalyzed by scandium tris(dodecylsulfate) – 2,2'-bipyridine complex in water. **2-d4** was also applicable to the monitoring of Mukaiyama aldol reactions in water catalyzed by the same scandium complex. As an extensive applications of the monitoring methodology, kinetic analyses were conducted and overall experimental rate-laws are described:

For direct-type aldol reactions,

$$\text{Initial Reaction Rate} = k[\mathbf{1}]_0^1[\text{Sc}]_0^1[\text{HCHO}]_0^0$$

And for Mukaiyama aldol reactions,

$$\text{Initial Reaction Rate} = k_1[\mathbf{4}]_0^{0.9}[\text{Sc}]_0^0 \frac{[\text{HCHO}]_0}{k_2[\text{HCHO}]_0 - k_3}$$

The completely different rate-laws suggest distinct roll of catalyst complex in each reaction mechanisms. 0th Order on formaldehyde in direct-type reaction is probably due to the slow deprotonation of **1**, however, it is difficult to explain another 0th order on scandium complex in Mukaiyama aldol reaction. The saturation of scandium species was suggested, but the true reason for this unusual kinetics is remain unknown. The elucidation of true catalyst species for Mukaiyama aldol reaction in water is highly desired in future.

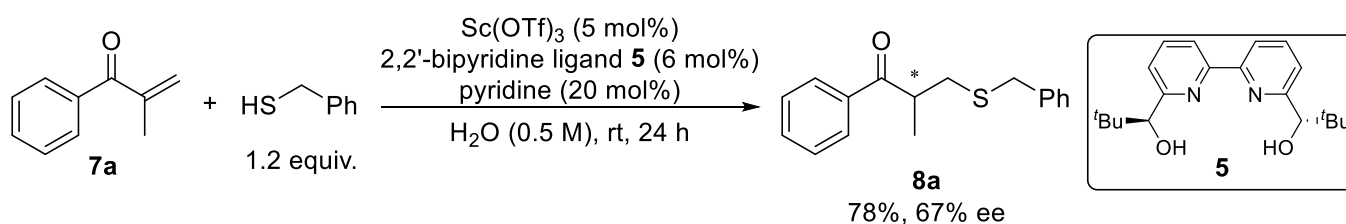
4. Monitoring study of liquid-liquid heterogeneous reactions: 1,4-addition/enantioselective protonation reactions in water

4-1. Introduction

It is important to show further applications toward various heterogeneous reaction systems to establish the monitoring strategy. In chapter 3, the monitoring strategy using DART-MS with an isotope-labelled internal standard was applied for the direct-type aldol reactions and Mukaiyama aldol reactions under micellar conditions to show successful reaction profiles. As the third example of the monitoring study, a heterogeneous reaction in the absence of surfactant was selected. Water-insoluble organic materials form large droplets under vigorous stirring during reactions, and reactions proceed in one phase of the mixture via an extractive manner or on the surface of the droplet. An important example is phase transfer catalysis^{110–112} employing water/organic solvent biphasic systems and ionic organic materials as intermediate transfer catalysts. If phases of heterogeneous reactions are easily separated when the stirring is stopped, *ordinary* aliquot-taking analysis is possible without any sample treatment.^{20,21} However, such a phase separation is not always promising. High viscosity of the phase or existence of an emulsifier would inhibit efficient phase separation for direct observation of the reaction system.

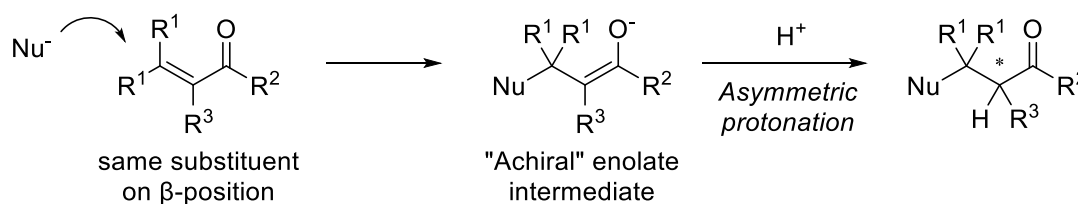
Scandium-catalyzed 1,4-addition/enantioselective protonation reactions were selected as good examples of non-micellar type catalytic reaction systems¹¹³ (Scheme 4-1).

Scheme 4-1. Scandium-catalyzed 1,4-addition/enantioselective protonation reactions



Stereoselective 1,4-addition reactions are highly important for the formation of complex molecules.^{114–116} In the selected examples, thia-Michael addition reactions were conducted in pure water with water-soluble scandium triflate as a catalyst. 2,2'-Bipyridine ligand **5** created an efficient chiral environment and 1,4-addition products were obtained with high enantioselectivities. Achiral enolate intermediate is expected in 1,4-addition reactions when substrate has same substituent on β -position, however, in this reaction the products are obtained with high enantioselectivity (Scheme 4-2). Such selective protonation reactions under highly protic conditions are quite rare and interesting.¹¹⁷ Of this great interest, this particular reaction was selected as a representative example.

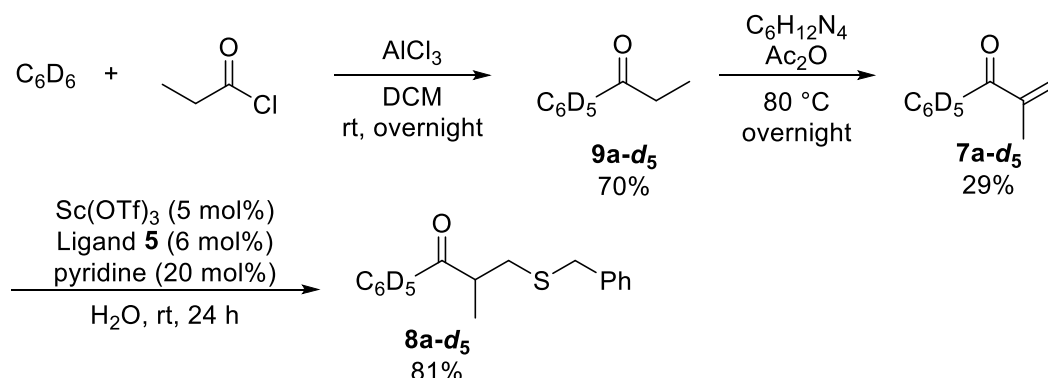
Scheme 4-2. 1,4-Addition/enantioselective protonation reactions



4-2. Initial trials

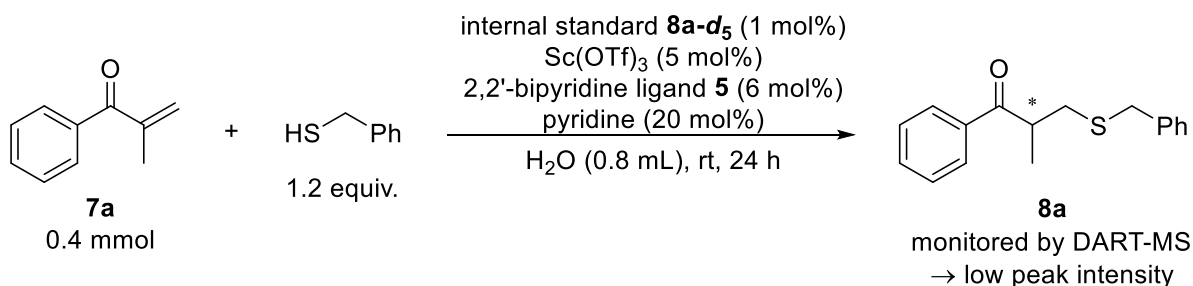
Deuterium labelled internal standard **8a-d₅** was prepared from commercial benzene-**d₆** as follows (Scheme 4-3). Friedel-Crafts acylation reaction under anhydrous condition was conducted to form propiophenone-**d₅** (**9a-d₅**), which was converted into α -methyl substituted enone **7a-d₅**.¹¹⁸ Under standard reaction conditions deuterium-labelled product **8a-d₅** was obtained in high yield with high deuterium purity. Obtained product was used after recrystallization.

Scheme 4-3. Preparation of deuterium-labelled internal standard



A synthesized internal standard **8a-d₅** was then used for the monitoring study. Due to its poor solubility in water, internal standard **8a-d₅** was added to a reaction vessel as a stock solution in ethyl acetate. After removal of solvent under continuous nitrogen flow, Sc(OTf)₃, 2,2'-bipyridine ligand **5** and water was added. After 1 hour of catalyst preparation, enone **7a** and benzyl mercaptan were successively added. The reaction was conducted in fume hood to avoid an odor of thiol and a small aliquot sample was taken by a glass capillary to bring DART ionization area manually. An ionization was conducted under standard DART-MS conditions previously determined in chapter 3 (Scheme 4-4, N₂ as carrier gas, 200 °C).

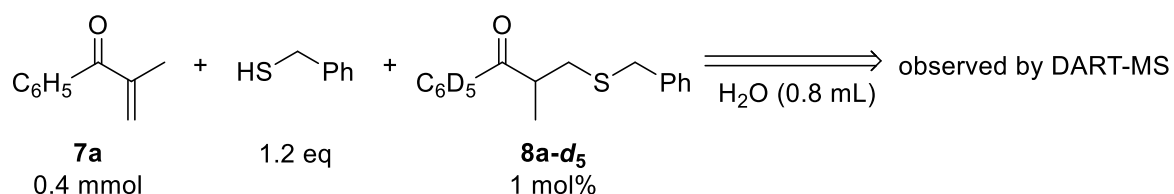
Scheme 4-4. Initial monitoring trial under standard reaction conditions



As a result, a peak intensity of a product **8a** at $m/z = 271$ gradually increased as the reaction proceeded, however, that of an internal standard **8a-d₅** at $m/z = 276$ was crucially low even after a long reaction time. In order to conduct a quantitative monitoring by the ratio of isotopes, an improvement of peak intensity was required. Monitoring

conditions of DART-MS were optimized for better detections. Starting material **7a**, benzyl mercaptan and deuterated internal standard **8a-d₅** was mixed in water and the mixture was analyzed by various conditions of DART-MS (Scheme 4-5).

Scheme 4-5. Monitoring conditions optimizations



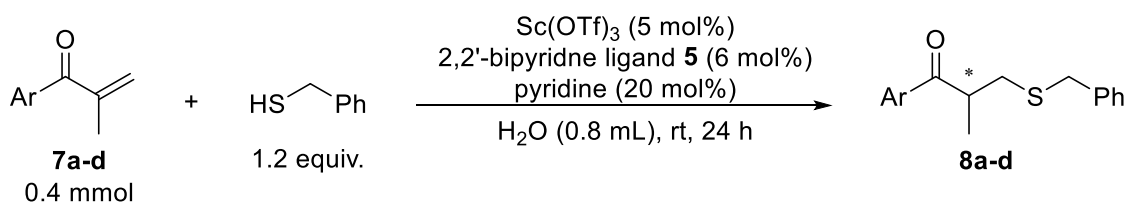
Entry	DART gas	DART temp. (°C)	m/z = 271 (8a)	m/z = 276 (8a-d ₅)
1	N ₂	200	ND	Weak
2	He	200	ND	Weak
3	He	400	Detected	Detected
4	He	100	ND	ND
5	N ₂	400	Detected	Detected

As a result, unfortunately, no good conditions were established. N₂, used in standard conditions in chapter 3, is generally considered to be a less efficient carrier gas of DART-MS than He.^{51,119} However, at 200 °C neither N₂ nor He ionized a deuterium labelled compound **8a-d₅** efficiently (entries 1, 2). At 400 °C by using He or N₂ as a carrier gas, the deuterium labelled compound **8a-d₅** was detected with acceptable peak intensity. But disappointingly, non-deuterium labelled compound **8a** was also detected in both case (entries 3, 5). It indicates that thia-Michael addition reaction was promoted under ionization conditions. This undesired reaction during ionization violated the ionization rules for quantitative monitoring, so those conditions were not applicable for reaction monitoring.

4-3. Substrate scope for good detection

The low peak intensity of internal standard **8a-d**₅ was probably due to an ion suppression effect caused by reaction components such as starting material **7a** or catalysts. An ionization tendency on DART-MS depends on desorption easiness and proton affinity of a molecule. In other word, a compound with lower boiling point and higher basicity is ionized better. In order to control the ionization properties of a reaction mixture, several types of the substrates were examined.

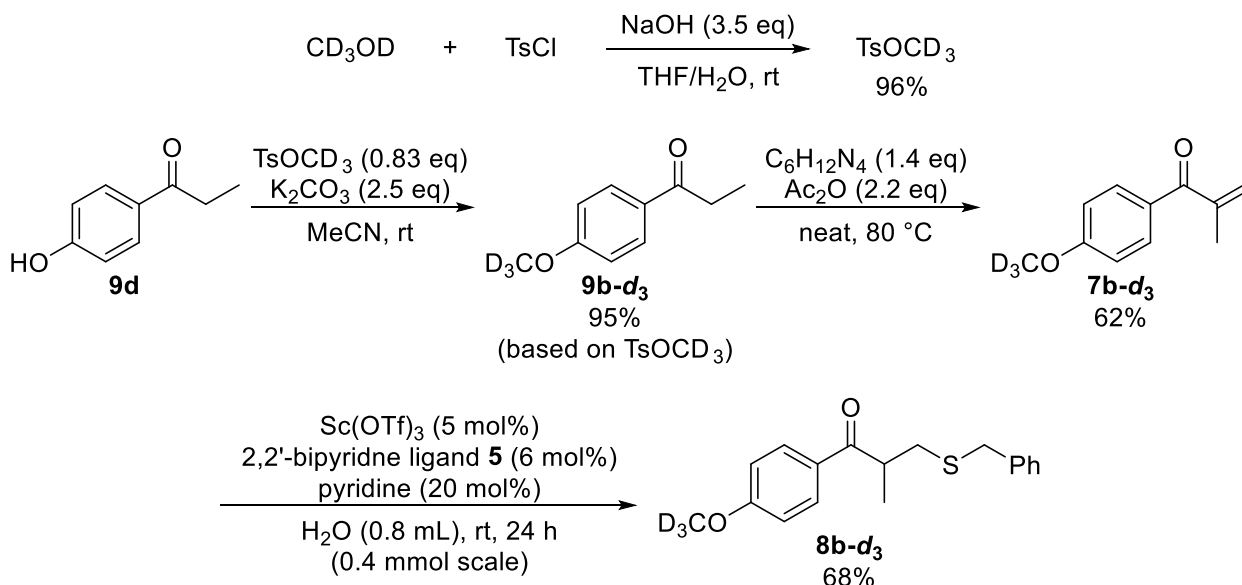
Scheme 4-6. Detection check with several substrates



Entry	Substrate (Ar)	DART condition	Detection of 8a-d	Product
1	7a (Ph)	Positive, He, 200 °C	No	8a
3	7b (4-(OMe)C ₆ H ₄)	Positive, He, 200 °C	Good	8b
4	7c (4-ClC ₆ H ₄)	Positive, He, 200 °C	Good	8c
5	7d (4-(OH)C ₆ H ₄)	Negative, He, 200 °C	Good	8d

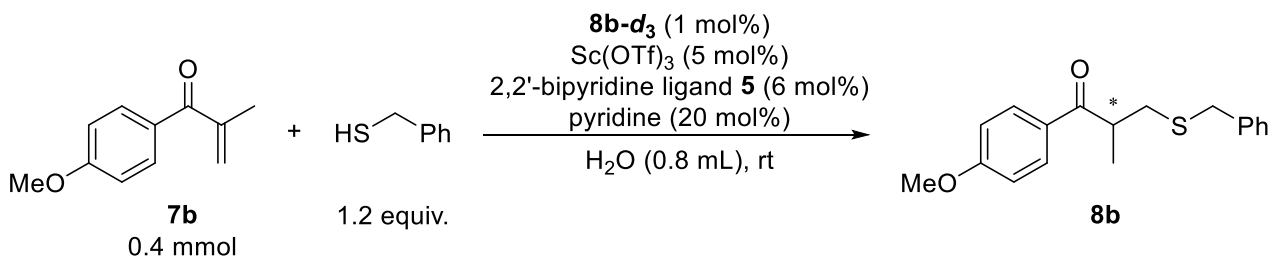
The reactions were conducted with substrates and the mixture was analyzed at early stage of the reaction under indicated conditions of DART-MS (Scheme 4-6). Applicability of substrates were judged from detections of each desired products **8a-d** at early reaction stages (within 10 minutes). As a result, products **8b** and **8c** were detected from corresponding reaction mixtures containing substrates **7b** and **7c** (Entries 2, 3). Acidic functional groups are often detected as its anion form under negative mode DART-MS. 4-Hydroxy substituted substrate **7d** was successfully applied to give the peak of desired product **8d** under negative mode at early stage of the reaction (entry 5). Among these 3 success, 4-methoxy substituted substrate **7b** was selected from viewpoint of synthetic availability. For the monitoring study, an internal standard **8b-d**₃ was synthesized by following procedure (Scheme 4-7).

Scheme 4-7. Preparation of deuterium labelled internal standard 8b-d₃



Methanol-**d**₄ was tosylated under basic conditions and obtained tosylmethane-**d**₃ was used as the reagent to introduce CD₃ group to 4-hydroxypropiophenone **9d**. After methylation reaction under basic conditions, **9b-d**₃ was obtained in high yield. α,β-Unsaturated enone **7b-d**₃ prepared by a methylenation reaction from **9b-d**₃ was submitted to 1,4-addition/protonation reactions to afford the desired deuterated internal standard **8b-d**₃.

Scheme 4-8. Monitoring trial with methoxy-substituted compounds



The reaction monitoring was then conducted with a newly prepared internal standard **8b-d**₃ by manual sampling. Both the peaks of internal standard **8b-d**₃ and reaction product **8b** were observed successfully with high S/N. Obtained SICs of *m/z* = 304 – 304.5 (Figure 4-2) and 301 – 301.5 (Figure 4-3) are shown in next page. The reaction profile of product **8b** was determined from the integrations of the peaks (Figure 4-1). A rapid increment of non-deuterated compound **8b** was suggested from the ratio of isotopes. As the reaction was considered to be too fast to determine its initial velocity, monitoring experiments were conducted for 3 times in larger amount of solvent to find more suitable reaction conditions (Scheme 4-9).

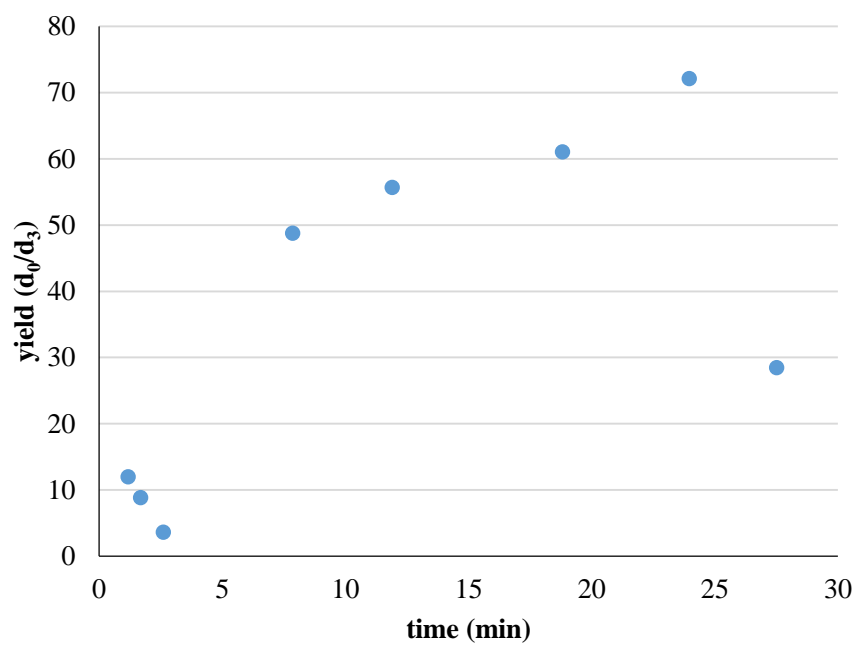


Figure 4-1. Reaction profile of Scheme 4-8

測定データ名: 20130622MASUD A922
 作成条件: マスクロ(MS[1] 質量電荷比: 304.00000..304.50000, 強度: 高さ)

実験日時: 2013/06/22 20:40:07
 イオン化モード: ESI+

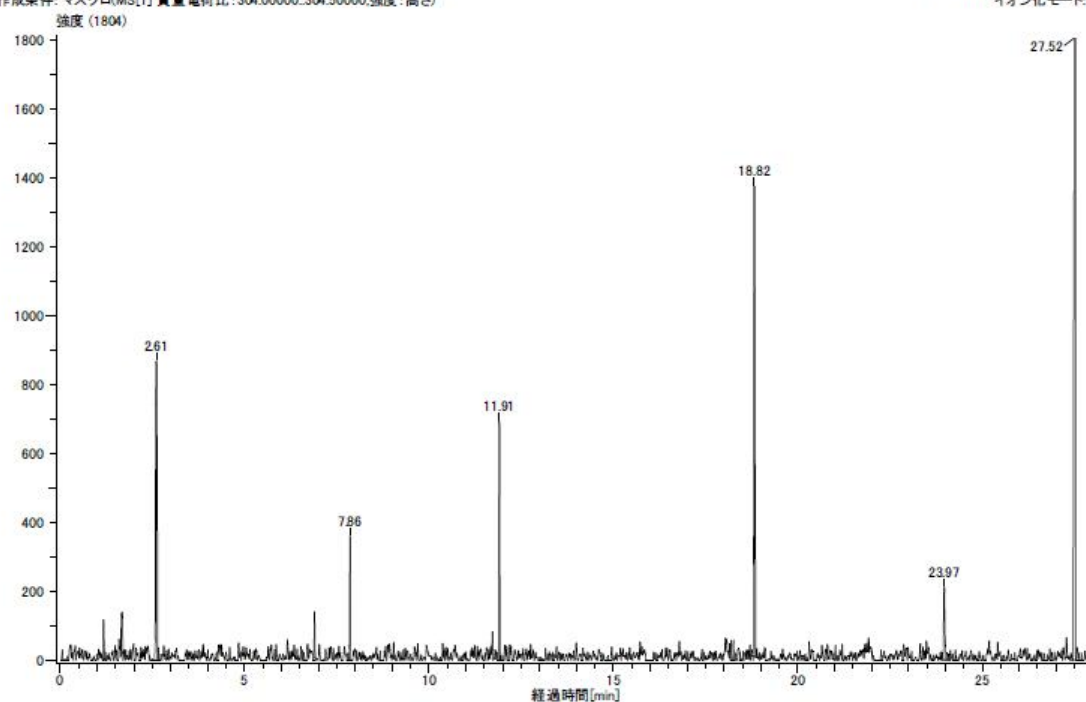


Figure 4-2. SIC of 8b-d₃ (m/z = 304.0 – 304.5)

測定データ名: 20130622MASUD A922
 作成条件: マスクロ(MS[1] 質量電荷比: 301.00000..301.50000, 強度: 高さ)
 x10³ 強度 (185219)

実験日時: 2013/06/22 20:40:07
 イオン化モード: ESI+

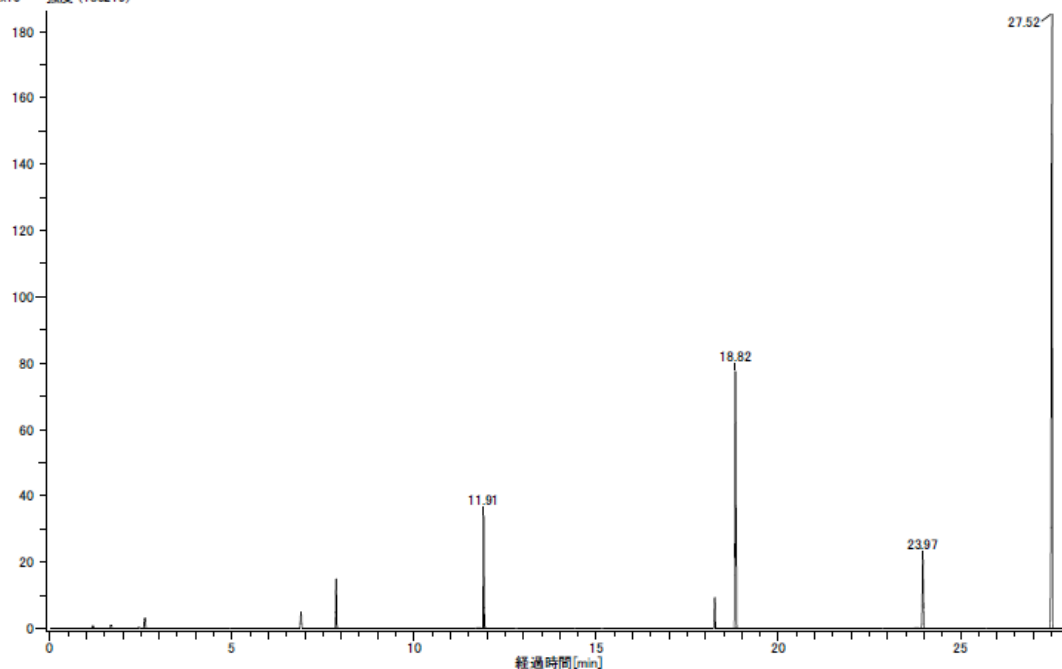
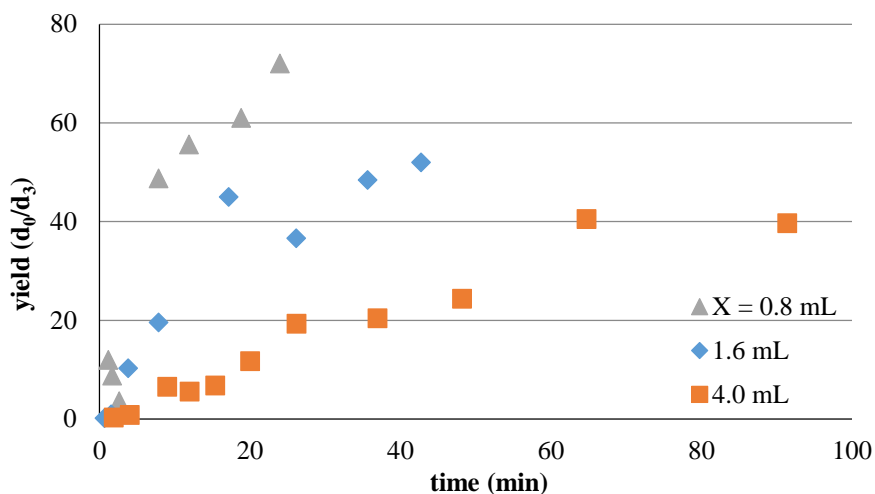
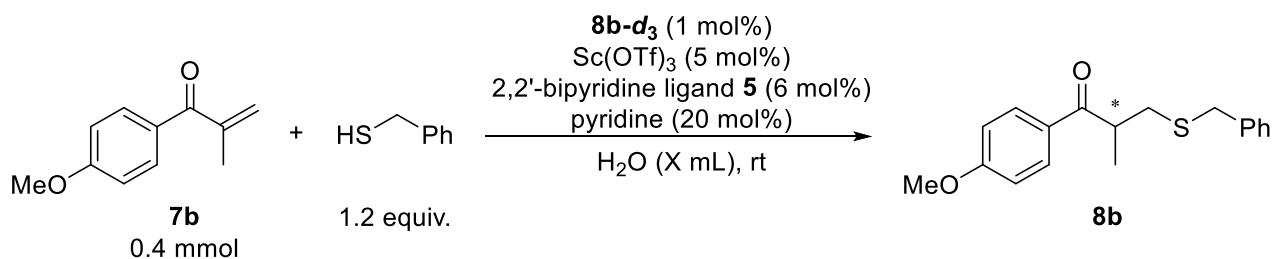


Figure 4-3. SIC of 8b (m/z = 301.0 – 301.5)

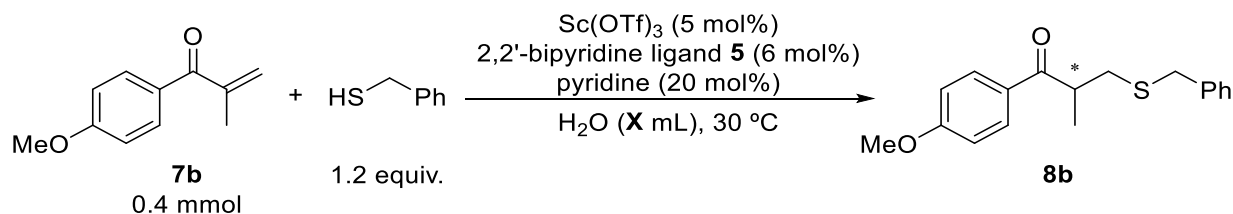
Scheme 4-9. Reaction monitoring trials under diluted conditions



A moderate reaction rate has some technical advantages. A number of data point per the reaction progress is increased, and local deviation range of material is minimized. In the presence of 1.6 mL of water (twice amount to the original conditions), the reaction proceeded slowly and the yield of **8b** reached 50 (d_0/d_3) at around 40 minutes. Under 5 times diluted conditions to the original, the reaction was more sluggish and a good linearity was observed on its profile. In order to conduct the reaction under diluted conditions, the details of reaction outcomes were examined extensively.

4-4. Condition optimizations for reproducibility

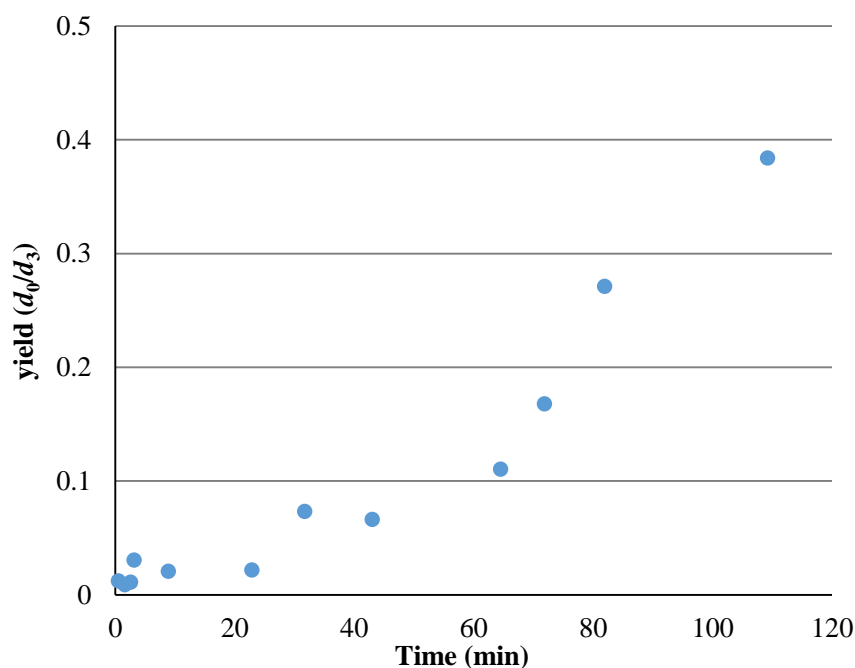
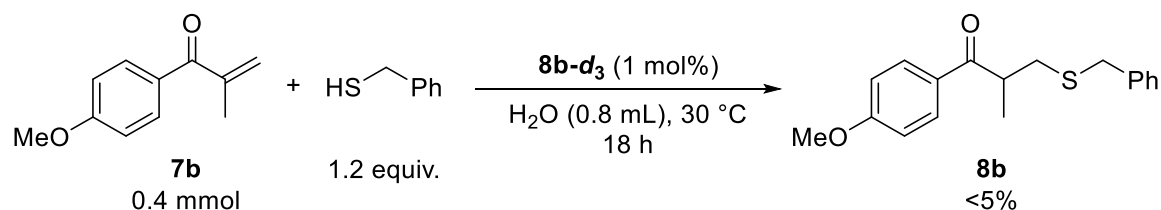
Scheme 4-10. Condition optimizations under diluted conditions



Entry	X (mL)	Yield (%)	ee (%)
1	0.8	85	54
2	1.6	93	45
3	4.0	89	21
4	4.0	80	28
5	4.0	82	28

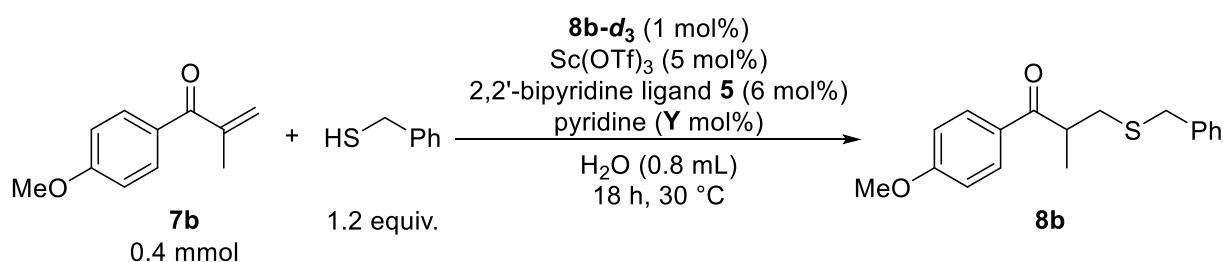
It is reported that with the substrate **7b** the desired product **8b** was obtained in 85% yield with 54% ee (entry 1).¹¹³ At lower concentration the product **8b** was obtained in high yield, though low selectivity was observed (entries 2 – 5). In the presence of 1.6 mL of water, the product **8b** was obtained in 93% yield with 45% enantioselectivity (entry 2). When the reaction was conducted in 4.0 mL of water, enantioselectivity was dropped to 21% (entry 3). This low ee was unfortunately reproducible in two replications (entries 4, 5). It was suggested that a background reaction were competitive to decrease the selectivity.

Scheme 4-11. Reaction monitoring in the absence of catalyst and base



In order to confirm the background pathway, the reaction was conducted in the absence of catalyst and base. However, the reaction did not proceed in the absence of scandium triflate, ligand **5** and base (Scheme 4-11). The reaction was monitored for 2 hours by DART-MS using **8b-d₃** as an internal standard, and less than 0.5 (d_0/d_3) of the product **8b** formation was observed. After 18 hours the reaction was quenched and its crude mixture was analyzed by ¹H-NMR with tetrachloroethane as an internal standard to detect 2.4% of the product (assumed to be a mixture of **8b** and **8b-d₃**). The low enantioselectivity observed at low concentration in Scheme 4-10 was therefore not due to the background reaction. The reaction was considered to be sensitive toward pH value of the reaction mixture because a stereo-determining step of this reaction is a protonation of an enolate intermediate.

Scheme 4-12. Reaction profiles with various base loadings



Entry	Y (mol%)	Yield (%)	ee (%)	Initial rate
1	5	81	68	2.20
2	5	-	-	1.74
3	5	-	-	1.51
4	10	89	65	1.66
5	20	-	-	1.95
6	20	-	-	1.36
7	20	-	-	1.20
8	20	-	-	1.22
9	30	-	-	0.53
10	40	85	65	0.13
11	40	-	-	0.67

The amount of solvent was fixed to 0.8 mL to avoid the decrease of enantioselectivity, and then the base loading was changed to confirm its influence to a reaction rate and enantioselectivity of the product **8b** (Scheme 4-12). In the presence of 5 mol% of pyridine, the reaction started rapidly to show linear initial reaction rate (Entries 1-3, Figure 4-4 as a representative; region from 0 to 20 min was used as its initial rate). On the other hand, 40 mol% of pyridine made the reaction rather sluggish and nearly 1 h of induction period was observed (Entries 10 and 11, Figure 4-5 as a representative; linear region after induction period was used as its initial rate). Interestingly, with different base loading the reaction rate was significantly changed without loss of enantioselectivity. The reactions were further monitored at 20 and 30 mol% base loading. In the presence of 20 mol% pyridine the monitoring was conducted 4 times to check the reproducibility of the reaction profile (Figure 4-6). Unfortunately, the reproducibility of the reaction profile was not excellent. Monitoring results of 11 initial reaction rates with different base loadings were summarized in Figure 4-7.

Additionally, it was found that the monitoring accuracy suddenly dropped around 50 (*d*₀/*d*₃) of the reaction progress in most cases. The reaction product **8b** is a solid while substrate **7b** and benzyl mercaptan are liquids. The solidification of product **8b** probably interfered the fast matter exchange between phases to keep an isotopic ratio homogeneous.

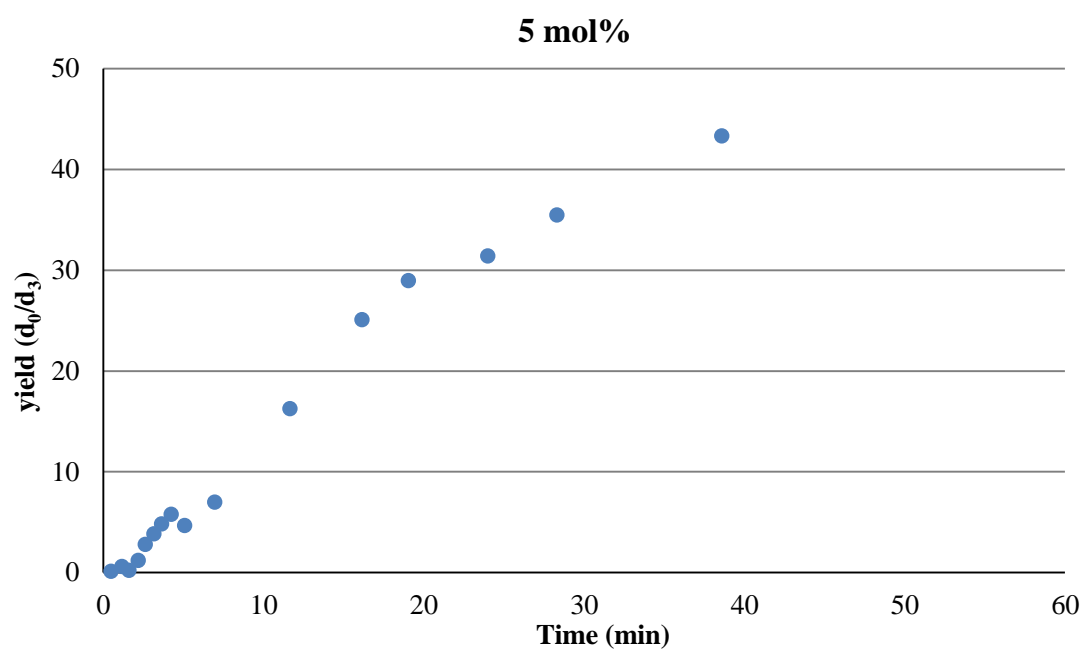


Figure 4-4. Entry 1, pyridine 5 mol%

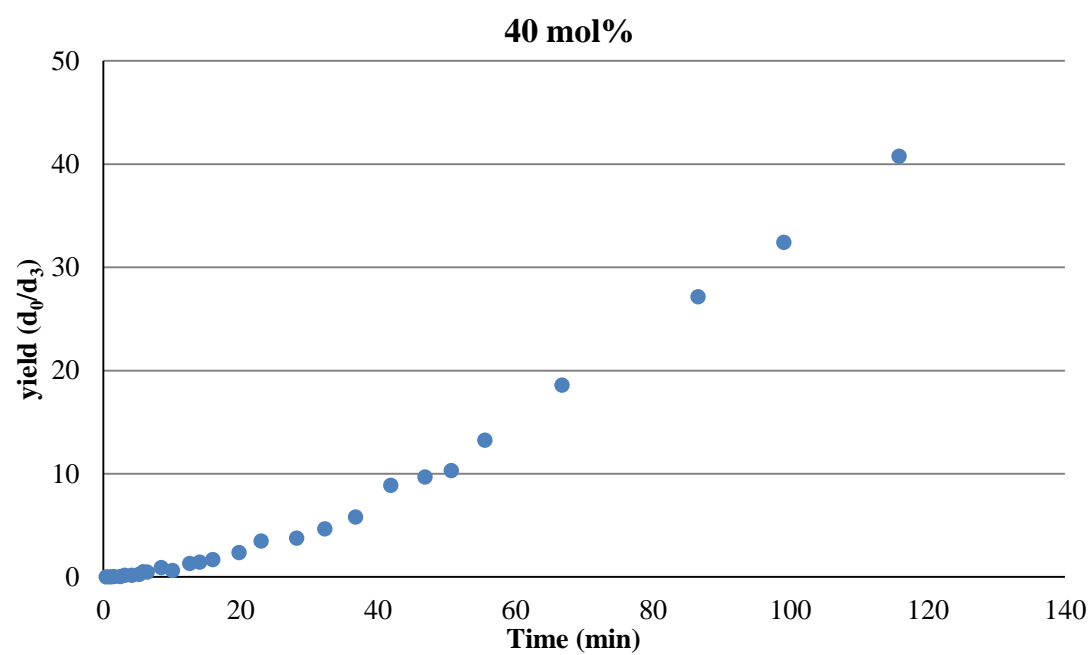


Figure 4-5. Entry 10, pyridine 40 mol%

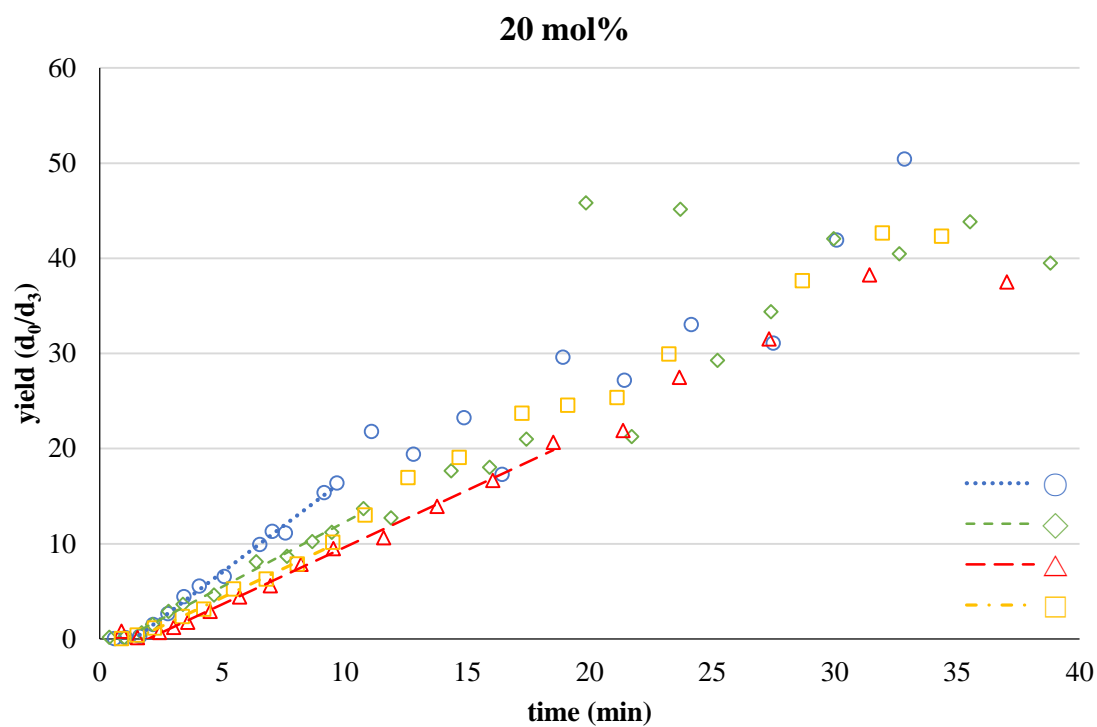


Figure 4-6. Reaction profiles of entries 5 – 8 (20 mol%)

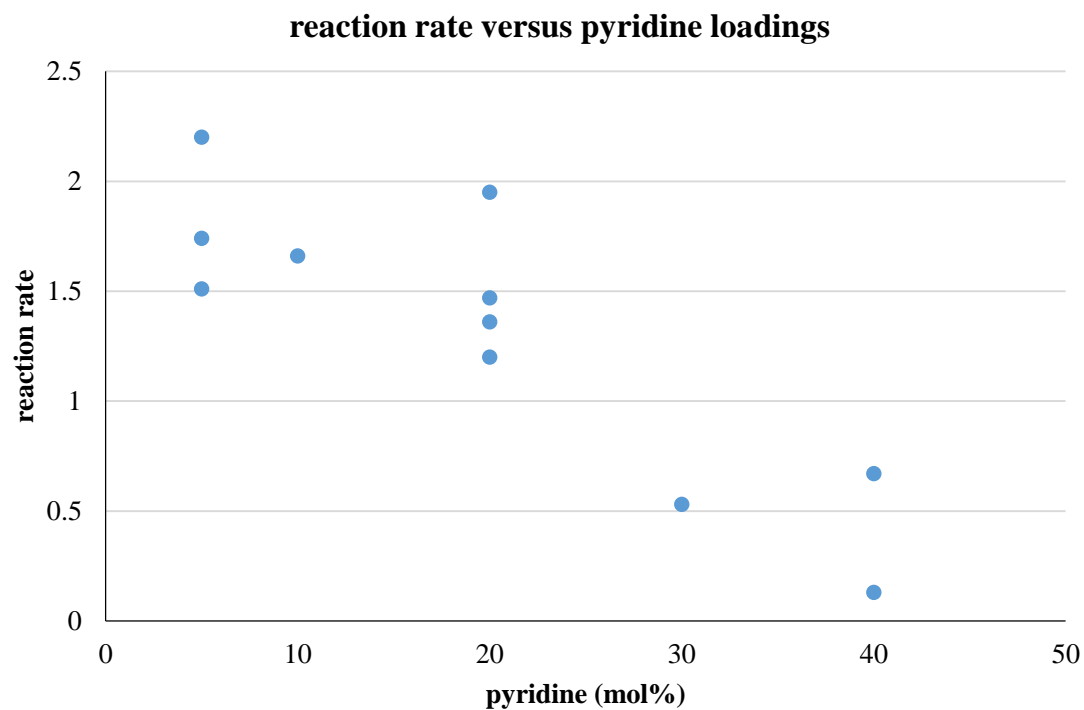
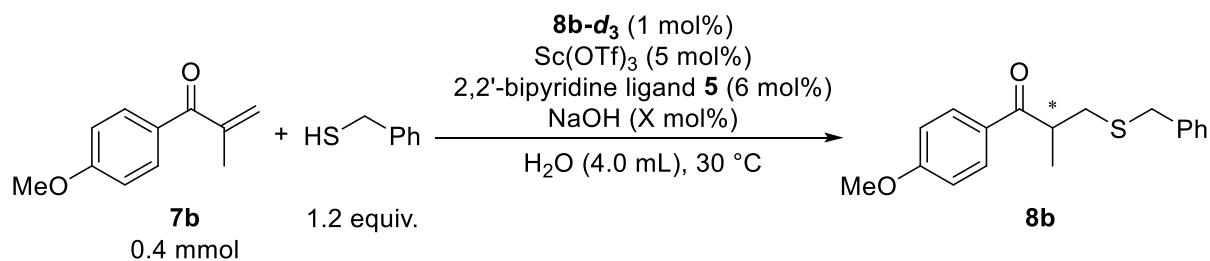
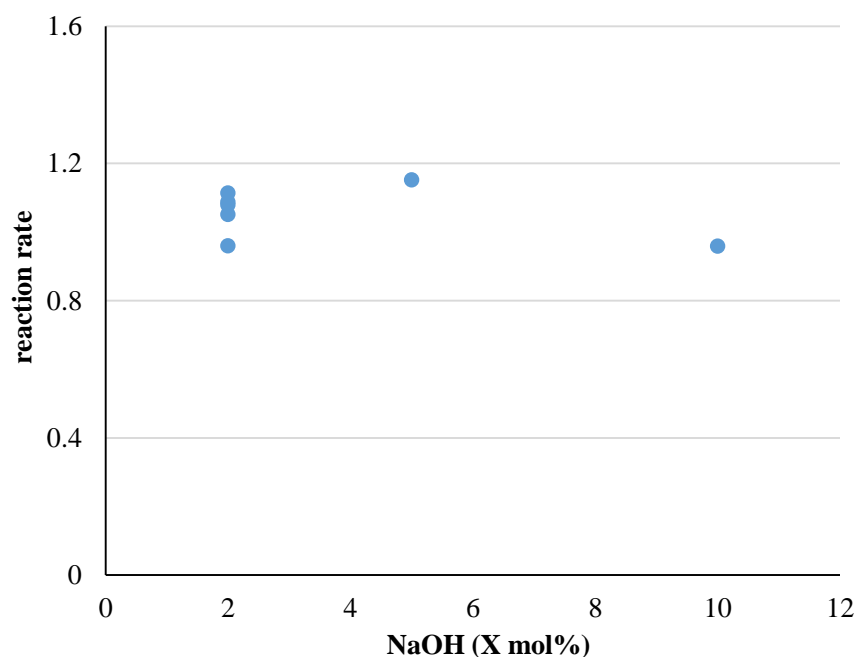


Figure 4-7. Reaction rate versus pyridine loading (Scheme 4-12)

Scheme 4-13. Enantioselective thia-Michael reactions with sodium hydroxide as a base



Entry	X (mol%)	Initial rate	Yield (%)	ee (%)
1	2	1.09	78	54
2	2	1.05	-	-
3	2	1.08	-	-
4	2	0.96	-	-
5	2	1.11	-	-
6	5	1.15	96	59
7	10	0.96	97	57
8	15	~12	Quant.	Rac.



In the course of extensive optimizations of conditions, it was found possible to catalyze the reaction well under diluted conditions by using sodium hydroxide as a base instead of pyridine (Scheme 4-13). The 0.4 mmol scale reaction was conducted with 4.0 mL water in the presence of 5 mol% of Sc(OTf)₃, 6 mol% of ligand **5** and 2 mol% of NaOH to furnish 78% yield of the product with 54% enantioselectivity (entry 1). An initial reaction rate was

rather sluggish than that of pyridine, but showed better reproducibility for 5 times trials (entries 1-5). Interestingly, reaction rate was constant while the loading of NaOH was changed from 2 mol% to 10 mol% (entries 6 and 7). With >15 mol% of NaOH, a reaction rate increased dramatically and enantioselectivity of the product was completely lost (entry 8). A test paper indicated that the pH value of reaction mixture after monitoring was larger than 7. It is assumed that Lewis acidic scandium catalyst was completely neutralized by NaOH and slight excess hydroxide worked as a base catalyst to promote 1,4-addition reaction of thiolate anion.

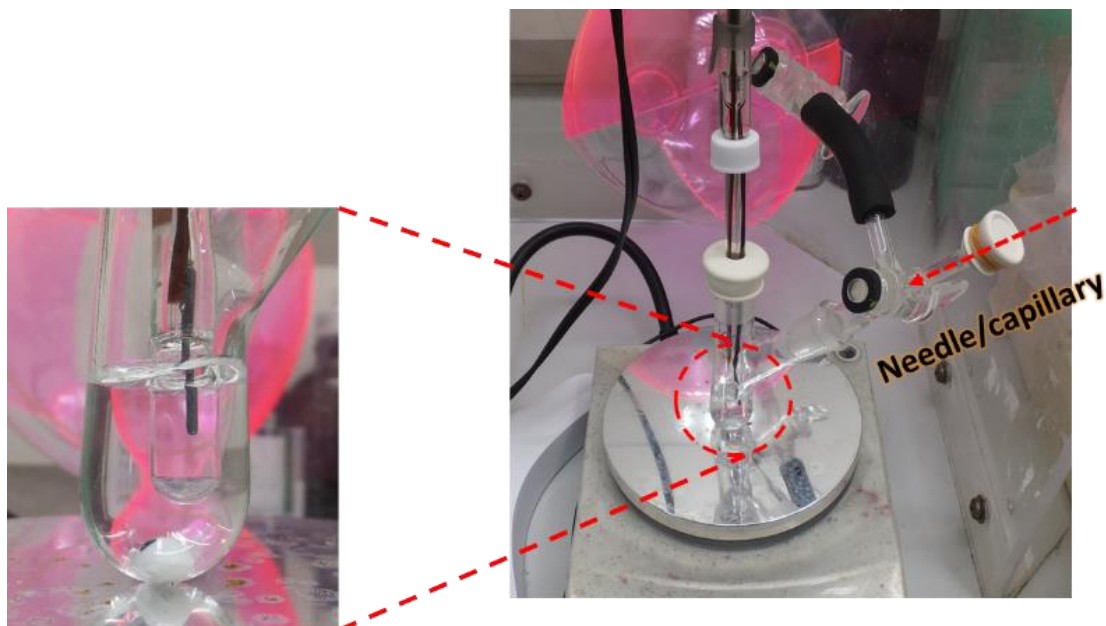
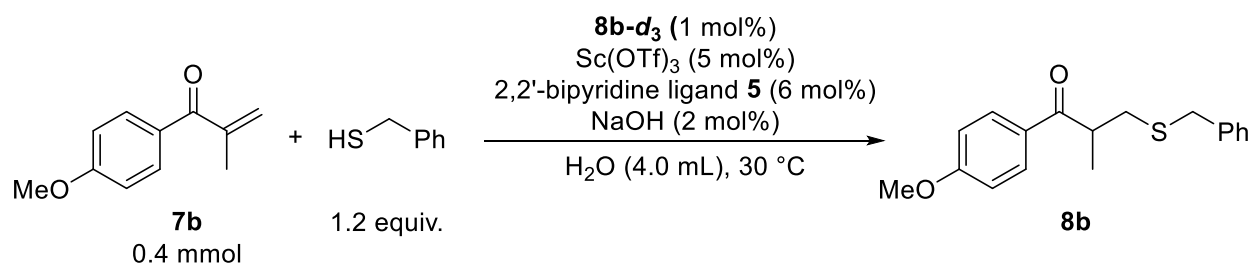
4-5. Reaction profiles and pH measurement

The thia-Michael reaction proceeds via addition step of thiol/thiolate to enone and following protonation step of enolate intermediate. Concentration of proton (pH of solution, in other word) can affect these two factors; deprotonation of thiol, protonation of product. The effect of pH value to the reaction rate was investigated by monitoring the reaction profile and pH profile simultaneously (Scheme 4-14). Horiba ToupH electrode was used for the real-time measurement of pH value. To avoid pH change by CO₂, the reaction was conducted under argon atmosphere. Aliquot sample for reaction monitoring by DART-MS was taken by glass capillary, which was led into flask by piercing septa with needle. See figure below the scheme for the details of the reaction set-up.

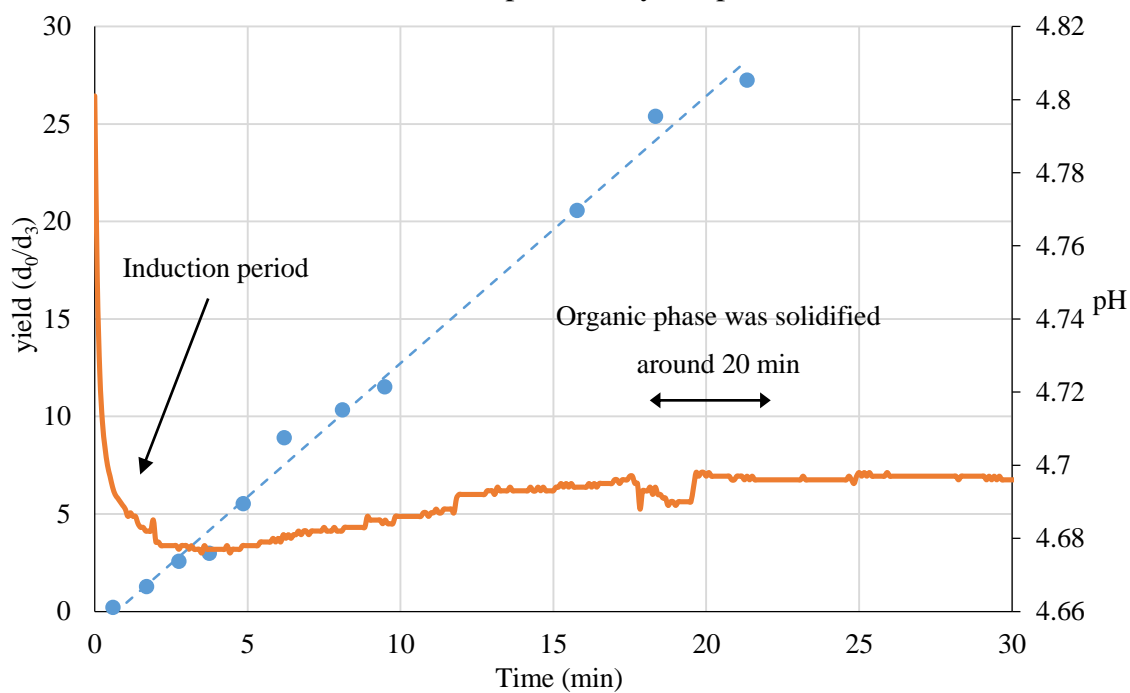
Monitoring results of reaction progress and pH value are shown in the bottom graph. On the very early stage of the reaction, a small induction period (less than 1 min) was observed. The similar induction periods have been observed in all the previous reaction monitorings. This induction period is in good agreement with the pH shift from 5 to 4.7. The pH change is probably induced by the change of catalyst structure, which is associated with the change of reactivities.

Additionally, from 17 to 20 min a small disturbment of pH measurement was observed. Formation of a solid material observed at this period was presumably the reason of a disturbment.

Scheme 4-14. Simultaneous monitoring of reaction and pH profiles



Reaction profile of yield/pH



4-6. Conclusion

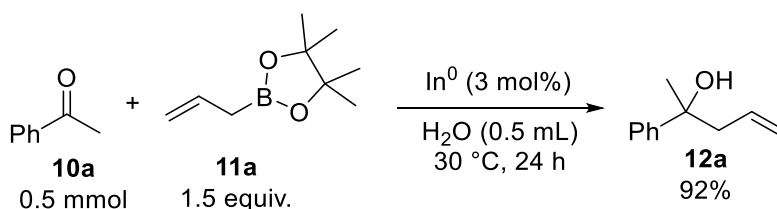
In chapter 4, the conditions of direct monitoring of heterogeneous reactions of organic materials in water were established. A slight modification of substrate structure was crucial to detect the desired peaks of an analyte and an internal standard with sufficient intensities. By using methoxy-substituted internal standard **8b-*d*₃**, a reaction profile was obtained with low deviation of data. The monitoring study revealed a negative dependency of the reaction rate to a pyridine loading and an independent manner of that to a loading of NaOH. A relationship between the reaction rate and the pH of the mixture was also pointed out.

5. Monitoring study of liquid-liquid-solid tri-phasic heterogeneous reactions: Indium(0) catalyzed allylation reactions in water

5-1. Introduction

Organic reactions promoted by solid catalysts have great attention nowadays for their robustness, reusability, and easy handlings. There are a number of examples of organic reactions in/on water with solid catalysts such as zeolites,¹²⁰ silica,¹²¹ clay, or metal/organocatalyst on solid supports. Organic materials are immiscible with water to create a biphasic system, and solid catalysts do not dissolve in both phases. So the reaction proceeds under a tri-phasic heterogeneous system: Organic phase, aqueous phase, and solid phase. Mechanistic analysis toward such a complicated system is highly problematic, especially a quantitative approach toward a water-organic-solid heterogeneous system has not been established well.

Scheme 5-1. Catalytic use of indium(0) for carbon-carbon bond transformations in water



In this section, an indium-catalyzed allylation reaction in water (Scheme 5-1) was selected as an example of tri-phasic heterogeneous organic reactions.¹²² Allylation reactions of simple ketones with allylboronates are promoted by indium(0) metal as a catalyst. In the representative example, acetophenone **10a** is allylated with pinacol allylboronate **11a** to furnish the desired homoallyl alcohol **12a** in high yield. It was reported that indium metal was aggregated during the reaction, but that it remained as a metal form. ICP-AES analysis after the reaction excluded the formation of soluble indium species. It is considered that the reaction is proceeding on the surface of indium metal, or isolated indium particles catalyze the reaction and go back to a bulk state (Figure 5-1).

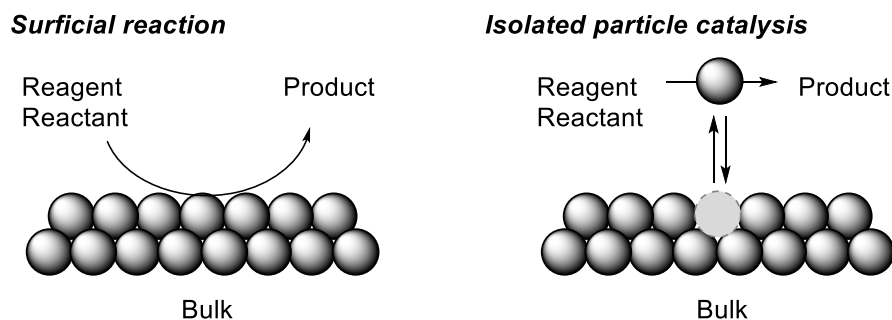
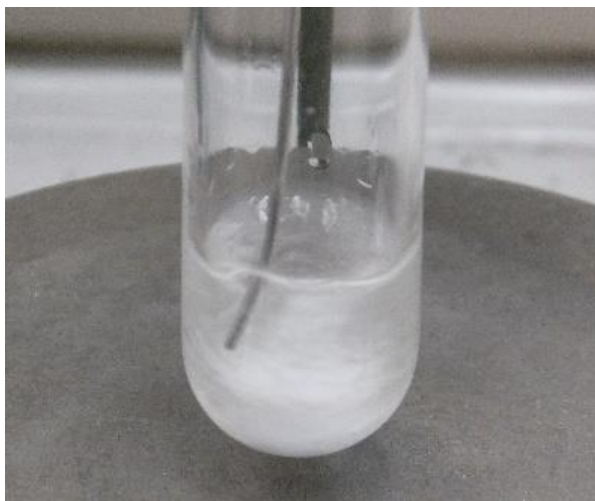
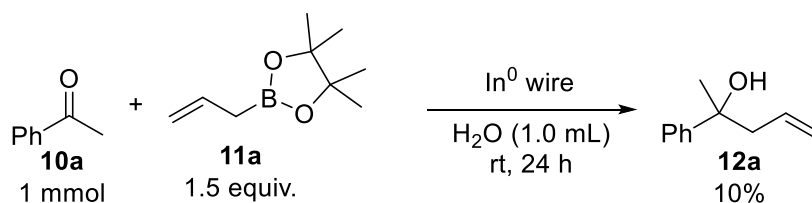


Figure 5-1. Surficial catalysis and isolated particle catalysis

Some control experiments reinforced surficial reaction mechanism. The reaction was conducted with indium metal wire by avoiding physical contact to a stirring bar (Scheme 5-2). Yield of the allylated product was low, but the reaction was surely promoted.

Scheme 5-2. Indium “wire” catalyzed reaction.



The reaction without a stirring bar promoted by vial shaking indicated that there were no aggregation without scratching force on indium metal (Scheme 5-3, Figure 5-2 and Figure 5-3). Indium powder purchased from Sigma-Aldrich® is ~60 mesh spherical particle (Figure 5-2, left) and its shape and size did not change during the reaction (Figure 5-2, right). Particle crushing and aggregation was observed in the presence of stirring bar (Teflon). Indium is a quite soft metal.

Scheme 5-3. Allylation reaction without stirring bar

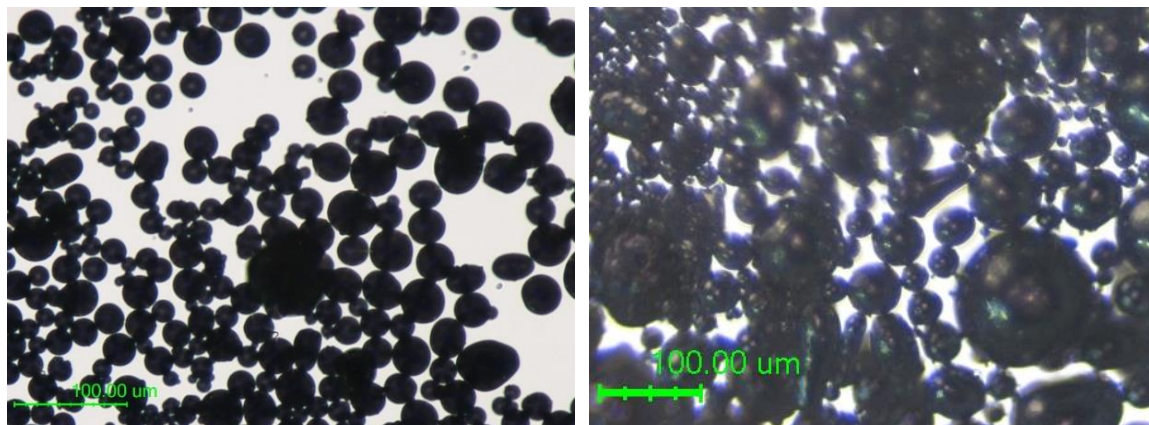
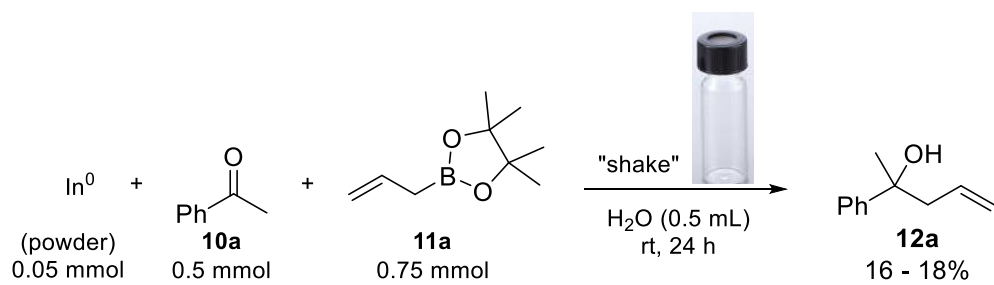


Figure 5-2. Indium powder. Before the reaction (left) and after the reaction (right)

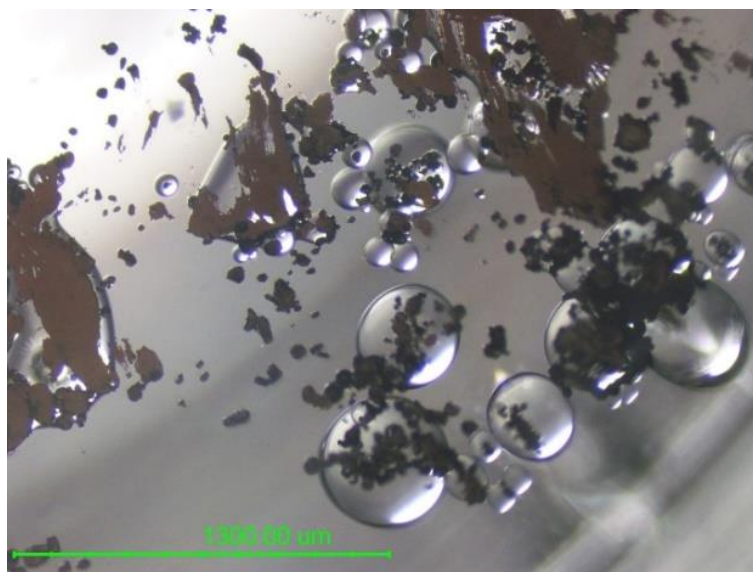
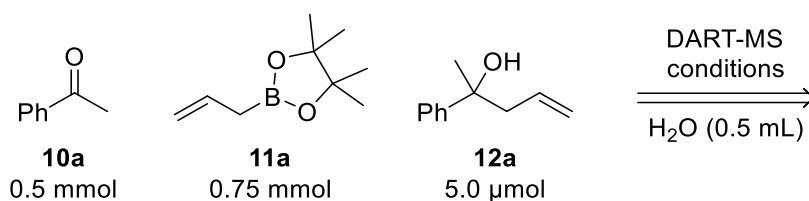


Figure 5-3. With stirring bar

5-2. Initial trials

In order to confirm that the monitoring strategy by using an isotope-labelled internal standard is applicably or not, the detection trial was conducted with a mixture of acetophenone, allylboronate and a trace amount of a reaction product in water. Firstly the detection of the reaction product **12a** in the mixture was examined. The mixture of starting material **10a**, allylboronate **11a** and a small amount of **12a** was placed in the reaction vessel on an auto-sampler and was analyzed by DART-MS with several detection conditions (Scheme 5-4).

Scheme 5-4. Ionization trials on DART-MS

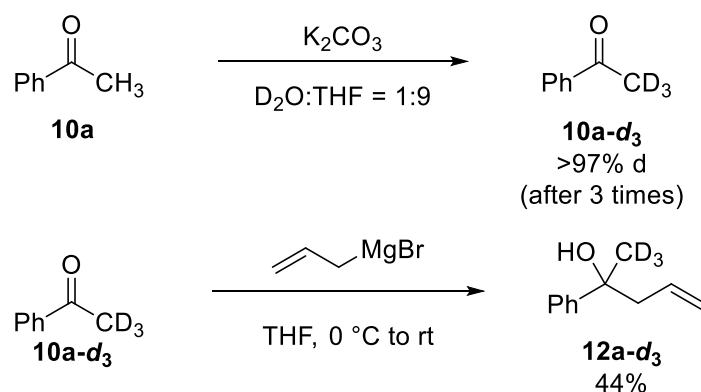


Entry	Gas	Temp. (°C)	Sampling rod	[12a +H] ⁺	[(12a +H ₂ O)+H] ⁺	[(12a -H ₂ O)+H] ⁺
1	N ₂	200	Glass tube ($\phi = 1.8$ mm)	ND	ND	ND
2	N ₂	200	Capillary	ND	ND	ND
3	He	200	Glass tube ($\phi = 1.8$)	ND	ND	Detected
4	He	200	Capillary	ND	Detected	Detected
5	He	400	Glass tube ($\phi = 1.8$)	ND	Detected	Detected

The conditions determined for Mukaiyama aldol reactions in chapter 3 (N₂ as carrier gas, 200 °C) was firstly employed (entries 1, 2). A small aliquot sample was taken by closed end of a melting point tube ($\phi = 1.8$ mm) or a glass capillary; however, no peak was observed of compound **12a**. It was suggested that nitrogen was not suitable carrier gas for the detection of compound **12a**. On the other hand, a corresponding peak of a dehydrated product of **12a** ([(**12a**-H₂O)+H]⁺) was observed by using helium as a carrier gas (entries 3, 4). The detection of simple proton adduct ([**12a**+H]⁺) was not stable under the conditions (entry 3). Detection of dehydrated cation of **12a** is reasonable due to the stability of tertiary cation species. At 400 °C gas temperature both the protonated and dehydrated cation was detected. The dehydrated cation was detected with the higher intensity as an elimination of the hydroxyl group was smoother at the high temperature (entry 5).

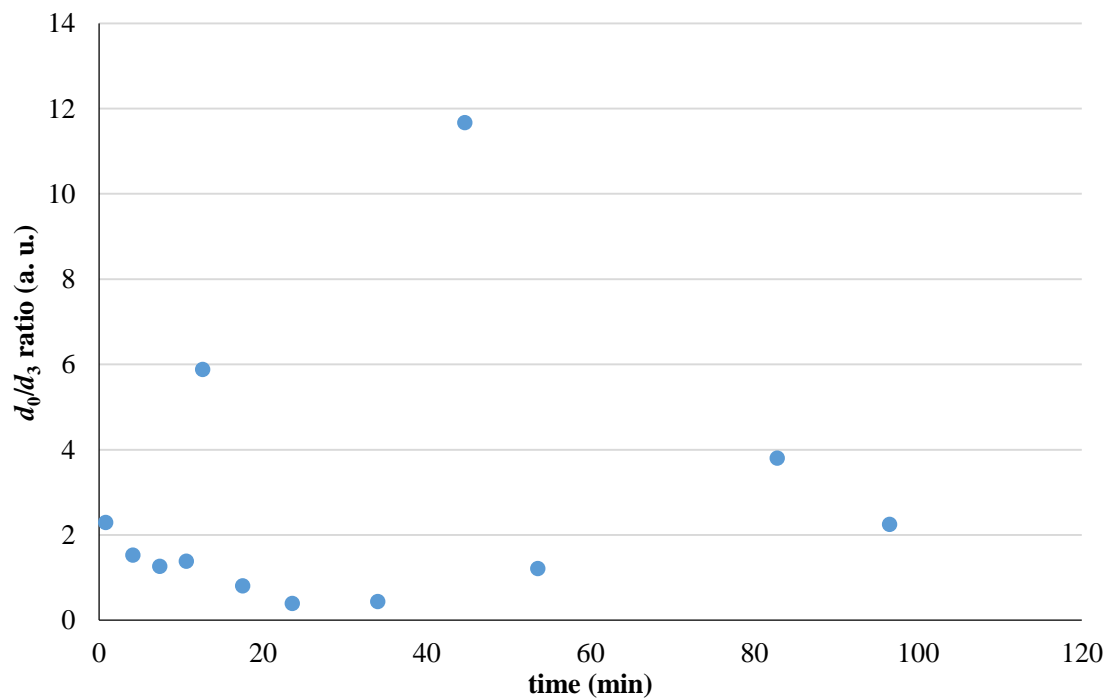
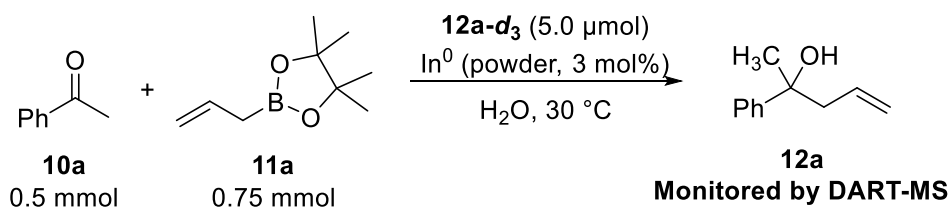
Toward the monitoring study, the deuterium-labelled compound **12a-d₃** was synthesized by simple reactions (Scheme 5-5). A proton on methyl group of acetophenone **10a** was exchanged into deuterium under basic conditions, and deuterated acetophenone **10a-d₃** was then allylated with commercial allylmagnesium bromide solution to furnish the labelled compound **12-d₃** in 44% yield.

Scheme 5-5. Preparation of an internal standard $12a-d_3$



The synthesized internal standard **12a-d₃** was then used for the monitoring study (Scheme 5-6). The internal standard **12a-d₃** was introduced to a flask as a methanol solution and the solvent was removed under N₂ flow. The indium powder, water, acetophenone **10a** and allylboronate **11a** were successively added and then the reaction was monitored by DART-MS (He, 200 °C).

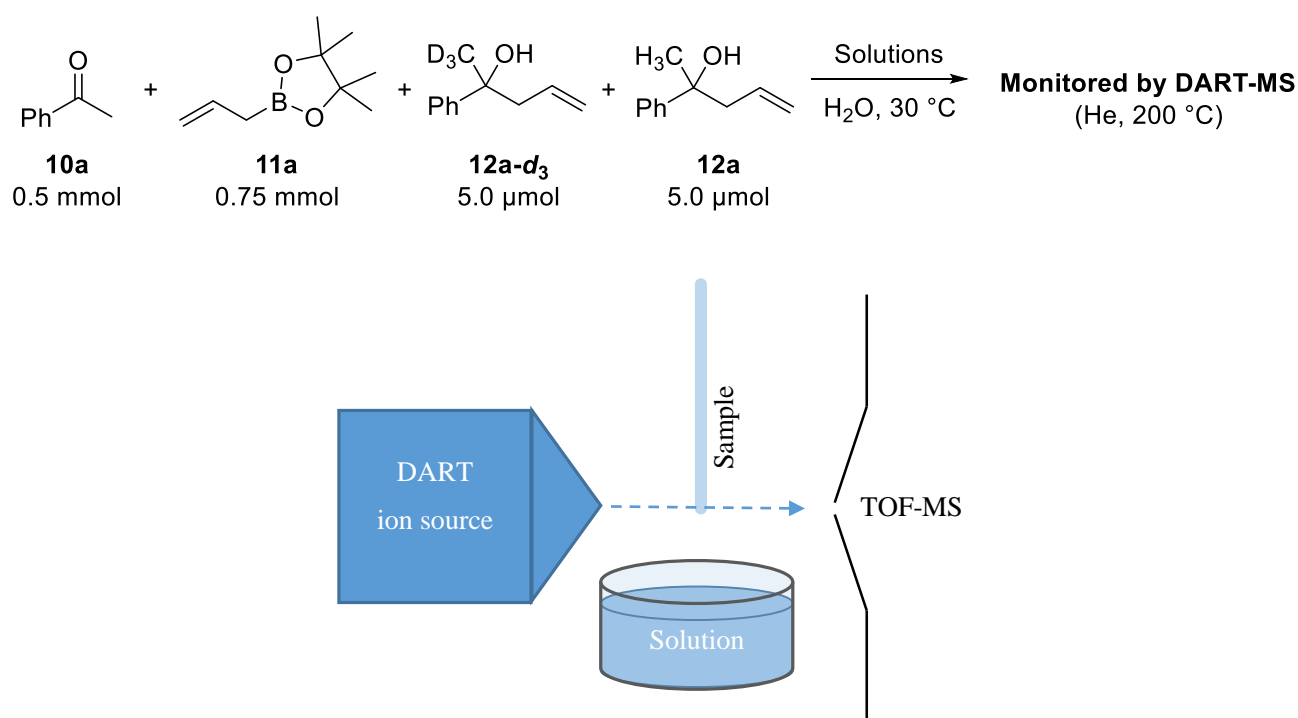
Scheme 5-6. Monitoring trial of the allylation reaction



The dehydrated peaks of the product **12a** and the internal standard **12a-*d*₃** were successfully observed with high peak intensities. However, the isotope ratio of **12a/12a-*d*₃** showed random result. A disturbance by background reaction under ionization conditions was highly doubted, so control experiment was conducted in the absence of indium catalyst.

Acetophenone **10a**, allylboronate **11a**, reaction product **12a** and internal standard **12a-*d*₃** were mixed in pure water at 30 °C and the mixture was ionized on DART-MS to conduct a repetitive analysis (Scheme 5-7: He as carrier gas, 200 °C). In the absence of the indium catalyst, the allylation reaction of **10a** with **11a** do not proceed and ratio of isotopes of product **12a/12a-*d*₃** is kept constant during the measurement. If the background reaction were not to proceed during the ionization, the detected ratio of **12a/12a-*d*₃** would be stable.

Scheme 5-7. The ionization experiment of 12a/12a-*d*₃ in the mixture



Entry	Solutions	Average peak intensity of 12a (<i>m/z</i> = 145)	Average 12a ratio (<i>d</i> ₀ / <i>d</i> ₃)	RSD (%)
1	None	1688	0.363	11.4
2	Pure water	3194	0.374	12.9
3	HCl _{aq.} (0.1 M)	4480	0.393	7.8
4	HCl _{aq.} (1.0 M)	5427	0.466	26.8
5	NH ₃ _{aq.} (1.0 M)	5749	0.471	21.6

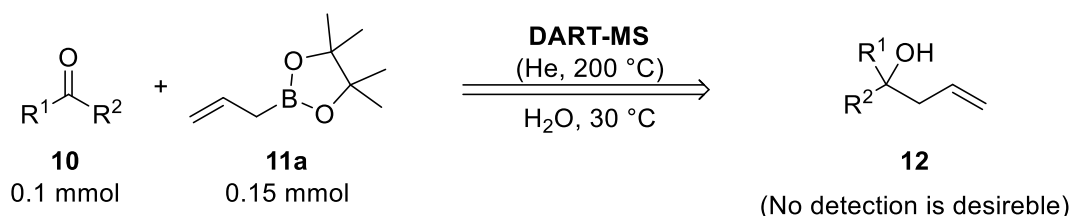
The result, however, showed a randomness indicating that the background reaction proceeded during the ionization (entry 1). The ratio of product **12a/12a-*d*₃** was not stable at all to show RSD = 11.4% within 18 repetitive ionizations by auto-sampler. In order to avoid the background reaction during the ionization, the ionization environment was modified. The ionization tendency of DART-MS is known to be dependent on the moisture around

the ionization region. Water was placed below ionization area and the same ionization experiment of the mixture was conducted (entry 2). As a result, an average ion intensity of desired product **12a** was increased; however, still the isotope ratio of **12a/12a-d₃** was not stable. An aqueous HCl was then examined for its volatility and the protonation ability, to find no stabilization effect (entries 3, 4). Finally an aqueous NH₃ was examined as organic compounds are sometimes detected as an ammonium adduct cation ([M+NH₄]⁺) on DART-MS analysis (entry 5). Unfortunately any expected ammonium adduct of **12a** was not observed, and the isotope ratio of **12a/12a-d₃** was not stable at all.

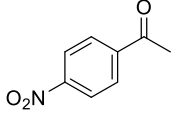
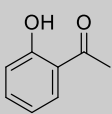
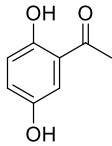
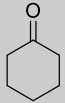
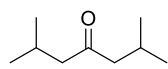
5-3. Reagent scope for detection conditions

From the control experiments in previous section, it is concluded that the combination of acetophenone **10a** and allylboronate **11a** was not suitable for DART-MS monitoring. In order to establish the monitoring conditions for the indium catalyzed allylation reactions, alternative substrates were examined extensively. The original article showed that various aromatic ketones and aliphatic ketones were applicable for the reactions.¹²² The scope was conducted by ionizing a mixture of various ketones and allylboronates in water under standard DART conditions. The detection of **12** is undesirable in the absence of the indium catalyst to avoid the background reaction during ionization under DART-MS conditions. Firstly the scope of ketone was conducted with allylboronate **11a** (Scheme 5-8).

Scheme 5-8. Reagent scope of ketone for the detection conditions



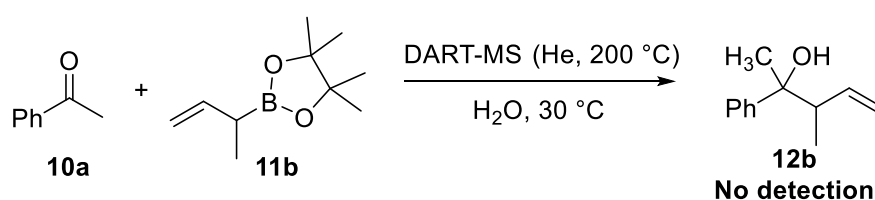
Entry	Ketone	[12+H] ⁺	[12+H ₃ O] ⁺	[12+NH ₄] ⁺	[12-OH] ⁺
1	(10a)	- (ND)	-	-	+ (detected)
2	(10b)	-	-	-	+
3	(10c)	+	+	+	+

4	 (10d)	-	+	-	+
5	 (10e)	+	+	+	+
6	 (10f)	+	+	+	+
7	 (10g)	-	-	+	+
8	 (10h)	+	+	+	-

As a result, in all cases any starting material **10** and allylboronate **11a** mixture gave protonated ($[M + H]^+$), hydrated ($[M + H_3O]^+$), dehydrated cation ($[M - OH]^+$) or ammonium adduct ($[M + NH_4]^+$) peaks of **12**; no ketone was found applicable for reaction monitoring. At this stage, it was concluded that the allylboronate **11a** was reactive enough toward any ketones under DART ionization conditions to proceed the allylation reaction on a gas phase.

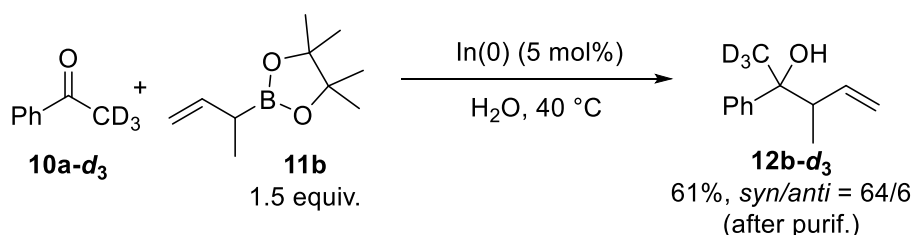
Secondary an allylboronate was examined. As a less reactive boronate than **11a**, α -methylallylboronate **11b** was chosen and ionization test was conducted with acetophenone **10a**.

Scheme 5-9. No background reaction of α -methylallylboronate under MS conditions



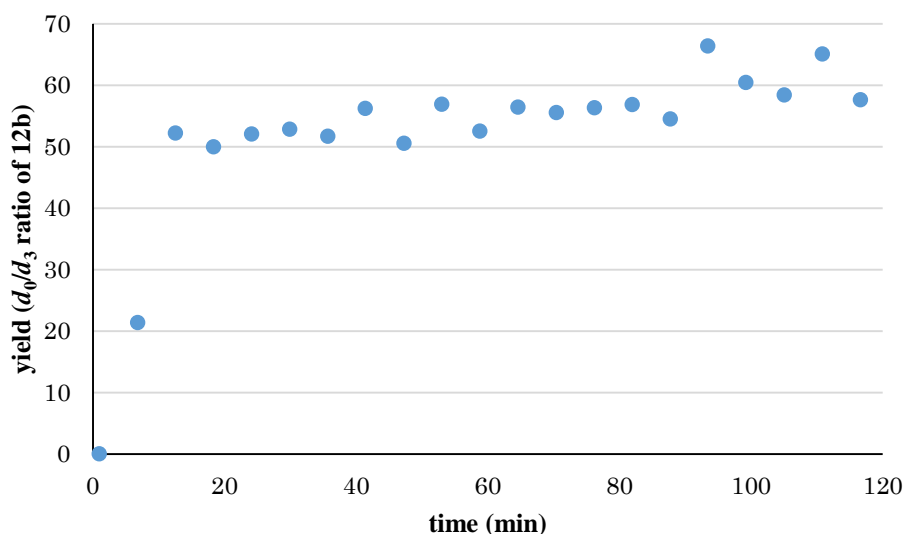
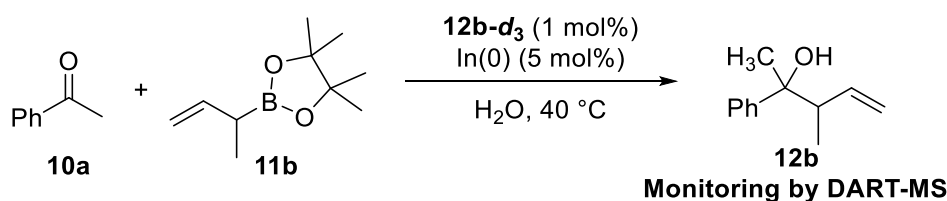
As a result, none of the protonated, hydrated, dehydrated cation or ammonium adduct peak of the product **12b** was observed, which indicated the background reaction of acetophenone **10a** and α -methylallylboronate **11b** did not take place. Internal standard **12b-d₃** was synthesized from labelled acetophenone **10-d₃** following reaction conditions of indium catalyzed allylation reactions (Scheme 5-10).

Scheme 5-10. Synthesis of 12b-d₃



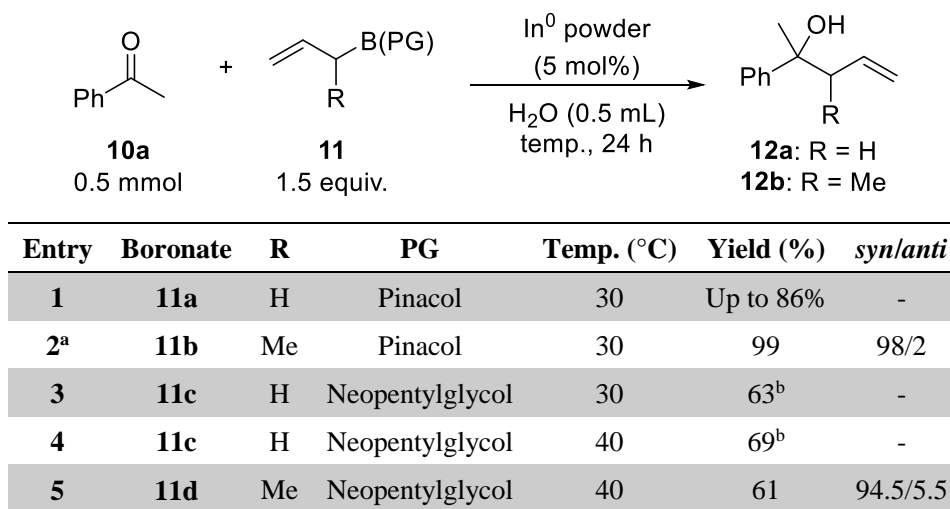
Synthesized internal standard **12b-d₃** was then used for the monitoring study of allylation reaction using α -methylallylboronate **11b** (Scheme 5-11). As the yield was relatively low in the internal standard preparation, reaction was expected to be slow and the monitoring was conducted with 5 minutes interval.

Scheme 5-11. Monitoring trial of allylation reaction using α -methylallylboronate



Interestingly, the resulted reaction profile of product **12b** indicated that the reaction was finished within 20 minutes. After that the ratio of isotopes **12b/12b-d₃** were stable to show 50 to 60% yield of the product. The change of allylboronate structure was promising for the control of the reactivity under ionization conditions. Generally allylboronates with 5-membered ring protecting groups are more reactive than those with 6-membered ones under reaction conditions both in organic solvents and in water.^{123,124} For the indium catalyzed allylation reactions, 6-membered allyl boronates were found applicable. Yield of the desired products **12a/12b** were not satisfactory with neopentylglycol allylboronate **11c** or α -methylallylboronate **11d**, while pinacol allylboronate **11a** and α -methylallylboronate **11b** furnish the products in high yields with excellent selectivity (Scheme 5-12).

Scheme 5-12. Allylation reactions with allylboronates 11a-11d

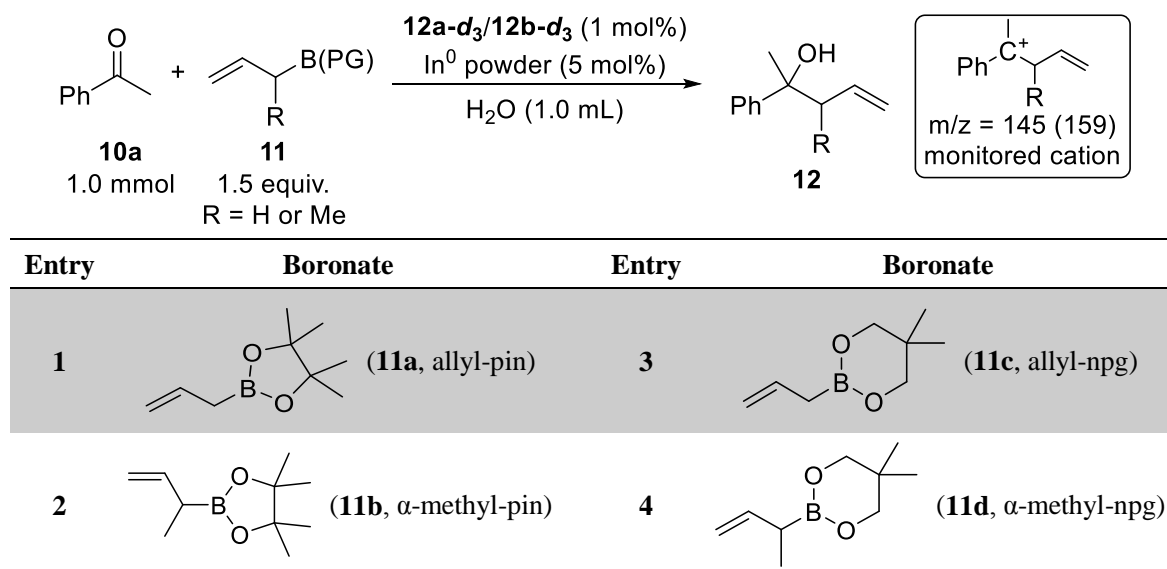


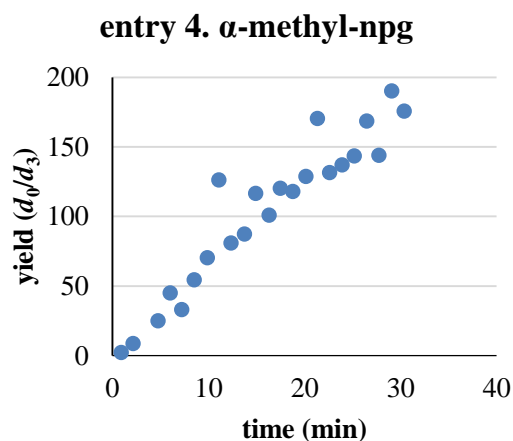
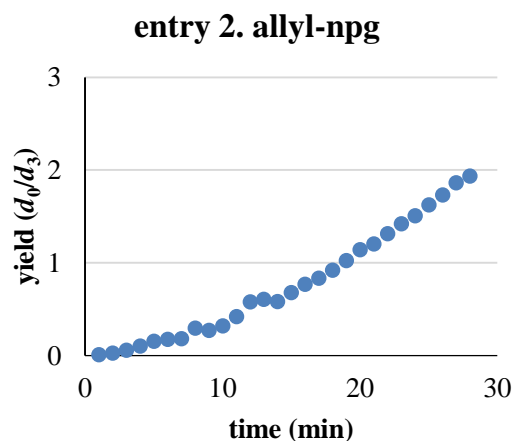
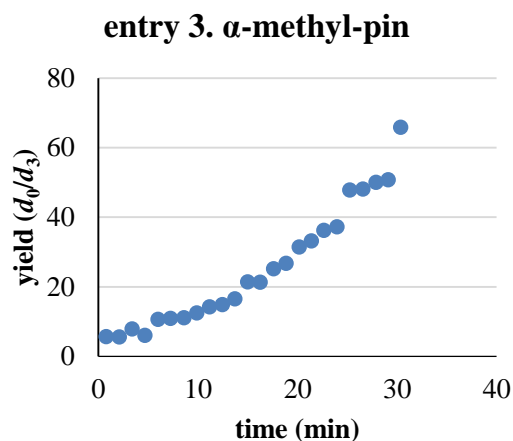
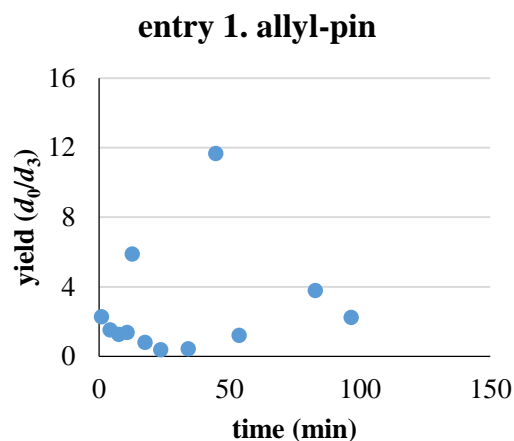
^a Reported results. ^b Determined by crude ¹H-NMR analysis with 4-dimethoxybenzene as an internal standard.

In the presence of 5 mol% indium metal, pinacol allylboronate **11a** gave the desired product up to 86% and α -methylallylboronate **11b** yielded the product quantitatively with 98/2 *syn* selectivity (entries 1, 2). On the other hand, neopentylglycol allylboronate **11c** gave the product only in 63% yield (entry 3). Yield was slightly improved to 69% at 40 °C. The conversion of acetophenone **10a** was not high with neopentylglycol α -methylallylboronate **11d** and the product **12b** was obtained in moderate yield with high selectivity (entry 5).

The same tendency was expected in gas phase, so several other allylboronates including 6-membered protecting groups were examined for their reactivities during ionization under the DART-MS conditions (Scheme 5-13).

Scheme 5-13. The reaction monitoring study with various allylboronates





As expected, the reaction of α -methylallylboronate **11c** was successfully monitored to show a curved reaction profile (entry 3). 6-Membered allylboronate **11b** and α -methylallylboronate **11d** were also applicable. These allylboronates did not react during ionization under gas phase to disturb the isotope ratio of the product **12a/12b**.

5-4. Conclusion

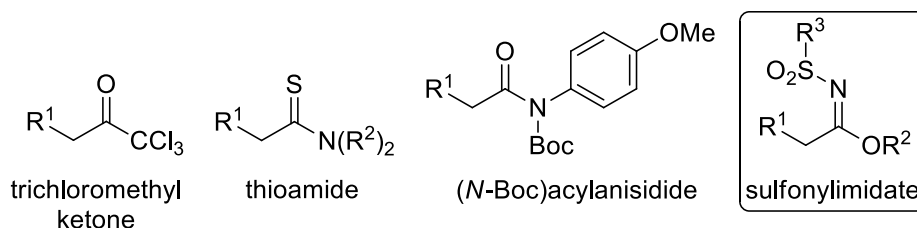
In this chapter the application of the real-time monitoring strategy using an isotope-labelled internal standard was shown for the indium catalyzed allylation reaction of a ketone as the representative examples. The background reaction of pinacol allylboronate **11a** with acetophenone **10a** under gas phase during ionization was problematic, but the problem was solved by using neopentylglycol allylboronate **11c** as an alternative reagent. Further improvement of reaction conditions for the reaction using **11c** was also shown.

6. Organosuperbase-catalyzed 1,4-addition reactions of sulfonylimidates

6-1. Introduction

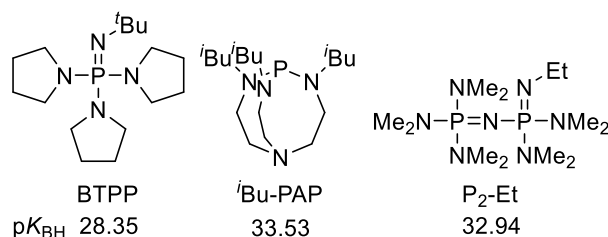
A catalytic carbon-carbon bond forming reaction by proton transfer is a highly efficient and atom-economical method for the construction of organic molecules.^{76,125–132} Deprotonation at α -position of carbonyl group to form enolate species is one of the most important preparation methods of carbon nucleophiles for the building of complex structure. However, especially in the case of simple alkyl esters having no activation group on its α -position, catalytic direct-type reactions are limited due to their less reactive α -protons. To the best of our knowledge, there is only one example of a base-catalyzed direct-type 1,2-addition reaction of simple alkyl esters.¹³³ To address the issue of high pK_a value of α -position on simple esters, some ester equivalents bearing no activation group on their α -positions have been developed such as trichloromethylketones,^{134,135} thioamides,¹³⁶ (*N*-boc)acylanisidides¹³⁷ and sulfonylimidates^{138–144} (Scheme 6-1).

Scheme 6-1. Ester equivalents for catalytic carbon-carbon bond forming reactions



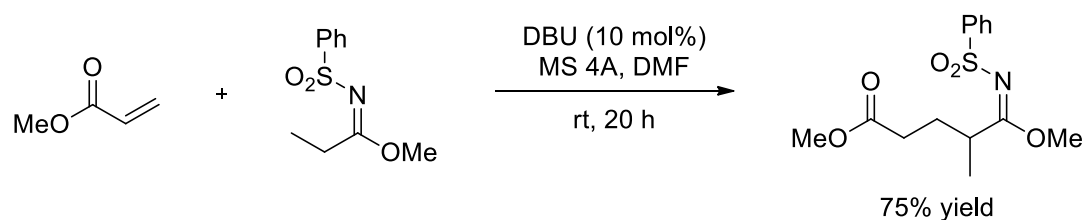
Successful utilizations of sulfonylimidates as nucleophiles have been shown in catalytic carbon-carbon bond-forming reactions, such as Mannich-type reactions with imines in the presence of DBU^{138,139,141} or alkaline earth metal alkoxides or amides as catalysts,^{141,142} allylic substitution reactions of allyl carbonates,¹⁴⁰ allyl acetates¹⁴⁰ or allylic alcohols with palladium catalysts.¹⁴³ Most recently, it was found that phosphorous-containing organosuperbases¹⁴⁵ such as phosphazenes^{146–148} (e.g. *tert*-butylimino-tri(pyrrolidino)phosphorane, BTPP) and proazaphosphatranes^{149–152} (e.g. *N,N,N'*-triisobutyl-2,5,8,9-tetraaza-1-phosphabicyclo[3.3.3]undecane, *i*Bu-PAP) (Scheme 6-2) were surprisingly efficient catalysts for Mannich-type reactions of sulfonylimidates with imines.¹⁴⁴ A unique reaction kinetics of an *i*Bu-PAP catalysis was revealed.

Scheme 6-2. Organosuperbases (pK_{BH} are values in MeCN¹⁵¹)



Michael addition reactions are among the most important and useful methods for carbon–carbon bond formation.^{114–116} Up to now, numerous examples of stereo-selective reactions, including asymmetric variants, have been reported.^{153–159} However, catalytic reactions using simple esters without an activation group or their equivalents are very limited. One example of DBU catalyzed 1,4-addition reaction of sulfonylimidate was reported¹³⁸ in our laboratory (Scheme 6-3). However, its entire reactivity or generality were still unknown.

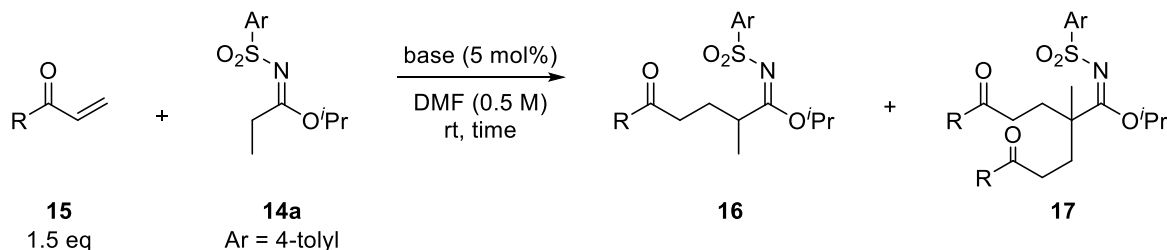
Scheme 6-3. DBU-catalyzed 1,4-addition reaction of sulfonylimidate¹³⁸



In this chapter, organosuperbase-catalyzed Michael addition reactions of sulfonylimidates with α,β -unsaturated esters and thioesters are described in a detail. The reaction showed excellent reactivity and diastereoselectivity in low-polarity solvents such as toluene.

6-2. 1,4-Addition reactions of sulfonylimidates with acrylates and analogues

Scheme 6-4. Investigations of 1,4-addition reactions of sulfonylimidates using acrylates and analogues^a



Entry	Acceptor	Base	Time (h)	Conversion ^b (%)	Isolated yield (%)
1	15a (R = OEt)	DBU	3	11	12 (16a)
2	15a	DBU	24	44	43
3	15a	BTPP	3	full	92
4	15a	P ₂ -Et	1.5	full	75 (16a) + 19 (17)
5	15a	^t Bu-PAP	3	< 30	12
6	15a	^t Bu-PAP	24	< 40	18
7	15b (R = O ^t Bu)	BTPP	3	94	90 (16b)
8	15c (R = Me)	BTPP	3	> 95	53 (16c)
9	15d (R = N(OMe)Me)	BTPP	24	full	45 (16d)

^a The reaction of sulfonylimidate **14a** (0.300 mmol) with acrylate (or analogues) **15** (0.450 mmol) was performed at room temperature in the presence of a catalytic amount of a base (0.015 mmol, used as a stock solution in DMF) unless otherwise noted. ^b Determined by ¹H-NMR analysis of the crude reaction mixture.

Control experiments with 5 mol% of DBU showed that the reactions of sulfonylimidate **14a** and ethyl acrylate **15a** were proceeded sluggishly to afford the desired adduct **16a** in 12% yield after 3 h or 43% yield after 24 h (Scheme 6-4, entries 1, 2). Preliminary investigations of phosphazene bases as catalysts showed excellent reactivity to achieve full conversion of **14a** in a very short time, yielding the adduct **16a** in higher yields (entries 3, 4). While BTPP base afforded **16a** in 92% yield, P₂-Et base gave **16a** in 75% yield with 19% yield of bis-adduct **17**. According to the strong basicity of proazaphosphatane, high yield of the reaction was expected by employing ^tBu-PAP as a catalyst. However, the dimerization (or polymerization) reaction of acrylate¹⁶⁰ took place to suppress the formation of the desired adduct (entries 5, 6).

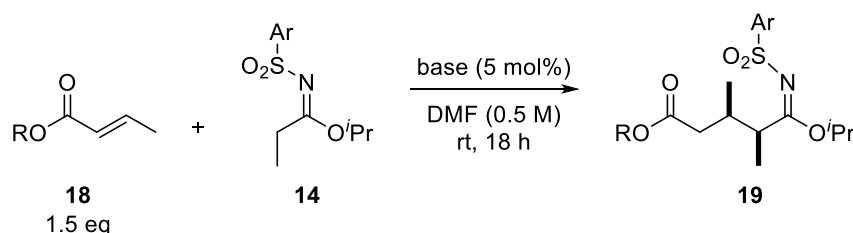
Other α,β-unsaturated carbonyl compounds were applicable for the reaction. ^tBu acrylate **15b** successfully yielded the desired product **16b** in excellent yield (entry 7). Methyl vinyl ketone **15c** and Weinreb amide **15d** gave moderate yields of the products **16c** and **16d**, respectively (entries 8, 9).

6-3. 1,4-Addition reactions of sulfonylimidates with crotonates and analogues

With the success of the reactions using acrylates in hand, ethyl crotonate **18a** was then chosen as a Michael

acceptor; however, the addition reaction of **14a** with **18a** did not proceed (Scheme 6-5, entries 1, 2). Further investigations showed that the substituents on sulfonylimidates, the ester part of the crotonate, and the basicity of the catalyst had a strong effect on reactivity. 2,5-Xylyl sulfonylimidate **14b** was more reactive than **14a** to give the adduct **19ba** in moderate yield (entry 3), and methyl crotonate **18b** could react with **14a** to afford **19ab** (entry 4) with ^tBu-PAP as a catalyst. By employing sulfonylimidate **14b** and methyl crotonate **18b**, 78% yield of the adduct **19bb** was obtained with moderate stereoselectivity (entry 5, *syn/anti* = 61/39). Interestingly, in contrast to the reactions with acrylates in Scheme 6-4, ^tBu-PAP catalyzed the desired reaction most effectively without promoting dimerization of crotonate esters (entries 5–7).

Scheme 6-5. Condition optimizations of 1,4-addition reactions to crotonates (1)^a



Entry	Sulfonylimidate	Acceptor	Base	Conversion ^b (%)	Isolated yield (%)	dr ^b (<i>syn/anti</i>)
1	14a (Ar = 4-tolyl)	18a (R = Et)	BTPP	NR	-	-
2	14a	18a	^t Bu-PAP	NR	-	-
3	14b (Ar = 2,5-xylyl)	18a	^t Bu-PAP	41	37 (19ba)	63/37
4	14a	18b (R = Me)	^t Bu-PAP	66	59 (19ab)	57/43
5	14b	18b	^t Bu-PAP	84	78 (19bb)	61/39
6	14b	18b	BTPP	NR	-	-
7	14b	18b	P ₂ -Et	60	60 (19bb)	61/39

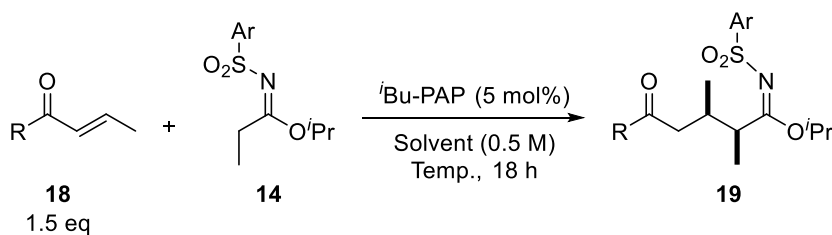
^a The reactions of sulfonylimidate **14** (0.300 mmol) with ester **18** (0.360 mmol) was performed at room temperature in the presence of a catalytic amount of a base (0.015 mmol, used as a stock solution in DMF). ^b Determined by ¹H-NMR analysis of the crude reaction mixture. The details of the determination of relative stereoconfigurations are shown in 0.

In order to improve the diastereoselectivity of the product, less polar solvents were examined; however, the reaction did not proceed well in THF (Scheme 6-6, entries 1–3). After investigations, thioester **18c** was found to be a good Michael acceptor to give the desired adduct **19bc** in high yield with good diastereoselectivity in toluene (entry 4). At the lower temperature, the more improved yield and selectivity were observed (entries 5, 6), and at –20 °C the product **19bc** was obtained in 99% yield with good diastereoselectivity (entry 6, *syn/anti* = 85/15). The reaction was sluggish at much lower temperature (–40 °C) to furnish the product in only 10% yield (entry 7).

Judging from the results in DMF in Scheme 6-5, bulkiness of the arylsulfonyl groups on sulfonylimidates were considered to be effective on the diastereoselectivity of products. For further improvement of the selectivity, the structure of the sulfonylimidates was again investigated in toluene with thioester **18c**. As expected, bulkiness of the arylsulfonyl group showed a significant effect on the selectivity. Compared with 2,5-xylyl sulfonylimidate **14b**, the less bulky 4-tolyl **14a** gave the product in lower selectivity (entry 8), and the more bulky mesityl **14c** (entry 9) or duryl **14d** (entry 10) showed higher selectivity. Moreover, 1-naphthyl **14e** and 2-naphthyl **14f** were examined with

expectation of high diastereoselectivity; however, the selectivities were not satisfactory (entries 11, 12).

Scheme 6-6. Condition optimizations of 1,4-addition reactions to crotonate/thiocrotonate (2)^a



Entry	Acceptor	Sulfonylelimide	solvent	Temp. (°C)	Isolated yield (%)	Dr ^b (syn/anti)
1	18b (R = OMe)	14b (Ar = 2,5-xylyl)	THF	rt	11 (19bb)	72/28
2	18b	14b	THF	50	9	65/35
3^c	18b	14b	THF	rt	trace	—
4	18c (R = S ^t Bu)	14b	toluene	rt	88 (19bc)	78/22
5	18c	14b	toluene	0	97	83/17
6	18c	14b	toluene	−20	99	85/15
7	18c	14b	toluene	−40	10	85/15
8	18c	14a (Ar = 4-tolyl)	toluene	−20	87 (19ac)	72/28
9	18c	14c (Ar = 2,4,6-Me ₃ C ₆ H ₂)	toluene	−20	87 (19cc)	88/12
10	18c	14d (Ar = 2,3,5,6-Me ₄ C ₆ H)	toluene	−20	88 (19dc)	93/7
11	18c	14e (Ar = 1-naphthyl)	toluene	−20	90 (19ec)	78/22
12	18c	14f (Ar = 2-naphthyl)	toluene	−20	99 (19fc)	76/24

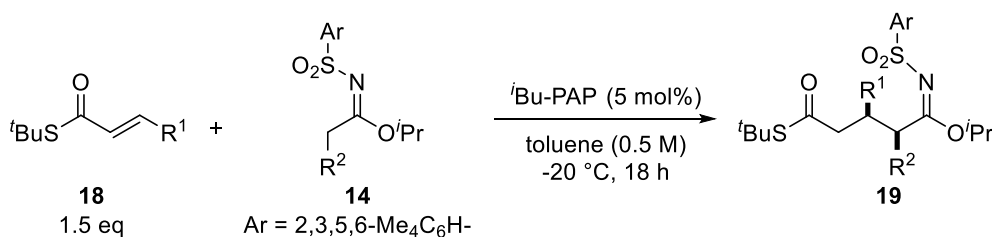
^a The reaction of sulfonylelimide **14** (0.300 mmol) with ester/thioester **18** (0.360 mmol) was performed in the presence of a catalytic amount of *t*Bu-PAP (0.015 mmol, used as a stock solution in the corresponding solvent) unless otherwise noted.

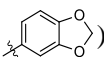
^b Determined by ¹H-NMR analysis of the crude reaction mixture. ^c P₂-Et phosphazene was used instead of *t*Bu-PAP.

6-4. Substrate scope

The substrate scope was then surveyed under the optimized conditions (Scheme 6-7). Aliphatic substituted thioesters **18d** and **18e** gave the products **19dd** and **19de**, respectively, in good to high yields with high diastereoselectivities (entries 2, 3). However, as the reactivity was low because of the bulkiness of the substituent at the R¹ position, a longer reaction time (entry 2) or higher catalyst loading (entry 3) was required. Aromatic substituted thioesters, regarded as cinnamic acid derivatives, were also successfully employed. A simple phenyl **18f** (entry 4), electron-donating group substituted **18g** and **18j** thioesters (entries 5, 8), electron-withdrawing group substituted **18h** and **18i** thioesters (entries 6, 7) yielded the corresponding products in high yields with good selectivities. Sulfonylimide **14g** also reacted to afford the desired Michael adduct **19gc** (entry 9).

Scheme 6-7. Substrate scope^a



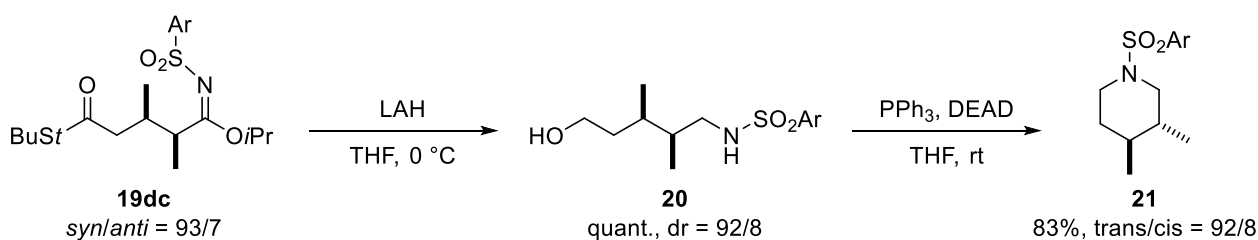
Entry	Thioester	Sulfonylimide	Isolated yield (%)	dr ^b (syn/anti)
1	18c (R ¹ = Me)	14d (R ² = Me)	88 (19dc)	93/7
2 ^c	18d (R ¹ = CH ₂ ^{<i>i</i>} Pr)	14d	77 (19dd)	93/7
3 ^d	18e (R ¹ = ^{<i>i</i>} Pr)	14d	60 (19de)	94/6
4 ^e	18f (R ¹ = Ph)	14d	89 (19df)	93/7
5	18g (R ¹ = <i>m</i> -CH ₃ C ₆ H ₄)	14d	quant. (19dg)	89/11
6	18h (R ¹ = <i>p</i> -BrC ₆ H ₄)	14d	96 (19dh)	91/9
7 ^f	18i (R ¹ = <i>p</i> -NO ₂ C ₆ H ₄)	14d	92 (19di)	87/13
8	18j (R ¹ = )	14d	96 (19dj)	91/9
9	18c	14g (R ² = Et)	56 (19gc)	88/12

^a The reaction of **14** (0.300 mmol) with **18** (0.360 mmol) was performed in the presence of a catalytic amount of *t*Bu-PAP (0.015 mmol, used as a stock solution in the corresponding solvent) unless otherwise noted. ^b Determined by ¹H-NMR analysis of the crude reaction mixture. ^c 48 h. ^d 10 mol%. ^e 48 h. ^f 0 °C.

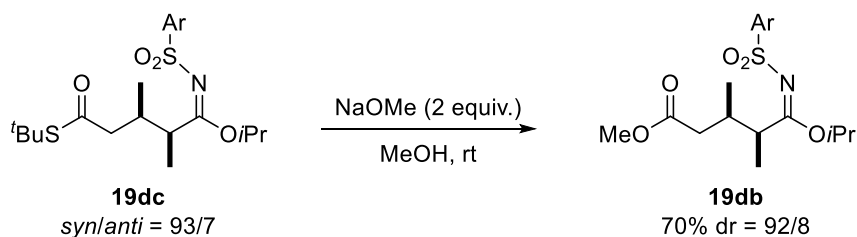
6-5. Further conversions of sulfonylimidate 1,4-adducts

Sulfonylimidate is a versatile ester surrogate and various conversion reactions are known.^{138,140–143} The Michael reaction product **19dc** was successfully converted to the corresponding amino alcohol **20** and ester **19db**. Product **19dc** was treated with lithium aluminum hydride (LAH) in THF to afford an amino alcohol **20** in quantitative yield without loss of stereoselectivity, and obtained amino alcohol **20** was successfully cyclized into dimethylpiperidine **21** under Mitsunobu conditions (**Scheme 6-8**). Methanolysis of the thioester moiety of product **19dc** was performed selectively using NaOMe with tolerance of the imidate moiety. It is considered that the *syn*-isomer of **19dc** reacted dominantly to afford the desired product **19db** in 70% yield with high diastereoselectivity (**Scheme 6-9**).

Scheme 6-8. Conversion to amino alcohol 20, piperidine derivative 21 (Ar = duryl)



Scheme 6-9. Conversion to methyl ester (Ar = duryl)

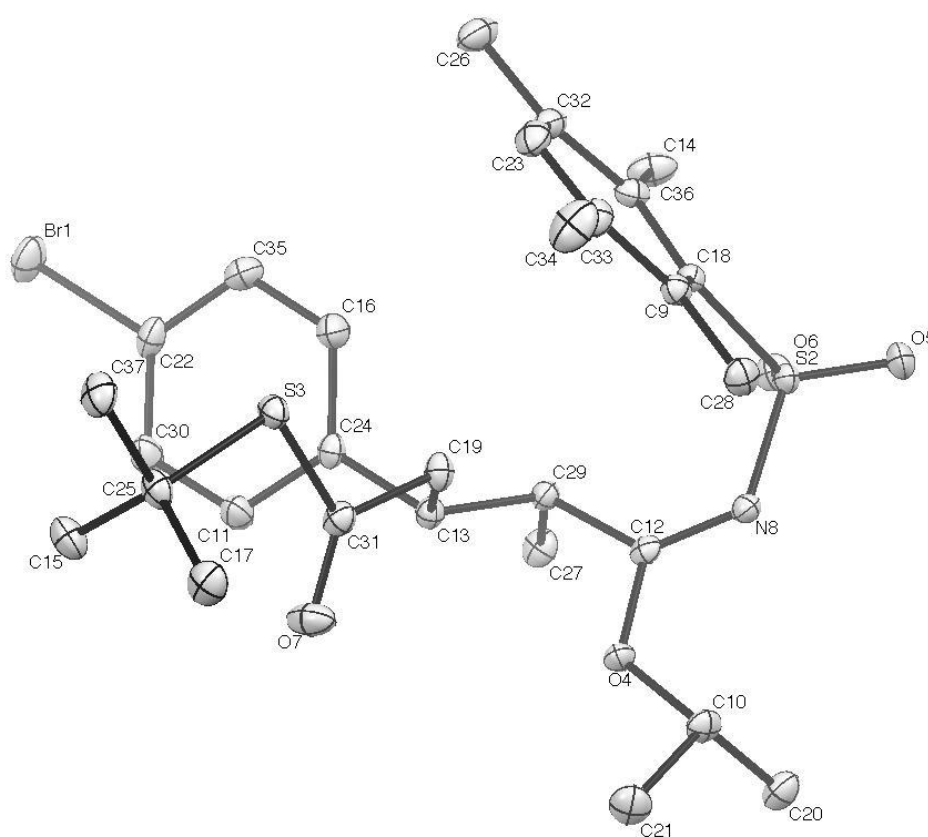


6-6. Determination of stereochemistry

Relative stereoconfiguration of **19dh** was determined by X-ray single crystallographic analysis. Relative stereoconfigurations of other aromatic substituted compounds **19df**, **19dg**, **19di**, and **19dj** were assigned by analogy of $^1\text{H-NMR}$ spectrometry.

Relative stereoconfiguration of **19dc** was assumed from the configuration of **21**. Relative stereoconfigurations of the other products were **19dd**, **19de**, **19gc**, **19ba**, **19ab**, **19bb**, **19bc**, **19ac**, **19cc**, **19dc**, **19ec**, and **19fc** were assigned by analogy of $^1\text{H-NMR}$ spectrometry.

Figure 6-1. X-ray single crystal structure of **19dh**¹⁶¹



6-7. Conclusion

In summary, highly diastereoselective Michael addition reactions of sulfonylimidates were developed using organosuperbases as highly efficient catalysts. α,β -Unsaturated thioesters were found to be suitable Michael acceptors to achieve highly stereoselective reactions in low-polarity solvents such as toluene. The diastereoselectivity of the products was successfully controlled by the steric bulkiness of the Ar group on the sulfonylimidates. The obtained products were successfully converted into an amino alcohol and an ester.

7. Summary and perspectives

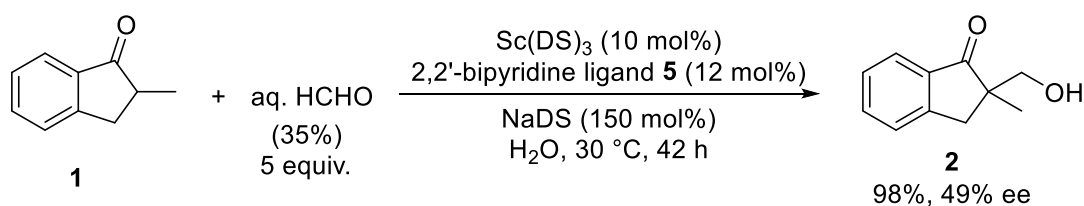
In this thesis, a novel real-time monitoring method for heterogeneous reactions and organosuperbase-catalyzed 1,4-addition reactions of sulfonylimidates with thioesters have been described.

Organic chemical reactions under heterogeneous conditions have been developed for years; however, detailed mechanistic studies have not been investigated enough due to technical problems of heterogeneity. To address the issue, a new monitoring method employing an auto-sampler DART-MS system with an isotope-labelled internal standard was established. In chapter 2, evaluations of an auto-sampler system were conducted to show its sampling ability with moderate reproducibility. For the quantitative monitoring study of heterogeneous reactions, an idea of isotope-labelled internal standard was introduced in this chapter.

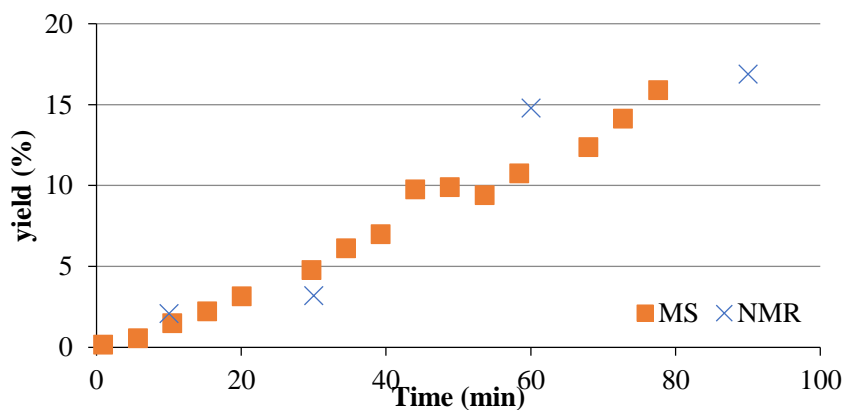
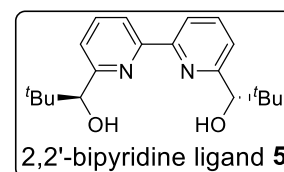
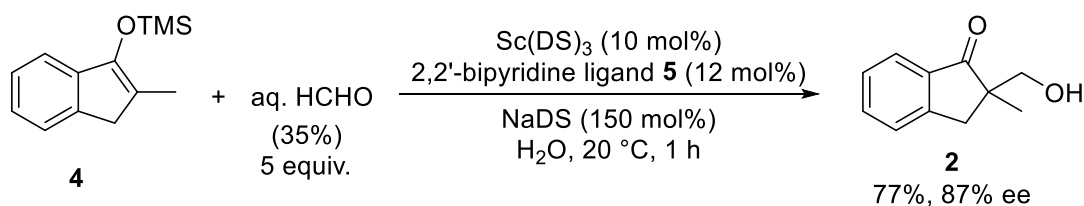
An advantage of isotope-labelled internal standard was confirmed in chapter 3. Deuterium-labelled compound **2-*d*₄** was synthesized and the monitoring study of direct-type aldol reactions in water was successfully conducted (Scheme 7-1). The same compound was applicable to the monitoring study of Mukaiyama aldol reactions in water.

Scheme 7-1. Real-time monitoring study of direct-type aldol reaction and Mukaiyama aldol reaction

Direct-type aldol reaction



Mukaiyama aldol reaction



Kinetics studies of direct-type aldol reactions and Mukaiyama aldol reactions were also shown in chapter 3. As a result of investigations, rate-laws of the reactions were determined as follows;

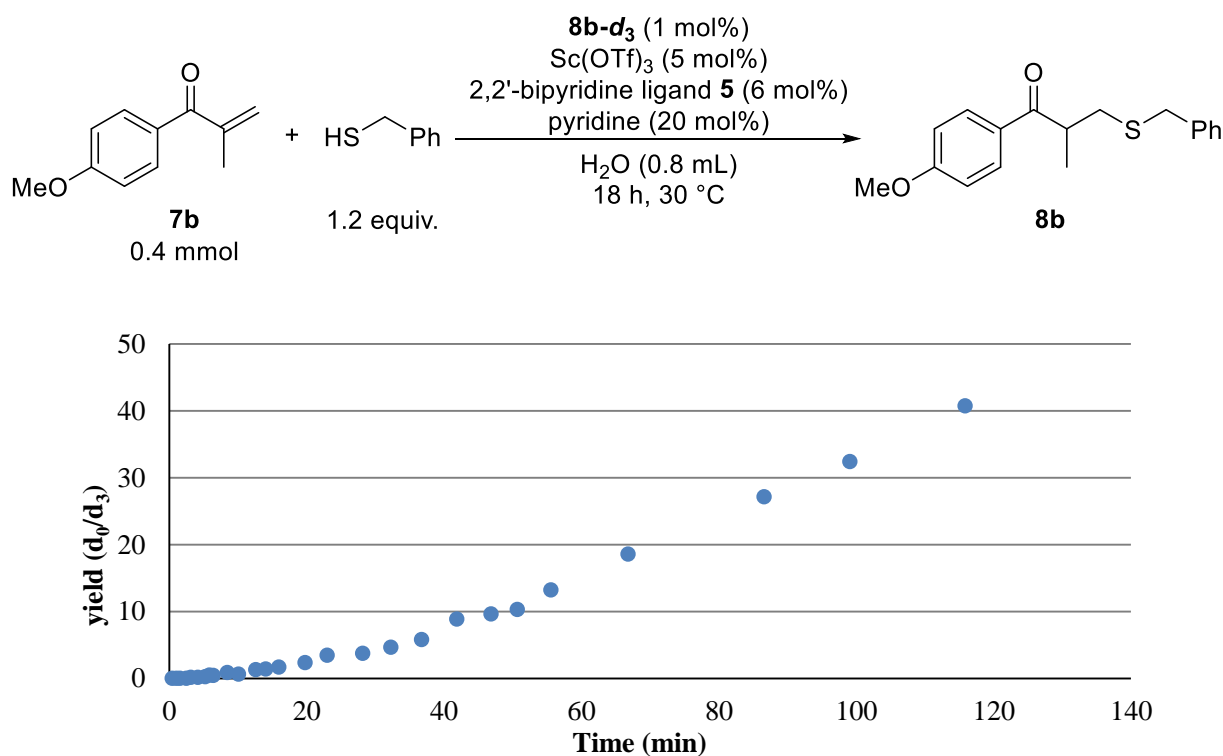
$$\text{for direct-type aldol reactions, Initial Reaction Rate} = k[\mathbf{1}]_0^1[\text{Sc}]_0^1[\text{HCHO}]_0^0$$

$$\text{for Mukaiyama aldol reactions, Initial Reaction Rate} = k_1[\mathbf{4}]_0^{0.9}[\text{Sc}]_0^0 \frac{[\text{HCHO}]_0}{k_2[\text{HCHO}]_0 - k_3}$$

With these results in hand, reaction mechanisms of aldol reactions were discussed in details.

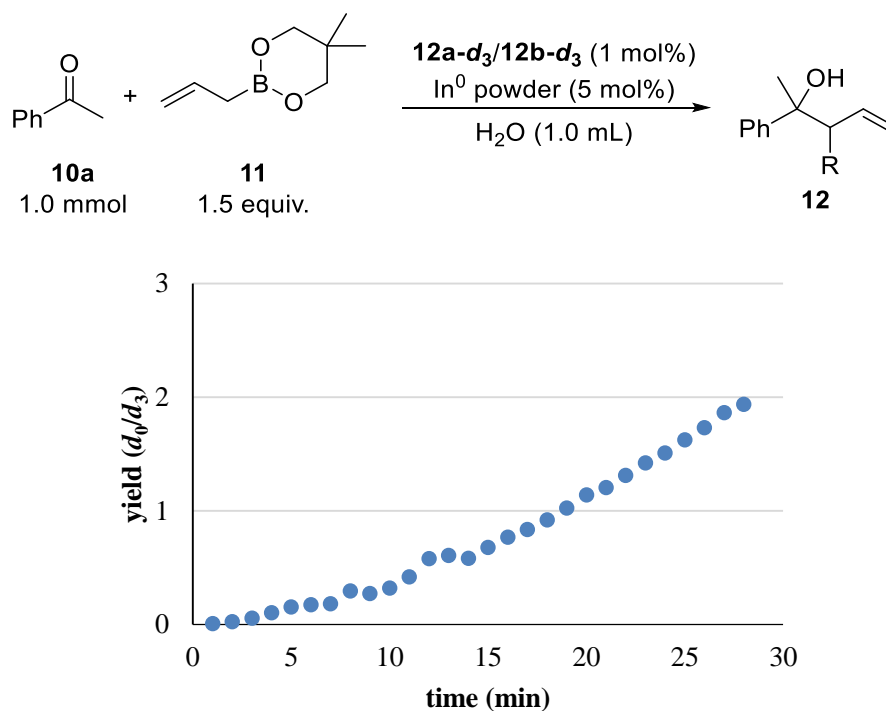
In chapter 4, a real-time monitoring method was applied for 1,4-addition/enantioselective protonation reactions as an example of liquid-liquid heterogeneous reactions. Slight modifications of monitoring conditions or substrate structure were required for the quantitative monitoring study. By using methoxy-substituted compound **8b**, desired peaks of **8b** and **8b-d₃** were observed with good intensities to give the smooth reaction profile (Scheme 7-2). The monitoring study revealed the existence of induction period, which was associated with the change of the pH value of reaction mixture by dual monitoring of reaction progress and the pH value of a reaction mixture.

Scheme 7-2. Real-time monitoring study of 1,4-addition/enantioselective protonation reactions in water



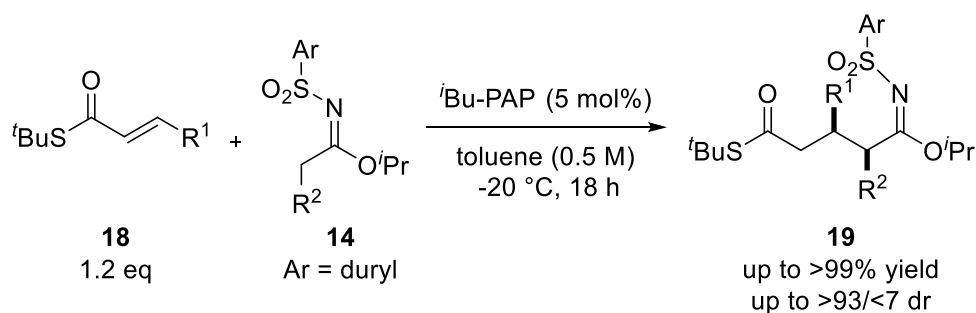
In chapter 5, a further application of the monitoring strategy was shown for indium(0) catalyzed allylation reactions in water as an example of a liquid-liquid-solid tri-phasic heterogeneous reaction. In the initial study, background reactions of acetophenone **10a** and pinacol allylboronate **11a** during ionization to prevent quantitative monitoring. Ketones and allylboronates were extensively examined to find α -methylallylboronate **11b** and 6-membered allylboronates **11c**, **11d** were effective for the quantitative reaction monitoring (Scheme 7-3).

Scheme 7-3. Real-time monitoring study of indium(0) catalyzed allylation reactions in water



Finally in chapter 6, highly diastereoselective Michael addition reactions of sulfonylimidates were developed using organosuperbases as highly efficient catalysts (Scheme 7-4). α,β -Unsaturated thioesters were found to be suitable Michael acceptors to achieve highly stereoselective reactions in low-polarity solvents such as toluene. The diastereoselectivity of the products was successfully controlled by the steric bulkiness of the Ar group on the sulfonylimidates. The obtained products were successfully converted into an amino alcohol and an ester.

Scheme 7-4. Organosuperbase-catalyzed 1,4-addition reactions of sulfonylimidates



8. Experimental

General

^1H and ^{13}C NMR spectra were recorded on JEOL JNM-ECX400, JNM-ECA500, and JNM-ECX600 spectrometers in CDCl_3 unless otherwise noted. Tetramethylsilane (TMS) and trace CHCl_3 in CDCl_3 served as internal standard ($\delta = 0, 7.26$) for ^1H NMR, and CDCl_3 served as internal standard ($\delta = 77.0$) for ^{13}C NMR. IR spectra were measured on a JASCO FT/IR-610 spectrometer. High Resolution Mass Spectra (HRMS) were recorded using a JEOL JMS T100TD spectrometer. Inductively Coupled Plasma (ICP) analyses were conducted with a SHIMADZU ICPS-7510 sequential plasma spectrometer. Preparative thin-layer chromatography (pTLC) was carried out using a plate with Wakogel B-5F. Caffeine, P1- t -Bu and P2-Et phosphazene bases were purchased from Aldrich Co., Ltd. and t -Bu-PAP base was prepared following reported method.¹⁶² All solvents were purchased from Wako Pure Chemical Industries as dry solvents. Deionized water from a MILLIPORE MilliQ machine (Gradient A10) was used as solvent without further treatment.

2. General aspects of quantitative monitoring using DART-MS

Experiment 2-1. Repetitive ionization experiment of caffeine using auto-sampler system

Standard solution of caffeine (400 ppm, 4 mL) in DCM was set into the reaction vessel on auto-sampler machine. Under standard conditions of DART-MS (Helium as carrier gas, 250 °C), ionization was conducted by using closed-end of glass tube (1.8 mm) as a sampling rod. Measurement was conducted for 18 times in each 2 set of experiments. Selected ion chromatograms of $m/z = 195.00\text{--}195.50$ (corresponding to $[\text{caffeine}+\text{H}]^+$ ion) were collected (Figure 2-5, Figure 2-6).

1 st set		2 nd set	
Peak area [Intens. • sec]		Peak area [Intens. • sec]	
	187535.5		222198
	202305		139013.8
	200832.2		227026.2
	204362.9		184267.7
	154393.5		199940.4
	315669.3		247348.7
	260854.7		185022.4
	246503.4		243320.9
	245727.5		237234.4
	238123.3		231811.4
	271915.6		203970.3
	243750.1		297203.9
	242721.4		252941.1
	252604		229058.6
	209949.7		258794.7
	203605.8		310424.1
	141266.8		267398.7
	187764.9		241028.5
Average	222771.4	Average	232111.3
Standard deviation	42775.63	Standard deviation	40843
RSD (%)	19.2	RSD (%)	17.6

Experiment 2-2. Calibration of auto-sampler by ICP-AES

Saturated aqueous CuSO_4 solution (4.0 mL) was placed in reaction vessel and auto-sampler was operated at 25 °C. The aliquot sample taken by closed-end of glass rod (1.8 mm) was sent to flask and diluted with 2 wt% aqueous sulfuric acid to 50.0 mL. Diluted sample was analyzed by ICP-AES to determine the concentration of Cu^{2+} to check the amount of sample taken by glass rod. As a result, the average amount of Cu^{2+} was determined as 0.182 ppm with 53.8% relative standard deviation for 10 repetitive measurements.

Results (ppm)	
0.367218	
0.190772	
0.140753	
0.096196	
0.109810	
0.122200	
0.121096	
0.129329	
0.347566	
0.194950	
Average	0.182 ppm
Standard deviation	0.0980
RSD (%)	53.8

Experiment 2-3. Calibration of auto-sampler by NMR

Pure anhydrous dimethylsulfoxide (4.0 mL) was placed in a reaction vessel and an aliquot sample was taken by closed-end of glass rod ($\phi = 1.8$ mm) into NMR tube containing 4.9 mg of tetrachloroethane in chloroform- d_1 . The amount of DMSO was determined by peak area of DMSO (2.62 ppm) relative to tetrachloroethane (5.91 ppm) as 1. 10 times of repetitive measurement revealed the average of the DMSO taken was 0.35 mg with 22.2% relative standard deviation.

Integrations of DMSO (2.62 ppm)	
Integrations of $(\text{CHCl}_2)_2$ (5.91 ppm)	
0.3941	
0.5258	
0.3895	
0.4003	
0.7164	
0.4276	
0.4489	
0.4773	
0.4476	
Average relative peak area	0.459
Standard deviation	0.102
RSD	22.2%

Experiment 2-4. Ionization experiment with readily sample-soaking materials

Tertiary alcohol **12b** in DCM (2.8 mg in 4 mL) was placed in a reaction vessel and an aliquot sample was taken by closed-end of a glass rod ($\phi = 1.8$ mm) to bring into ionization area of DART-MS (Helium as carrier gas, 250 °C).

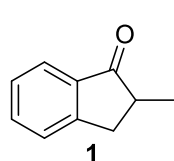
Raw data of peak area ($m/z = 159.00 - 159.50$) [Intensity * sec] for Figure 2-7 are shown in table.

29800.62	7122.23	31257.23	11918.9	7942.55	5556.45	19791.41	11292.14
28231.21	27858.2	10844.4	22644.98	8515.15	14518.79	12499.48	7054.44
7352	12455.9	10105.96	30723.48	10539.23	13480.55	13308.26	22402.88
19670.25	10363.66	8488.66	8086.68	33032.13	23030.12	9002.6	94734.64
12911.64	17364.42	8636.16	5845.13	14809.6	8783.6	26004.35	36471.33
10529.52	10915.33	57553.73	13132.62	9349.07	19752.28	9279.51	

Average = 17977.95, standard deviation = 15206.1, RSD = 84.6%.

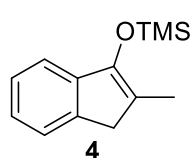
3. Monitoring study of chemical reaction under micellar conditions

Ketone **1**, silyl enol ether **4**, 2,2'-bipyridine ligand **5** were prepared following reported methods.^{95,97-99,163}



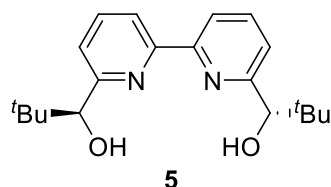
2-methylindan-1-one (**1**)⁹⁹

¹H-NMR (600 MHz): $\delta = 1.30$ (3H, d, $J = 7.5$ Hz), 2.67 – 2.73 (2H, m), 3.36 – 3.40 (1H, m), 7.35 (1H, dd, $J = 6.9, 8.2$ Hz), 7.44 (1H, d, $J = 8.2$ Hz), 7.57 (1H, dd, $J = 7.6, 6.9$ Hz), 7.74 (1H, $J = 7.6$ Hz); ¹³C-NMR (125 MHz): $\delta = 16.1, 34.7, 41.8, 123.7, 126.4, 127.1, 134.5, 136.1, 153.3, 209.2$.



2-methyl-1-trimethylsilyloxyind-1-ene (**4**)¹⁶⁴

¹H-NMR (500 MHz): $\delta = 0.27$ (9H, s), 1.97 (3H, s), 3.18 (2H, s), 7.12 (1H, dd, $J = 7.4, 5.7$), 7.18 (1H, d, $J = 7.4$), 7.24 (1H, dd, $J = 5.7, 7.4$), 7.31 (1H, d, $J = 7.4$); ¹³C-NMR (125 MHz): $\delta = 0.7, 12.4, 38.4, 117.2, 120.1, 123.3, 124.0, 125.9, 140.8, 142.7, 147.5$.



(S,S)-6,6'-bis(1-hydroxy-2,2-dimethylpropyl)-2,2'-bipyridine (**5**)^{97,98,163}

¹H-NMR (400 MHz): $\delta = 0.97$ (18H, s), 4.41 (2H, br s), 7.23 (4H, d, $J = 7.3$ Hz), 7.79 (2H, t, $J = 7.8$ Hz), 8.31 (2H, d, $J = 7.8$ Hz); ¹³C-NMR (100 MHz): $\delta = 25.9, 36.3, 80.2, 119.6, 123.1, 136.6, 153.8, 159.3$. HPLC (OD, hexanes/ⁱPrOH = 19/1, 1.0 mL/min; $t_R = 49.2$ min (S,S), ND for (R,R) isomer)

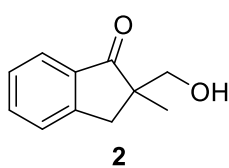
Representative procedures of direct-type aldol reactions and Mukaiyama aldol reactions under modified conditions (Scheme 3-2)

Modified procedure of direct-type aldol reaction

To a reaction vessel Sc(DS)₃ (33.6 mg, 0.0400 mmol), NaDS (173 mg, 0.600 mmol), 2,2'-bipyridine ligand **5** (15.7 mg, 0.0480 mmol) and water (0.63 mL) were added and stirred vigorously at 30 °C for an hour. Ketone **1** (58.5 mg, 0.400 mmol) and formaldehyde (35% aqueous solution, 167 μ L) were added successively. After 42 hours the reaction was quenched by adding DCM, aq. NaHCO₃ solution and brine. The mixture was extracted with DCM and dried over anhydrous Na₂SO₄. After removal of solvent under vacuum condition, a crude mixture was purified over preparative TLC (hexanes/ethyl acetate = 2/1) to afford the desired product **2** (69.2 mg, 0.392 mmol, 98%, 49% ee).

Modified procedure of Mukaiyama aldol reaction

To a reaction vessel $\text{Sc}(\text{DS})_3$ (33.6 mg, 0.0400 mmol), NaDS (173 mg, 0.600 mmol), 2,2'-bipyridine ligand **5** (15.7 mg, 0.0480 mmol), and water (1.83 mL) were added and stirred vigorously at 20 °C for an hour. Silyl enol ether **4** (87.3 mg, 0.400 mmol) and formaldehyde (35% aqueous solution, 167 μL) were added successively. After an hour the reaction was quenched by adding DCM, aq. NaHCO_3 solution and brine. The mixture was extracted with DCM and dried over anhydrous Na_2SO_4 . After removal of solvent under vacuum condition, a crude mixture was purified over preparative TLC (hexanes/ethyl acetate = 2/1) to afford the desired product **2** (54.1 mg, 0.307 mmol, 77%, 87% ee).

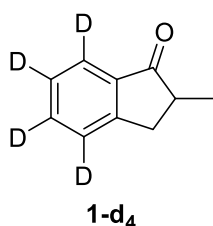


2-(hydroxymethyl)-2-methylindan-1-one (**2**)^{95,96}

The enantiomeric excess was determined by chiral HPLC analysis (OB-H, hexanes/ PrOH = 100/1, 1.0 mL/min. t_{major} = 41.0 min, t_{minor} = 50.1 min). $^1\text{H-NMR}$ (500 MHz): δ = 1.24 (3H, s), 2.48 (1H, br s), 2.89 (1H, d, J = 17.6 Hz), 3.26 (1H, d, J = 17.0 Hz), 3.62 (1H, dd, J = 10.8, 4.0 Hz), 3.83 (1H, dd, J = 10.2, 6.8 Hz), 7.34 – 7.38 (1H, m), 7.46 (1H, d, J = 7.4 Hz), 7.60 (1H, t, J = 7.4 Hz), 7.73 (1H, t, J = 7.1 Hz); $^{13}\text{C-NMR}$ (500 MHz): δ = 20.6, 37.8, 50.9, 67.6, 123.7, 126.2, 126.8, 134.6, 153.2, 211.2.

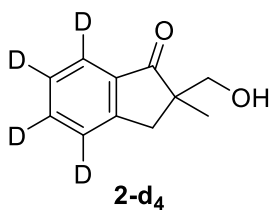
Synthesis of 2-**d**₄.

Pentadeuterated compound **1-d**₄ was synthesized by following Olah's method with slight modification.⁹⁹ Triflic anhydride (40 mL, 244 mmol) and water- d_2 (4.4 mL, 244 mmol) was mixed in a 100 mL round bottom flask and the mixture was heated at 90 °C for 2 hours under argon atmosphere. After the mixture became single phase, the mixture was allowed to room temperature and then benzene- d_6 (5.31 mL, 60 mmol) and methacrylic acid (2.53 mL, 30 mmol; treated with water- d_2 three times before use) were subsequently added. After stirring the mixture at 75 °C for overnight, the mixture was cooled to room temperature and poured into ice/water. The mixture was extracted with DCM (50 mL for 3 times) and combined organic phase was washed with saturated aq. NaHCO_3 until aqueous phase became basic. The organic phase was further washed with brine (30 mL, once) and dried over anhydrous Na_2SO_4 . After removal of solvent under vacuum, the mixture was poured into 1N aq. KOH/MeOH mixture (1/9, 10 mL) to stir for 10 min at room temperature. The mixture was acidified with saturated aq. NH_4Cl solution and extracted with DCM then dried over anhydrous Na_2SO_4 . This base treatment was conducted 3 times for full D-H exchange of carbonyl α -position. After the removal of solvent, the desired compound **1-d**₄ was obtained (3.86 g, 25.8 mmol, 86%). Obtained compound was used in next step after distillation (0.53 mmHg, 93 – 97 °C). Compound **2-d**₄ was obtained following modified procedure of direct-type aldol reactions described above.



2-methylindan-1-one-4,5,6,7-**d**₄ (**1-d**₄)

$^1\text{H-NMR}$ (500 MHz): δ = 1.31 (3H, d, J = 7.4 Hz), 2.66-2.74 (2H, m), 3.39 (1H, m), 7.35 (<0.01H), 7.44 (<0.01H), 7.57 (<0.01H), 7.74 (<0.01H), $^{13}\text{C-NMR}$ (500 MHz): δ = 16.1, 34.7, 123.4 (t, J = 25 Hz), 126.0 (t, J = 24.4 Hz), 126.7 (t, J = 24.4 Hz), 134.0 (t, J = 23.8 Hz), 136.1, 153.2, 209.3.



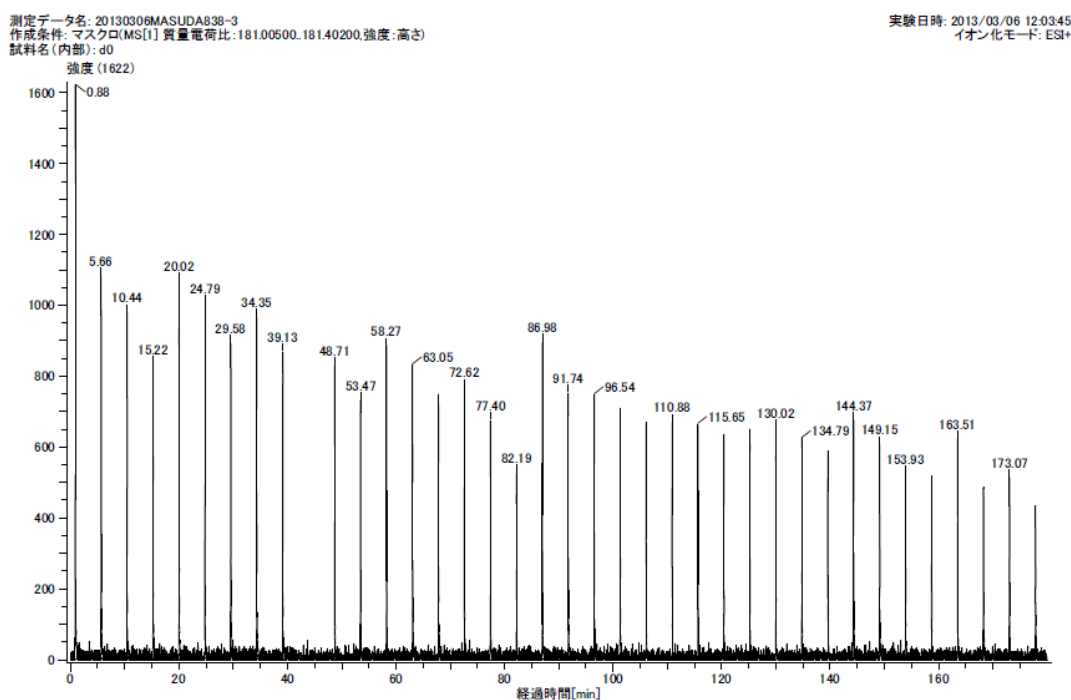
2-hydroxymethyl-2-methylindan-1-one-4,5,6,7-*d*₄ (2-*d*₄)

¹H-NMR (500 MHz): δ = 1.21 (3H, s), 2.78 (1H, br s), 2.88 (1H, d, *J* = 17.6 Hz), 3.27 (1H, d, *J* = 17.0 Hz), 3.60 (1H, d, *J* = 10.7 Hz), 3.81 – 3.85 (1H, m), 7.34 (trace) 7.45 (trace) 7.59 (trace) 7.70 (trace); ¹³C-NMR (125 MHz): δ = 20.6, 37.7, 50.9, 67.6, 123.7 (t, *J* = 26.2 Hz), 126.2 (t, *J* = 23.8 Hz), 134.6 (t, *J* = 23.8 Hz), 135.6, 153.2,

211.2.

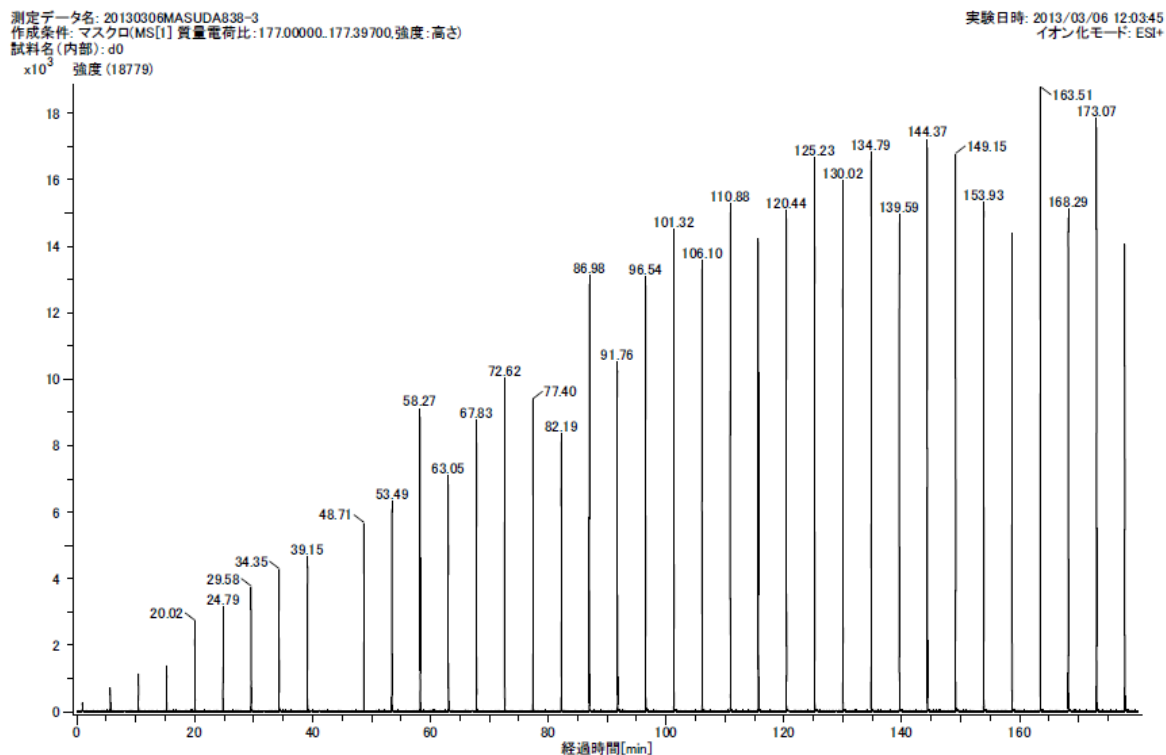
Raw SICs of Figure 3-1. Monitoring trial of direct-type aldol reactions

SIC of *m/z* = 181.005 – 181.402 (2-*d*₄)



Time (min)	Integration [Intens. • sec]	(continue)		(continue)	
0.88	5380.35	67.83	2360.42	130.02	1802.57
5.66	3404.75	72.62	2545.49	134.79	2452.86
10.44	2815.55	77.4	2086.96	139.59	1984.13
15.22	2679.48	82.19	1747.43	144.37	2043.92
20.02	3771.12	86.98	2719.86	149.15	1712.26
24.79	2661.25	91.74	2565.91	153.93	1985.81
29.58	2412.68	96.54	2278.01	158.71	2064.17
34.35	3378.44	101.32	2428.63	163.51	1592.98
39.13	2948.9	106.1	1676.33	168.27	1661.16
48.71	2345.05	110.88	1882.69	173.07	1426.01
53.47	2122.8	115.65	1890.01	177.85	1656.47
58.27	2113.54	120.44	1680.85		
63.05	2621.55	125.23	2161.47		

SIC of m/z = 177.000 – 177.397 (2)



Time (min)	Integration [Intens. • sec]	(continue)	
0.88	496.76	101.32	29826.96
5.66	1493.89	106.1	25561.68
10.44	2387.77	110.88	29551.6
15.22	2992.99	115.65	30317.78
20.02	6680.07	120.44	31640.96
24.79	5637.1	125.23	37941.77
29.58	8057.34	130.02	36440.3
34.35	10332.67	134.79	41041.43
39.15	10694.6	139.59	36015.46
48.71	11526.18	144.37	34542.22
53.49	14936.73	149.15	33463.36
58.27	16152.35	153.93	35842.54
63.05	13653.17	158.73	36005.95
67.83	17772.2	163.51	38724.74
72.62	22959	168.29	37070.39
77.4	18854.82	173.07	40472.98
82.19	18886.77	177.85	33047.43
86.98	26057.01		
91.76	24992.08		
96.54	27713.88		

Scheme 3-6. Comparative experiments between MS and NMR (1)

Detailed data of Scheme 3-6

Entry	Time (h)	NMR yield (%)	MS yield (% , estimated from d_0/d_4 ratio)	isolated yield
1	0.5	9.6	10.1	
2	0.5	8.1	9.9	
3	0.5	10.4	12.8	
4	1.0	11.6	15.5	
5	1.0	8.2	17.5	
6	1.0	11.5	14.1	13
7	2.0	34.1	39.0	
8	2.0	35.9	37.7	
9	2.0	31.0	30.9	
10	3.0	34.2	45.9	32
11	3.0	27.3	38.8	23
12	3.0	40.3	51.3	41
13	12	85.0	122	82
14	12	84.6	121	
15	12	88.7	124	

Scheme 3-7. Comparative experiments between MS and NMR (2): Late-stage addition of internal standard

A modified procedure of Scheme 3-7.

1. A reaction was conducted in the ABSENCE of an internal standard **2- d_4** at 0.2 mmol scale for indicated time.
2. A reaction was quenched by adding saturated aq. NaHCO_3 solution and brine, then a solution of an internal standard **2- d_4** (1 mol%) was added to a mixture. The mixture was extracted with dichloromethane (10 mL) for three times and the extract was dried over anhydrous Na_2SO_4 .
3. The crude mixture was analyzed by NMR and MS following a standard procedure.

Detailed data of Scheme 3-7.

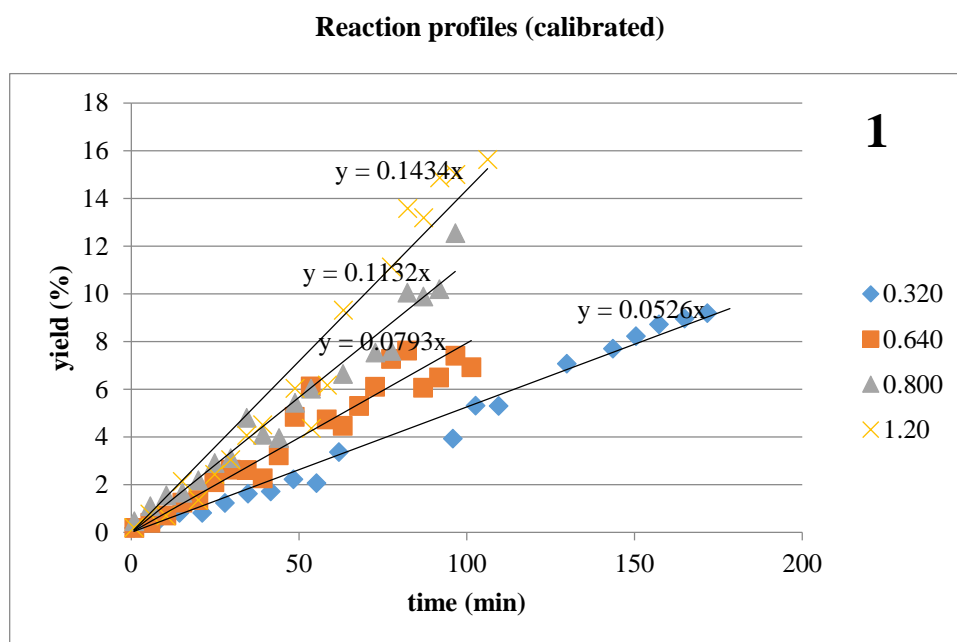
Entry	Time (h)	NMR yield (%)	MS d_0/d_4 (yield, estimated)
1	0.5	6.9	8.6
2	0.5	7.7	8.3
3	0.5	6.7	7.5
4	1.0	15.7	15.7
5	1.0	12.4	12.7
6	1.0	13.9	14.0
7	2.0	27.3	33.9
8	2.0	24.5	29.9
9	2.0	29.0	33.2
10	3.0	49.7	52.0
11	3.0	36.3	45.9
12	3.0	41.5	44.3
13	12	89.7	124
14	12	90.1	121
15	12	84.7	133

Figure 3-2. A calibration curve of the yield derived from isotope ratio

A calibration experiment was conducted by mixing compound **2** and **2-*d*₄** in several different ratios. An aqueous solution of compound **2-*d*₄** (5.055 g/L, 72.0 μL, 2.02 μmol as content) and 0.500, 1.00, 2.00, 5.00 and 10.00 mL of compound **2** solution in water (1.384 g/L) were mixed and analyzed by DART-MS (He as carrier gas, 200 °C). Each solution mixtures were analyzed 6 times and an average were taken for the calibration curve. Detailed data are shown in following table.

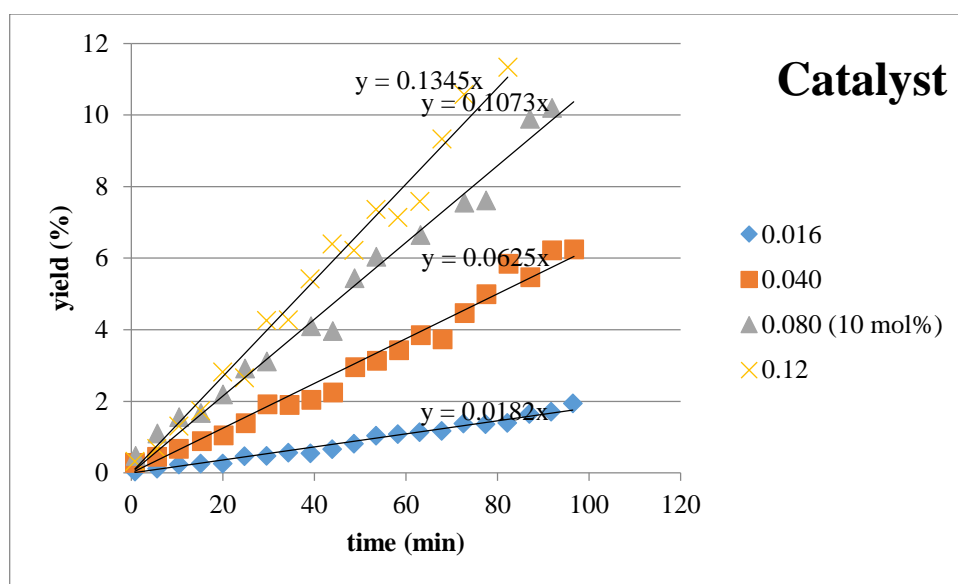
Molar ratio of 2/2-<i>d</i>₄	MS ratio of 2/2-<i>d</i>₄	Standard deviation of MS ratio
1.947	2.096	0.011442
3.893	4.390	0.117915
7.786	9.503	0.127548
19.47	25.19	0.343818
38.93	55.14	2.966017

Raw data of Scheme 3-9. Kinetic study on indanone



Loading of 1	Rate [yield/min]	Rate [mmol/h]
0.320	0.0526	0.026496
0.640	0.0793	0.03648
0.800	0.1132	0.05184
1.20	0.1434	0.07776

Raw data of Scheme 3-10. Kinetic study on scandium complex



Loading of Sc(DS) ₃	Rate [yield/min]	Rate [mmol/h]
0.016	0.0183	0.00912
0.04	0.0625	0.03168
0.08	0.1073	0.05184
0.12	0.1345	0.07008

Raw data of Scheme 3-11. Kinetic study on formaldehyde

HCHO [mol/L ⁻¹]	Rate [yield/min]	Rate [mmol/h]
0.25	0.0965	0.0480
0.25	0.0921	0.0459
0.5	0.0771	0.0384
0.5	0.1124	0.0560
0.75	0.0829	0.0413
1	0.1425	0.0710
1	0.1229	0.0612
1.25	0.1091	0.0543
1.5	0.0954	0.0475
1.5	0.1291	0.0643
2.5	0.1040	0.0518
2.5	0.1019	0.0508

Raw data of Scheme 3-14. Reaction monitoring trial of Mukaiyama-type aldol reactions, Figure 3-3, Figure 3-4 and Figure 3-5

Retention time (min)	m/z = 181	m/z = 177	m/z = 219	m/z = 249
0.76	2909.36	6873.64	19200.84	1221.11
2.26	1675.89	7715.37	15726.58	1219.47
3.73	1155.78	7985.79	33036.8	3466.03
5.22	952.24	11035.48	26759.08	2944.57
6.71	2129.66	27653.01	17708.38	5642.63
8.19	1178.11	22096.6	22462.67	6168.52
9.67	1432.17	31564.3	14263.59	6476.15
11.16	822.55	21127.9	27103.08	7635.83
12.64	450.82	14256.54	31978.94	5677.63
14.1	779.41	24755.57	30894.09	9287.71
15.6	970.3	35218.38	13839.78	7431.34
17.09	1450.86	50524.53	6881.12	7432.77
18.57	383.56	18330.47	34944.84	8593.84
20.05	697.89	30288.31	19582.53	9474.98
21.53	711.45	40374.37	20904.89	11072.14
23.02	983.14	52134.55	9358.05	8289.7
24.5	944.7	53994.72	10892.39	9180.81
25.98	1067.97	64409.61	5239.05	7102.55
27.47	810.9	58014.41	6203.93	6600.77
28.95	921.28	77216.93	2106.43	4146.18
30.43	740.89	56908.83	7486.19	8647.92
31.91	1090	79561.87	945.55	1818.97
33.41	923.07	69320.47	3079.26	4741.47
34.88	918.64	71091.18	4351.13	6789.95
36.36	582.84	54725.59	2355.77	3093.73
37.84	1127.73	101380.6	1410.77	3417.18
39.33	870.37	77298.12	5637.12	7743.71
40.83	1172.39	104375.4	1291	3153.14
42.29	1202.39	111291	1638.79	4330.27
43.77	1059.64	98812.7	1642.1	3205.61
45.27	782.26	70203.01	483.25	1893.49
48.24	1105.02	95557.51	560	1439.22
49.71	1148.73	100984.6	576.43	963.09
51.19	1258.78	105463.2	473.85	1117.84
52.69	919.03	76738.61	102.89	244.93
54.17	756.91	64362.1	326.96	718.46
55.64	847.96	76524.19	306.51	692.77
58.6	997.91	82943.77	236.36	884.1
60.1	1177.68	113214.3	402.82	1323.6
61.58	1063.92	104894.1	198.43	750.82
63.07	1437.34	126943.3	149.55	1171.74
64.53	872.25	84258.59	259.69	539.6
67.5	738.64	74418.43	257.99	548.61
69	948.31	89549.5	215.9	565.54
70.48	1002.95	95999.63	408.35	1194.68

Raw data of Scheme 3-20. Kinetic study on catalyst

Loading of Sc(DS)3 (mmol)	Rate [yield/min]	Rate [mmol/h]
0.02	1.6589	0.398136
0.02	1.6676	0.400224
0.02	2.067	0.49608
0.016	1.7202	0.412848
0.012	2.0225	0.4854
0.04	1.8137	0.435288
0.004	1.4021	0.336504
0.004	1.5105	0.36252
0.002	1.7159	0.411816
0.008	1.7891	0.429384

Raw data of Scheme 3-21. Kinetic experiment on silyl enol ether 4

Loading of 4 (mmol)	Rate [yield/min]	Rate [mmol/h]
0.4	1.2436	0.298464
0.3	1.1965	0.28716
0.2	1.1785	0.28284
0.1	0.4087	0.098088
0.2	1.0224	0.245376
0.4	1.6589	0.398136
0.4	1.6676	0.400224
0.4	2.067	0.49608

Raw data of Scheme 3-22. Kinetic experiment on formaldehyde

HCHO [mol/L]	Rate [yield/min]	Rate [mmol/h]
0.5	1.6589	0.398136
0.5	1.6676	0.400224
0.5	2.067	0.49608
0.1	1.0022	0.240528
0.2	1.224	0.29376
0.3	1.1852	0.284448
0.05	0.5932	0.142368
0.3	1.7768	0.426432
0.4	1.734	0.41616

4. 1,4-additionenantioselective protonation reactions in water

Ketones **7a** – **7d** were synthesized following reported procedure.¹¹⁸ The standard reaction procedure for monitoring study was followed by the reported one.¹¹³ Internal standard **8a-d₅** and **8b-d₃** were synthesized as follows.

Synthesis of **8a-d₅**.

To a dried 200 mL 2-neck flask anhydrous AlCl₃ (10.0 g, 75 mmol) and 50 mL of DCM was placed under argon atmosphere. The mixture was cooled down to 0 °C and benzene-d₆ (4.43 mL, 50 mmol) was slowly added. After addition of the reagent, the mixture was stirred at room temperature for overnight. The reaction was poured into ice/water mixture and extracted with DCM (100 mL x 3). Combined organic layer was washed with saturated aq. NaHCO₃ solution (50 mL x 2), water (50 mL) and brine (30 mL). After dryness over anhydrous Na₂SO₄ solvent was removed under reduced pressure. Crude mixture was directly distilled to afford the desired propiophenone-d₅ (**9a-d₅**, 4.89 g, 35 mmol, 70%) which was successfully converted into ketone **7a-d₅** and internal standard **8a-d₅** following reported procedures.

Synthesis of **8b-d₃**.

4-Hydroxypropiophenone **9d** (3.73g, 24.8 mmol) was treated with tosylmethane-d₃ (3.92g, 20.7 mmol) prepared from methanol-d₄ and anhydrous K₂CO₃ (8.58g, 62.1 mmol) in 80 mL of acetonitrile at room temperature for overnight. To a mixture 100 mL of water was added and the phase was separated. Aqueous phase was extracted with ethyl acetate (50 mL x 3) and combined organic phase was washed with brine. After dryness over anhydrous Na₂SO₄ the solvent was removed *in vacuo*. Further purification over silica gel column chromatography (hexanes/ethyl acetate = 9/1 → 5/1) afforded the desired product **9b-d₃** (3.03 g, 19.7 mmol, 95% based on TsOCD₃) which was further converted into **7b-d₃** and **8b-d₃** following reported procedures.

1-Phenyl-2-methylprop-2-en-1-one (7a)¹¹³

¹H-NMR (400 MHz): δ = 2.07 (3H, s), 5.62 (1H, s), 5.91 (1H, s), 7.42 (2H, dd, *J* = 7.3, 7.3 Hz), 7.52 (1H, t, *J* = 7.3 Hz), 7.73 (2H, d, *J* = 7.3 Hz); ¹³C-NMR (100 MHz): δ = 18.6, 127.0, 128.1, 129.3, 131.9, 137.6, 143.7, 198.2.

1-(Phenyl-d₅)-2-methylprop-2-en-1-one (7a-d₅)

¹H-NMR (500 MHz): δ = 2.07 (3H, s), 5.62 (1H, s), 5.91 (1H, s), 7.42 (trace), 7.52 (trace), 7.73 (trace, <0.03H); ¹³C-NMR (125 MHz): δ = 18.6, 127.0, 127.6 (t, *J* = 24.4 Hz), 128.9 (t, *J* = 25.6 Hz), 131.4 (t, *J* = 23.8 Hz), 137.4, 143.7, 198.3.

1-(4-methoxyphenyl)-2-methylprop-2-en-1-one (7b)¹¹³

¹H-NMR (400 MHz): δ = 2.06 (3H, s), 3.85 (3H, s), 5.53 (1H, s), 5.79 (1H, s), 6.91 (2H, d, *J* = 6.9 Hz), 7.78 (2H, d, *J* = 6.9 Hz); ¹³C-NMR (100 MHz) δ = 18.9, 55.2, 113.3, 124.6, 129.8, 131.7, 143.7, 162.9, 196.9.

1-(4-methoxyphenyl)-2-methylprop-2-en-1-one (7b)

¹H-NMR (500 MHz): δ = 2.06 (3H, s), 3.85 (trace), 5.53 (1H, s), 5.79 (1H, s), 6.91 (2H, d, *J* = 6.9 Hz), 7.78 (2H, d, *J* = 6.9 Hz); ¹³C-NMR (100 MHz) δ = 19.0, 54.6 (tt, *J* = 21.5, 21.5), 113.4, 124.6, 129.9, 131.8, 143.9, 163.0, 197.1.

1-(4-chlorophenyl)-2-methylprop-2-en-1-one (7c)¹¹³

¹H-NMR (400 MHz): δ = 2.03 (3H, s) 5.56 (1H, s) 5.88 (1H, s) 7.37 (2H, d, J = 8.4), 7.66 (2H, d, J = 8.4 Hz); ¹³C-NMR (100 MHz): δ = 18.6, 127.0, 128.5, 130.8, 135.9, 138.4, 143.6, 197.0.

1-(4-hydroxyphenyl)-2-methylprop-2-en-1-one (7d)⁹⁹

¹H-NMR (400 MHz): δ = 2.07 (3H, s), 5.57 (1H, s), 5.83 (1H, s), 6.92 (2H, d, J = 6.9 Hz), 7.74 (2H, d, J = 6.9 Hz); ¹³C-NMR (100 MHz) δ = 19.1, 115.3, 125.7, 129.1, 132.5, 143.6, 160.9, 198.8.

propiophenone-d₅ (9a-d₅)¹⁶⁵

¹H-NMR (500 MHz): δ = 1.22 (3H, t, J = 7.4 Hz), 2.99 (2H, q, J = 7.4 Hz), 7.44 (trace), 7.53 (trace), 7.96 (trace, <0.03H); ¹³C-NMR (125 MHz): δ = 8.1, 31.6, 127.4 (t, J = 24.4 Hz), 127.9 (t, J = 25.0 Hz), 132.2 (t, J = 24.4 Hz), 136.6, 200.6.

4-methoxypropiophenone-d₃ (9b-d₃)¹⁶⁶

¹H-NMR (500 MHz): δ = 1.21 (3H, t, J = 7.4 Hz), 2.95 (2H, q, J = 7.4 Hz), 6.92 (2H, d, J = 9.1 Hz), 7.93 (2H, d, J = 9.1 Hz); ¹³C-NMR (125 MHz) δ = 8.40, 31.4, 113.6, 130.0, 130.2, 163.3, 199.4.

3-benzylthio-2-methyl-1-phenylpropan-1-one (8a)¹¹³

¹H-NMR (600 MHz): δ = 1.10 (3H, d, J = 6.9 Hz), 2.47 (1H, dd, J = 6.9, 13.1 Hz), 2.88 (1H, dd, J = 6.9, 13.1 Hz), 3.48 (1H, ddt, J = 6.9, 6.9, 6.9 Hz), 3.65 (2H, s), 7.18 – 7.24 (5H, m), 7.38 (2H, dd, J = 7.6, 6.9 Hz), 7.49 (1H, t, J = 6.9 Hz), 7.79 (2H, d, J = 7.6 Hz); ¹³C-NMR (150 MHz) δ = 17.6, 34.6, 37.2, 41.0, 127.0, 128.2, 128.4, 128.6, 128.8, 133.0, 136.1, 138.4, 202.7.

3-benzylthio-2-methyl-1-(phenyl-d₅)propan-1-one (8a-d₅)

¹H-NMR (600 MHz): δ = 1.10 (3H, d, J = 6.9 Hz), 2.47 (1H, dd, J = 6.9, 13.1 Hz), 2.88 (1H, dd, J = 6.9, 13.1 Hz), 3.48 (1H, ddt, J = 6.9, 6.9, 6.9 Hz), 3.66 (2H, s), 7.18 – 7.24 (5H, m), 7.38 (trace), 7.49 (trace), 7.79 (trace); ¹³C-NMR (150 MHz) δ = 17.6, 34.7, 37.2, 41.0, 127.0, 127.6 – 128.4 (multiplets), 128.5, 128.8, 133.0 (t, J could not be determined), 136.0, 138.4, 202.7.

3-benzylthio-2-methyl-1-(4-methoxyphenyl)propan-1-one (8b)¹¹³

¹H-NMR (400 MHz): δ = 1.20 (3H, d, J = 6.9 Hz), 2.51 (1H, dd, J = 6.8, 12.8 Hz), 2.92 (1H, dd, J = 6.9, 12.8 Hz), 3.49 (1H, dd, J = 6.9, 14.2 Hz), 3.70 (2H, s), 3.86 (3H, s), 6.91 (2H, d, J = 9.2 Hz), 7.22 – 7.30 (5H, m), 7.83 (2H, d, J = 9.2 Hz); ¹³C-NMR (100 MHz) δ = 17.8, 34.9, 37.2, 40.6, 55.4, 113.7, 126.9, 128.5, 128.8, 129.1, 130.6, 138.5, 163.5, 201.2.

3-benzylthio-2-methyl-1-(4-methoxy-d₃-phenyl)propan-1-one (8b-d₃)

¹H-NMR (400 MHz): δ = 1.20 (3H, d, J = 6.9 Hz), 2.51 (1H, dd, J = 6.8, 12.8 Hz), 2.91 (1H, dd, J = 6.9, 12.8 Hz), 3.49 (1H, dd, J = 6.9, 14.2 Hz), 3.70 (2H, s), 3.86 (trace), 6.90 (2H, d, J = 9.2 Hz), 7.22 – 7.30 (5H, m), 7.84 (2H, d, J = 9.2 Hz); ¹³C-NMR (100 MHz) δ = 17.7, 34.9, 37.2, 40.6, 54.6 (t, J = 21.6 Hz), 113.7, 126.9, 128.4, 128.8, 129.1, 130.5, 138.4, 163.5, 201.2.

Raw data of Scheme 4-8. Monitoring trial with methoxy-substituted compounds, Figure 4-1, Figure 4-2 and Figure 4-3

Time (min)	m/z = 304	m/z = 301
1.18	141.24	1693.41
1.68	294.2	2599.04
2.61	2258.23	8190.89
7.86	429.83	20962.13
11.91	730.35	40666.48
18.82	2229.94	136166.6
23.97	479	34530.94
27.52	12927.02	367848.6

Raw data of Scheme 4-9. Reaction monitoring trials under diluted conditions

X = 1.6 mL			X = 4.0 mL		
Time (min)	m/z = 304	m/z = 301	Time (min)	m/z = 304	m/z = 301
0.68	1605.98	296.5	1.88	14721.37	4826.4
1.55	2853.11	2892.73	4.02	11867.66	10296.74
3.83	1231.05	12742.91	9.02	11930.34	78660.29
7.84	1878.66	36805.32	11.97	12350.12	69394.56
17.16	2039.97	91796.6	15.4	10541.94	72156.96
26.15	9646.01	353533.9	20.02	8138.98	95508.59
35.65	3890.19	188382.5	26.18	1878.61	36373.26
42.74	876.06	45560.75	36.94	7449.91	152103.8
			48.17	6580.64	160735.8
			64.75	3260.33	132264.3
			78.89	884.65	83320.8
			91.4	1375.33	54572.69
			101.93	560.01	85128.1

Raw data of Scheme 4-11. Reaction monitoring in the absence of catalyst and base

Time (min)	m/z = 304	m/z = 301
0.53	42536.75	526.06
1.63	51702.98	453.91
2.58	187523.7	2108.28
3.15	95844.64	2929.49
8.89	77577.85	1600.62
22.89	184318.4	4005.62
31.73	53420.98	3914.12
43.05	69400.5	4593.54
64.52	48607.18	5375.56
71.9	83909.6	14092.4
81.93	51575.79	13988.14
109.22	116294	44651.76

Raw data of Figure 4-4. Entry 1, pyridine 5 mol%

Time (min)	m/z = 304	m/z = 301
0.48	21535.19	2976.44
1.16	17802.8	10918.01
1.61	12894.08	2941.23
2.18	17450.26	21422.57
2.61	13877.65	39070.3
3.16	9906.04	38134.77
3.63	18347.88	88798.7
4.23	36570.61	211886.6
5.06	51971.22	243715.9
6.94	40230.6	280985.3
11.64	33652.83	547785.2
16.14	27423.27	688371.5
19.04	17191.63	497915.5
23.99	20717.39	651061.1
28.3	19799.14	702429.6
38.58	15935.69	690480

Raw data of Figure 4-5. Entry 10, pyridine 40 mol%

Time (min)	m/z = 304	m/z = 301
0.38	22986.85	276.23
1.01	37673.21	955.56
1.54	83220.65	2396.48
2.48	51076.31	2744.43
3.13	7665.44	1276.45
4.13	53044.02	8689.27
5.23	28250.44	7709.02
5.84	52514.31	27178.95
6.41	83316.33	38452.54
8.44	25116.77	22909.89
10.09	18431.31	11788.58
12.61	21697.8	28723.98
14.05	35706.93	50855.05
15.94	36088.9	60965.96
19.75	46499.94	110407.3
23	19158.25	66485.29
28.15	49383.39	186238.2
32.26	63485.95	296332.6
36.73	28363.1	164727.9
41.86	13147.67	116896.7
46.82	38470.33	372187.7
50.64	35789.59	369147.9
55.54	36427.61	482894.3
66.77	40214.11	747927.5
86.57	46546.53	1264215
99.08	22498.84	729783.8
115.83	25121.42	1024288

Raw data of Figure 4-6. Reaction profiles of entries 5 – 8 (20 mol%)

Trial 1			Trial 2		
Time (min)	m/z = 304	m/z = 301	Time (min)	m/z = 304	m/z = 301
0.6	12883.22	564.69	0.38	9790.42	1557.87
1.05	24232.21	2823.07	1.01	6026.35	736.31
1.63	21582.93	5621.36	1.71	2471.78	1607.3
2.18	5592.69	8362.88	2.16	20695.94	31231.91
2.78	9607.4	25372.13	2.81	6075.8	17611.34
3.43	9371.2	41736.22	3.36	11583.6	41861.86
4.06	5737.25	31813.13	3.97	16504.4	43815.93
5.08	16940.62	110869.6	4.67	8484.46	39091.66
6.53	8885.32	88213.55	5.89	14096.45	57316.54
7.04	7054.3	79678.64	6.39	8848.38	71602.09
7.58	6397.28	71290.76	7.64	17476.43	151363.2
9.16	4914.41	75585.81	8.67	12671.13	129669.6
9.68	4743.89	77720.38	9.47	15749.34	176262.4
11.09	851.2	18552.78	10.77	22100.31	302599.4
12.81	10524.01	204418.2	11.89	11224.29	142775.9
14.87	10626.02	247001.5	14.35	7108.05	125545.2
16.44	32923.06	569190.6	15.92	11066.58	199592.1
18.91	9028.88	267144	17.42	8340.44	174949.3
21.42	11326.54	307846.5	19.85	917.6	42036.53
24.15	1221.63	40371.67	21.72	8467.87	179890.7
27.49	6807.33	211607.5	23.7	1742.08	78657.07
30.08	6490.52	272142.9	25.22	6385.08	186879.2
32.85	6526.03	329060.9	27.4	11436.77	393210.1
			29.96	5222.6	219628.1
			32.65	9824.71	397613.8
			35.54	18986.03	832463.1
			38.81	20806.28	821568.7
			42.56	5013.54	161310.3
			46.57	11703.69	571560.7
			53.1	24864.32	560434.2

Trial 3			Trial 4		
Time (min)	m/z = 304	m/z = 301	Time (min)	m/z = 304	m/z = 301
0.88	18777.88	14839.19	0.48	26181.74	-372.3
1.54	17336.37	2508.66	0.88	49862.98	1684.35
2.44	14911.54	9975.51	1.53	32867.61	12764.22
3.02	4460.7	5431.82	2.23	35336.97	40874.22
3.59	22809.57	39484.55	3.37	30137.95	70503.33
4.51	6868.49	19853.9	4.25	39822.02	124258.8
5.71	10363.47	45651.08	5.46	32362.61	169548
6.97	34410.09	191694.3	6.8	54879.91	345338
8.22	6835.88	53657.47	8.06	55860.36	440048.5
9.54	11935.26	113240.4	9.51	58286.59	591216.6
11.59	24595.55	261794	10.83	17494.4	227626.6
13.77	16984.37	236601.3	12.59	21749.61	368723.9

(trial 3 continue)			(trial 4 continue)		
16.05	12632.26	210151.8	14.68	22175.43	423066.2
18.52	12794.53	264118	17.24	23733.77	562836.3
21.37	17239.67	377688.5	19.11	16265.75	399437.8
23.67	11362.36	312380.7	21.12	18357.21	465343.4
27.33	5845.8	184213.8	23.24	22323.62	668304.6
31.43	5748.45	219961	25.57	43848.69	953876.7
37.04	12562.6	471311.4	28.69	38942.38	1466337
41.82	17895.03	640127.3	31.95	28580.14	1219059
46.81	4783.79	194498	34.32	23178.95	981186
51.25	22341.57	755441.8			
57.73	18710.04	626549.5			
65.1	14962.81	523120.2			
76.03	9794.55	471491			
84.09	6177.94	421260.8			
92.22	913.01	67728.09			
97.17	6656.73	391000.8			
109.23	4405.19	355155.4			
113.51	24059.39	1115986			

Raw data of Scheme 4-14. Simultaneous monitoring of reaction and pH profiles

Reaction profile

Time (min)	m/z = 304	m/z = 301
0.62	8041.28	1607.04
1.7	10583.39	13546.03
2.75	18483.59	47350.85
3.75	8918.38	26585.46
4.86	10328.77	57122.3
6.2	16168.23	143939.3
8.1	11524.31	119164.5
9.46	30433.27	350675.3
15.78	20496.62	421373.1
18.34	17232.49	437586
21.34	24148.63	657952.1

pH profile

Time (min)	pH	(continue)		(continue)		(continue)		(continue)		(continue)	
0.00	4.801	5.08	4.678	10.17	4.686	15.25	4.695	20.33	4.697	25.42	4.697
0.08	4.751	5.17	4.678	10.25	4.686	15.33	4.694	20.42	4.697	25.50	4.697
0.17	4.725	5.25	4.678	10.33	4.686	15.42	4.695	20.50	4.697	25.58	4.697
0.25	4.712	5.33	4.678	10.42	4.686	15.50	4.694	20.58	4.697	25.67	4.697
0.33	4.705	5.42	4.679	10.50	4.686	15.58	4.695	20.67	4.697	25.75	4.697
0.42	4.7	5.50	4.679	10.58	4.686	15.67	4.694	20.75	4.697	25.83	4.697
0.50	4.697	5.58	4.679	10.67	4.686	15.75	4.694	20.83	4.696	25.92	4.698
0.58	4.694	5.67	4.679	10.75	4.687	15.83	4.694	20.92	4.696	26.00	4.697
0.67	4.692	5.75	4.679	10.83	4.687	15.92	4.694	21.00	4.697	26.08	4.697
0.75	4.691	5.83	4.68	10.92	4.686	16.00	4.694	21.08	4.697	26.17	4.697
0.83	4.69	5.92	4.679	11.00	4.687	16.08	4.694	21.17	4.697	26.25	4.697

0.92	4.689	6.00	4.68	11.08	4.687	16.17	4.695	21.25	4.696	26.33	4.697
1.00	4.688	6.08	4.679	11.17	4.688	16.25	4.694	21.33	4.697	26.42	4.697
1.08	4.686	6.17	4.681	11.25	4.687	16.33	4.695	21.42	4.696	26.50	4.697
1.17	4.687	6.25	4.68	11.33	4.687	16.42	4.694	21.50	4.697	26.58	4.697
1.25	4.686	6.33	4.681	11.42	4.688	16.50	4.695	21.58	4.696	26.67	4.697
1.33	4.686	6.42	4.68	11.50	4.688	16.58	4.695	21.67	4.696	26.75	4.697
1.42	4.684	6.50	4.681	11.58	4.688	16.67	4.695	21.75	4.696	26.83	4.697
1.50	4.683	6.58	4.681	11.67	4.688	16.75	4.695	21.83	4.696	26.92	4.697
1.58	4.683	6.67	4.682	11.75	4.687	16.83	4.695	21.92	4.696	27.00	4.697
1.67	4.682	6.75	4.681	11.83	4.691	16.92	4.695	22.00	4.696	27.08	4.697
1.75	4.682	6.83	4.682	11.92	4.692	17.00	4.696	22.08	4.696	27.17	4.697
1.83	4.682	6.92	4.682	12.00	4.692	17.08	4.696	22.17	4.696	27.25	4.697
1.92	4.685	7.00	4.681	12.08	4.692	17.17	4.695	22.25	4.696	27.33	4.697
2.00	4.679	7.08	4.682	12.17	4.692	17.25	4.696	22.33	4.696	27.42	4.697
2.08	4.679	7.17	4.682	12.25	4.692	17.33	4.696	22.42	4.696	27.50	4.697
2.17	4.678	7.25	4.682	12.33	4.692	17.42	4.696	22.50	4.696	27.58	4.697
2.25	4.678	7.33	4.682	12.42	4.692	17.50	4.697	22.58	4.696	27.67	4.697
2.33	4.678	7.42	4.682	12.50	4.692	17.58	4.697	22.67	4.696	27.75	4.697
2.42	4.678	7.50	4.683	12.58	4.692	17.67	4.695	22.75	4.696	27.83	4.697
2.50	4.678	7.58	4.682	12.67	4.692	17.75	4.695	22.83	4.696	27.92	4.697
2.58	4.678	7.67	4.682	12.75	4.692	17.83	4.688	22.92	4.696	28.00	4.697
2.67	4.678	7.75	4.682	12.83	4.693	17.92	4.693	23.00	4.696	28.08	4.697
2.75	4.677	7.83	4.683	12.92	4.693	18.00	4.693	23.08	4.696	28.17	4.697
2.83	4.678	7.92	4.682	13.00	4.693	18.08	4.693	23.17	4.697	28.25	4.696
2.92	4.678	8.00	4.682	13.08	4.692	18.17	4.694	23.25	4.696	28.33	4.697
3.00	4.678	8.08	4.682	13.17	4.694	18.25	4.692	23.33	4.696	28.42	4.697
3.08	4.677	8.17	4.683	13.25	4.693	18.33	4.694	23.42	4.696	28.50	4.697
3.17	4.678	8.25	4.683	13.33	4.693	18.42	4.692	23.50	4.696	28.58	4.697
3.25	4.677	8.33	4.683	13.42	4.693	18.50	4.692	23.58	4.696	28.67	4.697
3.33	4.677	8.42	4.683	13.50	4.693	18.58	4.691	23.67	4.696	28.75	4.697
3.42	4.677	8.50	4.683	13.58	4.694	18.67	4.691	23.75	4.696	28.83	4.697
3.50	4.676	8.58	4.683	13.67	4.693	18.75	4.689	23.83	4.696	28.92	4.697
3.58	4.678	8.67	4.683	13.75	4.693	18.83	4.69	23.92	4.696	29.00	4.697
3.67	4.677	8.75	4.683	13.83	4.693	18.92	4.69	24.00	4.696	29.08	4.697
3.75	4.677	8.83	4.683	13.92	4.693	19.00	4.689	24.08	4.696	29.17	4.696
3.83	4.677	8.92	4.686	14.00	4.693	19.08	4.69	24.17	4.696	29.25	4.697
3.92	4.677	9.00	4.685	14.08	4.693	19.17	4.69	24.25	4.696	29.33	4.696
4.00	4.677	9.08	4.685	14.17	4.693	19.25	4.69	24.33	4.696	29.42	4.697
4.08	4.677	9.17	4.685	14.25	4.694	19.33	4.69	24.42	4.696	29.50	4.696
4.17	4.677	9.25	4.685	14.33	4.693	19.42	4.69	24.50	4.696	29.58	4.697
4.25	4.677	9.33	4.685	14.42	4.693	19.50	4.69	24.58	4.696	29.67	4.696
4.33	4.678	9.42	4.684	14.50	4.694	19.58	4.694	24.67	4.697	29.75	4.696
4.42	4.676	9.50	4.685	14.58	4.693	19.67	4.698	24.75	4.696	29.83	4.696
4.50	4.677	9.58	4.684	14.67	4.694	19.75	4.697	24.83	4.695	29.92	4.696
4.58	4.677	9.67	4.684	14.75	4.693	19.83	4.698	24.92	4.697	30.00	4.696
4.67	4.677	9.75	4.684	14.83	4.693	19.92	4.698	25.00	4.698		
4.75	4.677	9.83	4.686	14.92	4.693	20.00	4.697	25.08	4.697		
4.83	4.678	9.92	4.686	15.00	4.693	20.08	4.698	25.17	4.698		
4.92	4.678	10.00	4.686	15.08	4.694	20.17	4.697	25.25	4.697		
5.00	4.678	10.08	4.686	15.17	4.694	20.25	4.697	25.33	4.698		

5. Indium(0) catalyzed allylation reactions in water

Ketone **10a-d₃**, Allylboronate **11a – 11d** were prepared following reported method.^{123,167–170} Ketones **10a – 10h** were purchased from TCI Co., LTD. Indium powder was purchased from Aldrich Co. Internal standard **12a-d₃** was synthesized as follows. Internal standard **12b-d₃** was synthesized following reported standard reaction procedure.

Preparation of 12a-d₃.

To a solution of acetophenone-d₃ (**10a-d₃**; 1.23 g, 10 mmol) in anhydrous THF, a commercial allylmagnesium bromide solution (Aldrich; 1M, 12 mL) was added dropwise at 0 °C. The mixture was stirred 3 hours at room temperature and then was quenched with 1N aq. HCl solution. The mixture was extracted with ethyl acetate and combined organic layer was washed with brine. After dryness over Na₂SO₄ the material was purified over silica gel column chromatography to afford the target compound **12a-d₃** (730 mg, 4.42 mmol, 44%).

Phenylpent-4-en-2-ol (12a-d₃)

¹H-NMR (400 MHz): δ = 1.55 (trace), 2.08 (1H br s), 2.51 (1H, dd, J = 8.4, 13.2 Hz), 2.70 (1H, dd, J = 6.5, 13.2 Hz), 5.11-5.16 (2H, m), 5.57-5.70 (1H, m), 7.20-7.45 (5H, m); ¹³C-NMR (100 MHz): δ = 30.0 (multiplet), 48.4, 73.6, 119.4, 124.7, 126.6, 128.1, 133.6, 147.6.

3-Methyl-2-phenyl-4-penten-2-ol (12b-d₃)

(*syn* isomer) ¹H-NMR (500 MHz): δ = 0.85 (3H, d, J = 6.8 Hz), 1.50 (trace), 1.86 (1H, br s), 2.51 – 2.61 (1H, m), 5.09 – 5.13 (2H, m), 5.77 – 5.85 (1H, m), 7.22 – 7.25 (1H, m), 7.33 – 7.43 (4H, m); ¹³C-NMR (125 MHz): δ = 14.7, 48.8, 75.6, 116.6, 124.8, 126.5, 127.9, 139.8, 146.9.

Raw data of Scheme 5-6. Monitoring trial of the allylation reaction

Time (min)	m/z = 148	m/z = 145
0.83	36945.29	84579.88
4.13	36881.84	56384.04
7.41	44969.61	56855.06
10.67	55614.67	76799.11
12.65	2738.14	16112.49
17.55	4405.37	3562.82
23.6	12032.63	4765.67
34.05	19515.2	8510.26
44.69	8404.11	98102.53
53.59	9552.75	11575.37
82.81	1501.28	5702.57
96.55	5845.2	13117.95

Raw data of Scheme 5-11. Monitoring trial of allylation reaction using α -methylallylboronate

Time (min)	m/z = 162	m/z = 159
0.94	146244.6	6343.66
6.76	169771.5	3630286
12.51	79691.72	4161838
18.3	80518.28	4022886
24.08	69690.97	3629325
29.9	67762.27	3579593
35.65	61689.11	3187996
41.38	12263.23	689872.5
47.22	77877.12	3936027
53	64283.79	3657826
58.79	71449.87	3754863
64.55	49086.26	2770308
70.38	63715.82	3539038
76.16	59825.66	3369743
81.92	61953.02	3521009
87.72	53814.23	2933860
93.4	2209.07	146713.7
99.2	10434.6	630836
105	21537.55	1258121
110.78	16159.9	1051764
116.58	26605.66	1533784

Raw data of Scheme 5-13. The reaction monitoring study with various allylboronates

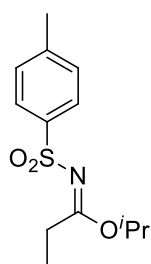
entry 2.			entry 3.			entry 4.		
Time (min)	m/z = 148	m/z =145	Time (min)	m/z = 162	m/z = 159	Time (min)	m/z = 162	m/z = 159
0.79	80443.94	801.88	0.88	3053.22	17358.84	0.91	1348.79	3237.98
1.68	125776.9	3373.2	2.18	2732.34	15326.48	2.15	1562.06	13660.36
4.19	156998.8	8993.27	3.44	2790.33	22210.2	4.74	1669.42	41733.37
5.54	164967.5	17346.73	4.74	4331.14	26260.33	6.01	1570.63	70707.58
8.11	158464	24748.88	5.99	3055.7	32724.67	7.21	1057.07	34986.45
9.39	65239.38	11495.66	7.26	2639.85	28990.04	8.49	770.17	42016.58
10.61	122375.9	22572.27	8.59	3870.77	43127.81	9.88	1324.21	93328.42
11.89	177135.5	52395.14	9.87	4301.51	53961.52	11.06	245.83	31070.65
13.17	81129	22101.25	11.14	4487.13	64217.38	12.34	934.3	75645.24
14.47	96951.73	31271.3	12.44	3997.83	59447.76	13.72	1139.87	99722.45
15.8	166889.6	70014	13.7	4043.4	66894.34	14.91	664.82	77621.41
17.04	152854.5	88695.19	14.99	3627.92	77751.79	16.29	1546.77	156325.3
18.37	177950.8	108339.9	16.22	3659.35	78148.57	17.47	770.95	92731.75
19.67	118884.4	69408.82	17.57	3460.53	87279.86	18.76	938.2	110777.6
20.95	151621.4	103013.8	18.85	3760.82	100655.4	20.14	1105.63	142501.7
22.22	69236.16	53265.39	20.15	5105.62	160839.2	21.32	957.14	163274.7
23.43	96979.91	81008.14	21.35	4894.31	162794.1	22.6	979.86	128983.2
24.72	154317.1	142339.2	22.63	3050.56	110743.3	23.89	1148.56	157505
26.02	68801.88	70582.63	23.95	3238.97	120790.6	25.17	1726.48	248034.3
27.32	112952	128991.6	25.2	3309.75	158322.9	26.49	607.91	102548.5
28.6	68295.4	82362.14	26.48	3141.09	151310.4	27.73	824.07	118613.5
29.88	115317.5	151451.7	27.77	3625.15	181333.3	29.05	1000.83	190350.5
31.15	102954.1	146463.6	29.11	4809.19	244438.9	30.37	1409.16	247661.3
32.5	146325.1	220834.6	30.36	3145.05	207091.6			
33.78	122035.8	198183.4						
35.01	136773.1	237020.7						
36.35	138305	257716.9						
37.58	142351.4	275799.6						

Topic 6. Organosuperbase-catalyzed 1,4-addition reactions of sulfonylimidates

Typical procedure for the preparation of sulfonylimidates and compound information

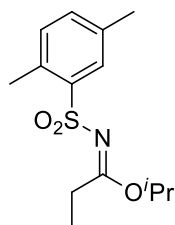
All sulfonylimidates were prepared following the reported methods.¹³⁸ To a solution of the crude propionimide HCl salt (5.00 g, 33.0 mmol, 1.0 equiv) prepared from Pinner reaction in dichloromethane (100 mL), Et₃N (13.8 mL, 99.0 mmol, 3.0 equiv), 4-toluenesulfonyl chloride (6.29 g, 33.0 mmol, 1.0 equiv), and DMAP (403 mg, 3.3 mmol, 10 mol%) were added at rt. The reaction mixture was stirred until 4-toluenesulfonyl chloride was consumed (22 h). The mixture was poured into saturated aq. NH₄Cl solution, and extracted with DCM. The organic layers were combined and dried over anhydrous Na₂SO₄. Filtration and evaporation of the solvents afforded the crude product, which was purified by column chromatography on silica gel and recrystallized from hexane/EtOAc (4/1) to give the pure sulfonylimidate **14a**. (7.15 g, 80%)

Isopropyl *N*-(4-toluenesulfonyl)-propionimide (**14a**)¹³⁸



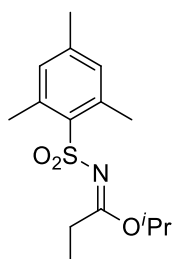
¹H NMR (CDCl₃) δ = 7.82 (d, 2H, J = 8.5 Hz), 7.29 (d, 2H, J = 7.9 Hz), 5.10 (septet, 1H, J = 6.2 Hz), 2.88 (q, 2H, J = 7.6 Hz), 2.42 (s, 3H), 1.23 (d, 6H, J = 6.2 Hz), 1.21 (t, 3H, J = 6.2 Hz); ¹³C NMR (CDCl₃) δ = 176.3, 142.9, 139.4, 129.3, 126.4, 71.9, 27.8, 21.5, 21.1, 10.1.

Isopropyl *N*-(2,5-xylenesulfonyl)-propionimide (**14b**)¹³⁸

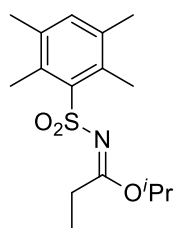


¹H NMR (CDCl₃) δ = 8.20 (s, 1H), 6.90 (d, 1H, J = 7.4 Hz), 6.84 (dd, 1H, J = 7.4, 1.4 Hz), 4.74 (septet, 1H, J = 6.3 Hz), 2.91 (q, 2H, J = 7.4 Hz), 2.77 (s, 3H), 1.94 (s, 3H), 1.07 (t, 3H, J = 7.4 Hz), 0.83 (d, 6H, J = 6.3 Hz); ¹³C NMR (CDCl₃) δ = 176.2, 141.2, 135.9, 134.4, 133.0, 132.2, 128.9, 71.2, 28.4, 21.1, 20.6, 20.2, 10.4.

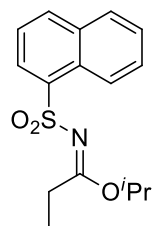
Isopropyl *N*-(2,4,6-trimethylbenzenesulfonyl)-propionimide (**14c**)



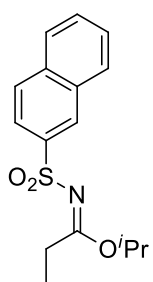
White crystal; ¹H NMR (CDCl₃) δ = 6.91 (s, 2H), 5.01 (septet, 1H, J = 6.2 Hz), 2.81 (q, 2H, J = 7.4 Hz), 2.63 (s, 6H), 2.27 (s, 3H), 1.21-1.15 (m, 9H); ¹³C NMR (CDCl₃) δ = 176.0, 141.7, 138.5, 136.4, 131.5, 71.4, 27.8, 22.7, 21.4, 20.9, 10.1; IR (neat) 2981, 2940, 1596, 1559, 1541, 1466, 1457, 1384, 1310, 1235, 1153, 1104, 1089, 1072, 1061 cm⁻¹; HRMS (DART) Exact mass calcd for C₁₅H₂₄NO₃S [M+H]⁺, 298.1477. Found 298.1482.

Isopropyl *N*-(2,3,5,6-tetramethylbenzenesulfonyl)-propionimide (14d)

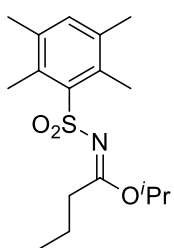
White crystal; ^1H NMR (CDCl_3) δ = 7.05 (s, 1H), 4.98 (septet, 1H, J = 6.2 Hz), 2.73 (q, 2H, J = 7.4 Hz), 2.48 (s, 6H), 2.19 (s, 6H), 1.16 (d, 6H, J = 6.2 Hz), 1.10 (t 3H, J = 7.4); ^{13}C NMR (CDCl_3) δ = 176.0, 140.2, 135.6, 135.1, 134.5, 71.4, 27.8, 21.4, 20.7, 17.9, 10.1; IR (neat) 2982, 2948, 2885, 1589, 1559, 1541, 1522, 1507, 1464, 1459, 1438, 1385, 1375, 1354, 1297, 1233, 1139, 1106, 1086, 1071 cm^{-1} ; HRMS (DART) Exact mass calcd for $\text{C}_{16}\text{H}_{26}\text{NO}_3\text{S}$ $[\text{M}+\text{H}]^+$, 312.1633. Found 312.1651.

Isopropyl *N*-(1-naphthalenesulfonyl)-propionimide (14e)

White crystal; ^1H NMR (C_6D_6) δ = 8.84 (d, 1H, J = 8.9 Hz), 8.24 (d, 1H, J = 7.6 Hz), 7.20 (d, 2H, J = 8.3 Hz), 7.09 (t, 1H, J = 8.3 Hz), 6.91 (t, 1H, J = 7.6 Hz), 6.71 (t, 1H, J = 7.6 Hz), 4.31 (septet, 1H, J = 6.2 Hz), 2.65 (q, 2H, J = 7.6 Hz), 0.77 (t, 3H, J = 7.6 Hz), 0.44 (d, 6H, J = 6.2 Hz); ^{13}C NMR (C_6D_6) δ = 176.4, 138.6, 134.6, 133.7, 129.1, 128.9, 128.3, 127.6, 126.7, 126.6, 124.3, 71.6, 28.4, 20.9, 10.3; IR (neat) 3057, 2982, 2942, 2883, 1588, 1507, 1465, 1384, 1358, 1309, 1265, 1235, 1201, 1160, 1131, 1102, 1090, 1071, 1030 cm^{-1} ; HRMS (DART) Exact mass calcd for $\text{C}_{16}\text{H}_{20}\text{NO}_3\text{S}$ $[\text{M}+\text{H}]^+$, 306.1164. Found 306.1184.

Isopropyl *N*-(2-naphthalenesulfonyl)-propionimide (14f)

White crystal; ^1H NMR (C_6D_6) δ = 8.44 (s, 1H), 7.83 (dd, 1H, J = 8.6, 1.7 Hz), 7.24 (d, 1H, J = 8.9 Hz), 7.19-7.14 (m, 2H), 6.90-6.87 (m, 1H), 6.83 (t, 1H, J = 7.6 Hz), 4.45 (septet, 1H, J = 6.2 Hz), 2.65 (q, 2H, J = 7.6 Hz), 0.79 (t, 3H, J = 7.2 Hz), 0.54 (d, 6H, J = 6.2 Hz); ^{13}C NMR (C_6D_6) δ = 176.1, 140.5, 134.9, 132.5, 129.4, 129.2, 128.4, 128.3, 127.7, 127.3, 123.1, 71.6, 28.3, 20.9, 10.4; IR (neat) 3059, 2982, 2883, 1593, 1558, 1541, 1506, 1465, 1385, 1358, 1308, 1235, 1154, 1130, 1103, 1077, 1030 cm^{-1} ; HRMS (DART) Exact mass calcd for $\text{C}_{16}\text{H}_{20}\text{NO}_3\text{S}$ $[\text{M}+\text{H}]^+$, 306.1164. Found 306.1182.

Isopropyl *N*-(2,3,5,6-tetramethylbenzenesulfonyl)-butanimide (14g)

White crystal; ^1H NMR (CDCl_3) δ = 7.13 (s, 1H), 5.07 (septet, 1H, J = 6.2 Hz), 2.75 (t, 2H, J = 7.7 Hz), 2.56 (s, 6H), 2.27 (s, 6H), 1.70-1.62 (m, 2H), 1.23 (d, 6H, J = 6.2 Hz), 0.93 (t, 3H, J = 7.4 Hz); ^{13}C NMR (CDCl_3) δ = 175.3, 140.2, 135.6, 135.1, 134.6, 71.3, 36.0, 21.4, 20.8, 19.4, 17.9, 13.7; IR (neat) 3232, 2968, 2936, 2875, 1719, 1697, 1686, 1591, 1464, 1365, 1338, 1305, 1258, 1208, 1142, 1100, 1016 cm^{-1} ; HRMS (DART) Exact mass calcd for $\text{C}_{17}\text{H}_{28}\text{NO}_3\text{S}$ $[\text{M}+\text{H}]^+$, 326.1790. Found 326.1759.

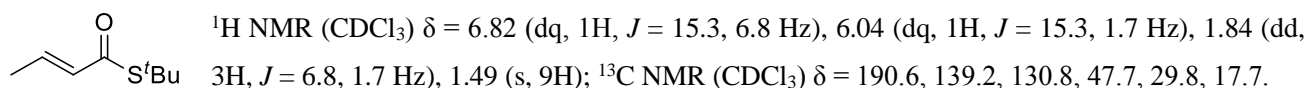
Preparation of Michael acceptors and compound information

Michael acceptors **15a-d**, **18a** and **18b** were purchased from Tokyo Chemical Industry Co., Ltd. or Aldrich Co., Ltd. *S*-*tert*-Butyl thiocrotonate **18c** was prepared as follows; crotonoyl chloride (5 mL, 52 mmol) was added carefully at 0 $^{\circ}\text{C}$ to a mixture of $t\text{-BuSH}$ (7 mL, 62 mmol), Et_3N (10.8 mL, 78 mmol) and DMAP (315 mg, 2.7 mmol)

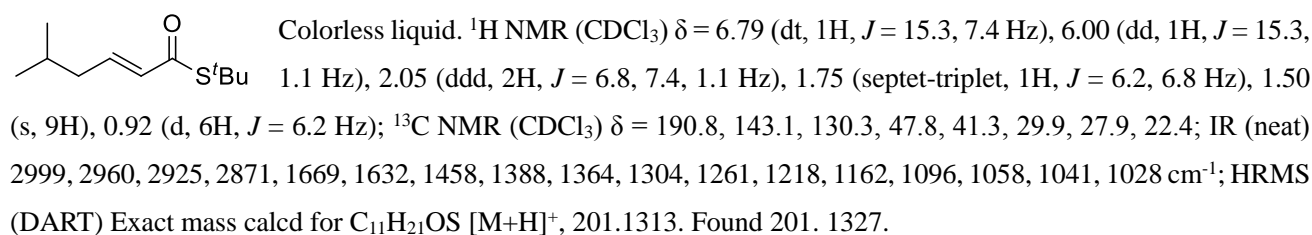
in 50 mL of THF. After addition, the mixture was stirred for 24 h at rt and then the reaction was quenched by adding H₂O (100 mL). The mixture was extracted with Et₂O (50 mL × 3) and combined organic layers were washed with brine and then dried over anhydrous Na₂SO₄. The crude material was distilled (79 °C / 18 mmHg) to afford pure *tert*-butyl thiocrotonate **18c** (4.67 g, 62%).

Other thioesters were synthesized by HWE reactions following reported method.¹⁷¹

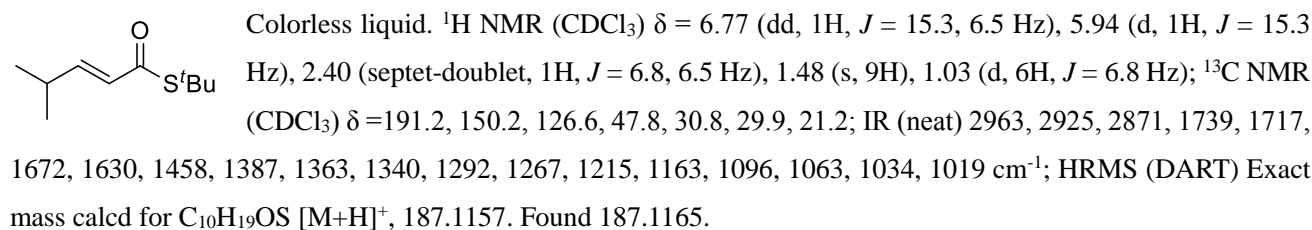
(*E*)-*S*-*tert*-butylbut-2-enethiate (18c**)**¹⁷²



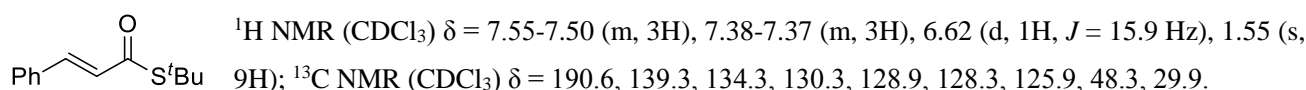
(*E*)-*S*-*tert*-butyl-5-methylhex-2-enethiate (18d**)**



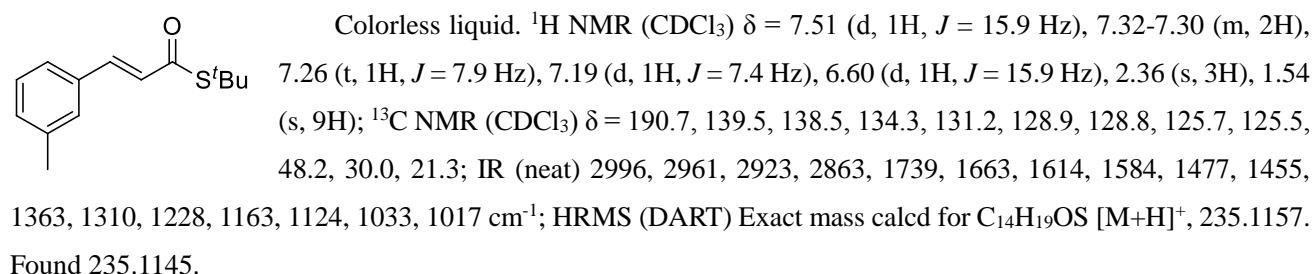
(*E*)-*S*-*tert*-butyl-4-methylpent-2-enethiate (18e**)**



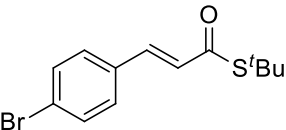
(*E*)-*S*-*tert*-butyl-3-phenylprop-2-enethiate (18f**)**¹⁷³



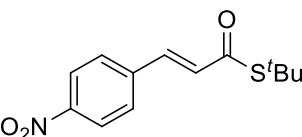
(*E*)-*S*-*tert*-butyl-3-(3-methylphenyl)prop-2-enethiate (18g**)**



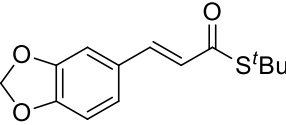
(E)-S-tert-butyl-3-(4-bromophenyl)prop-2-enethiate (18h)

 Pale yellow crystal. ¹H NMR (CDCl₃) δ = 7.50 (d, 2H, *J* = 8.5 Hz), 7.46 (d, 1H, *J* = 15.9 Hz), 7.37 (d, 2H, *J* = 8.5 Hz), 6.59 (d, 1H, *J* = 15.9 Hz), 1.54 (s, 9H); ¹³C NMR (CDCl₃) δ = 190.3, 137.8, 133.3, 132.1, 129.6, 126.4, 124.5, 48.5, 29.9; IR (neat) 3031, 2996, 2967, 2913, 2890, 1739, 1658, 1612, 1583, 1560, 1487, 1453, 1400, 1363, 1320, 1291, 1216, 1203, 1160, 1069, 1034, 1012 cm⁻¹; HRMS (DART) Exact mass calcd for C₁₃H₁₆BrOS [M+H]⁺, 299.0105. Found 299.0153.

(E)-S-tert-butyl-3-(4-nitrophenyl)prop-2-enethiate (18i)

 Yellow crystal. ¹H NMR (CDCl₃) δ = 8.24 (d, 2H, *J* = 8.7 Hz), 7.67 (d, 2H, *J* = 8.7 Hz), 7.54 (d, 1H, *J* = 16.0 Hz), 6.71 (d, 1H, *J* = 16.0 Hz), 1.56 (s, 9H); ¹³C NMR (CDCl₃) δ = 189.9, 136.1, 129.6, 128.8, 124.2, 48.9, 29.8; IR (neat) 2970, 2927, 2867, 1739, 1720, 1653, 1616, 1596, 1520, 1475, 1458, 1413, 1364, 1345, 1274, 1218, 1162, 1127, 1109, 1033, 1014 cm⁻¹; HRMS (DART) Exact mass calcd for C₁₃H₁₆NO₃S [M+H]⁺, 266.0851. Found 266.0818.

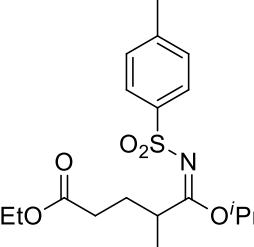
(E)-S-tert-butyl-3-(benzo-[d][1,3]-dioxol-5-yl)prop-2-enethiate (18j)

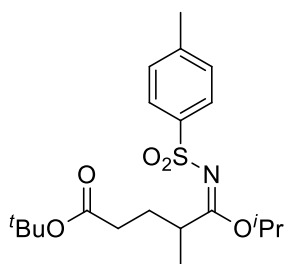
 White crystal. ¹H NMR (CDCl₃) δ = 7.45 (d, 1H, *J* = 15.8 Hz), 7.01-7.00 (m, 2H), 6.80 (d, 1H, *J* = 8.9 Hz), 6.46 (d, 1H, *J* = 15.8 Hz), 6.00 (s, 2H), 1.54 (s, 9H); ¹³C NMR (CDCl₃) δ = 190.5, 149.7, 148.3, 139.0, 128.7, 124.8, 124.0, 108.6, 106.5, 101.5, 48.2, 29.9; IR (neat) 3054, 2989, 2968, 2897, 1739, 1659, 1598, 1504, 1489, 1448, 1363, 1262, 1128, 1035, 1015 cm⁻¹; HRMS (DART) Exact mass calcd for C₁₄H₁₇O₃S [M+H]⁺, 265.0898. Found 265.0860.

General procedure of Michael addition reaction of sulfonylimidates and compound information

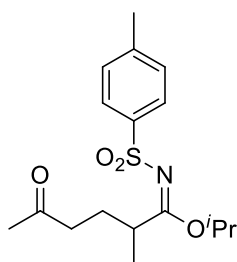
Sulfonylimidate **14d** (93.4 mg, 0.300 mmol) and thioester **18c** (60 μL, 3.60 mmol) were placed in a well-dried reaction tube, and were dissolved in toluene (0.55 mL) under Ar. The mixture was cooled to -20 °C and *i*Bu-PAP soln. in toluene (110.9 g·L⁻¹, 46 μL, 5 mol%) was added. The mixture was stirred for 18 h and then sat. NH₄Cl aq was added. The mixture was extracted with DCM (15 mL × 3) and dried over anhydrous Na₂SO₄. After filtration and removal of the solvents under reduced pressure, ¹H-NMR analysis of the crude product was conducted with 1,1,2,2-tetrachloroethane as an internal standard. Purification of the crude product was performed by preparative TLC (Hexane/EtOAc = 5/1) to afford the desired product **19dc** (120.5 mg, 88%).

Isopropyl 2-methyl-5-ethoxy-5-oxo-N-(4-toluenesulfonyl)-pentanimidate (16a)

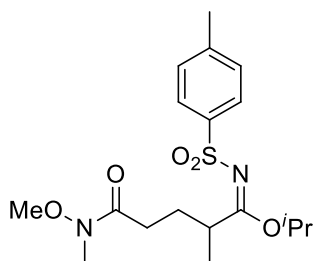
 White solid; ¹H NMR (CDCl₃) δ = 7.81 (d, 2H, *J* = 7.9 Hz), 7.29 (d, 2H, *J* = 7.9 Hz), 5.02 (septet, 1H, *J* = 6.2 Hz), 4.13 (q, 2H, *J* = 7.4 Hz), 3.66-3.61 (m, 1H), 2.42-2.34 (m, 4H), 2.28-2.21 (m, 1H), 2.01-1.94 (m, 1H), 1.85-1.78 (m, 1H), 1.27-1.21 (m, 12H); ¹³C NMR (CDCl₃) δ = 177.3, 172.7, 142.9, 139.3, 129.2, 126.4, 71.7, 60.3, 38.1, 31.8, 28.7, 21.4, 21.0, 20.9, 17.6, 14.1; IR (neat) 2981, 2937, 2877, 1736, 1596, 1461, 1378, 1353, 1307, 1261, 1157, 1093, 1038 cm⁻¹; HRMS (DART) Exact mass calcd for C₁₈H₂₈NO₅S [M+H]⁺, 370.1688. Found 370.1674.

Isopropyl 2-methyl-5-*tert*-butoxy-5-oxo-*N*-(4-toluenesulfonyl)-pentanimidate (16b)

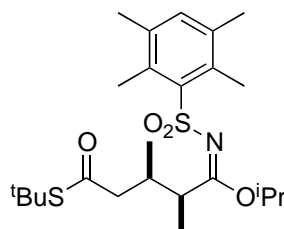
Colorless oil; ^1H NMR (CDCl_3) δ = 7.81 (d, 2H, J = 8.5 Hz), 7.29 (d, 2H, J = 8.5 Hz), 5.02 (septet, 1H, J = 6.2 Hz), 3.62 (dq, 1H, J = 15.3, 6.8 Hz), 2.41 (s, 3H), 2.33-2.26 (m, 1H), 2.19-2.13 (m, 1H), 1.97-1.90 (m, 1H), 1.80-1.74 (m, 1H), 1.45 (s, 9H), 1.24-1.20 (m, 9H); ^{13}C NMR (CDCl_3) δ = 177.4, 142.0, 142.8, 139.5, 129.2, 126.4, 80.2, 71.6, 38.1, 33.0, 28.8, 27.9, 21.3, 20.9(2), 20.8(7), 17.6; IR (neat) 2980, 2936, 2877, 1730, 1596, 1459, 1368, 1307, 1261, 1215, 1156, 1093 cm^{-1} ; HRMS (DART) Exact mass calcd for $\text{C}_{20}\text{H}_{35}\text{N}_2\text{O}_5\text{S}$ $[\text{M}+\text{NH}_4]^+$, 415.2267. Found 415.2289.

Isopropyl 2-methyl-5-oxo-*N*-(4-toluenesulfonyl)-hexanimidate (16c)

White solid; ^1H NMR (CDCl_3) δ = 7.81 (d, 2H, J = 7.9 Hz), 7.30 (d, 2H, J = 7.9 Hz), 5.03 (septet, 1H, J = 6.2 Hz), 3.57-3.53 (m, 1H), 2.56-2.49 (m, 1H), 2.42 (s, 3H), 2.40-2.35 (m, 1H), 2.14 (s, 3H), 1.94-1.87 (m, 1H), 1.80-1.73 (m, 1H), 1.24 (d, 3H, J = 6.2 Hz), 1.22 (d, 3H, J = 6.2 Hz), 1.18 (d, 3H, J = 6.8 Hz); ^{13}C NMR (CDCl_3) δ = 207.6, 177.7, 142.9, 139.5, 129.3, 126.4, 71.7, 41.0, 38.3, 29.8, 27.6, 21.4, 21.0, 20.9, 17.9; IR (neat) 2982, 2936, 2876, 1718, 1593, 1495, 1458, 1417, 1357, 1305, 1227, 1216, 1156, 1093, 1018 cm^{-1} ; HRMS (DART) Exact mass calcd for $\text{C}_{17}\text{H}_{29}\text{N}_2\text{O}_4\text{S}$ $[\text{M}+\text{NH}_4]^+$, 357.1848. Found 357.1808.

Isopropyl 2-methyl-5-methoxymethylamino-5-oxo-*N*-(4-toluenesulfonyl)-pentanimidate (16d)

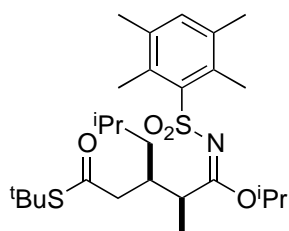
Colorless oil; ^1H NMR (CDCl_3) δ = 7.81 (d, 2H, J = 7.9 Hz), 7.29 (d, 2H, J = 7.9 Hz), 5.03 (septet, 1H, J = 6.0 Hz), 3.68 (s, 3H), 3.65-3.60 (m, 1H), 3.17 (s, 3H), 2.54-2.37 (m, 5H), 2.01-1.93 (m, 1H), 1.87-1.79 (m, 1H), 1.24-1.21 (m, 9H); ^{13}C NMR (CDCl_3) δ = 177.7, 142.8, 139.5, 129.2, 126.4, 71.7, 61.1, 38.4, 28.6, 21.4, 21.0, 20.9, 17.7; IR (neat) 2980, 2938, 2876, 1738, 1665, 1591, 1459, 1418, 1383, 1358, 1304, 1215, 1181, 1156, 1092, 1067 cm^{-1} ; HRMS (DART) Exact mass calcd for $\text{C}_{18}\text{H}_{29}\text{N}_2\text{O}_5\text{S}$ $[\text{M}+\text{H}]^+$, 385.1797. Found 385.1776.

Isopropyl 2,3-dimethyl-5-*tert*-butylthio-5-oxo-*N*-(2,3,5,6-tetramethylbenzenesulfonyl)-pentanimidate (19dc)

Obtained as diastereomer mixture; Colorless oil; ^1H NMR (CDCl_3) δ = 7.14 (s, 1H), 5.09 (septet, 1H, J = 6.2 Hz), 3.16-3.13 (m, 1H), 2.56 (s, 6H), 2.28-2.19 (m, 8H), 2.07-2.02 (m, 1H), 1.44 (s, 9H), 1.29-1.24 (m, 6H), 1.16 (d, 3H, J = 6.8 Hz), 0.92 (d, 3H, J = 6.8 Hz); ^{13}C NMR (CDCl_3) δ = 199.1, 177.3, 140.1, 135.6, 135.2, 134.4, 71.3, 49.2, 47.8, 44.0, 33.9, 29.6, 21.2, 21.1, 20.7, 17.8, 16.3, 15.5; IR (neat) 2969, 2929, 2878, 1738, 1717, 1683, 1590, 1459, 1383, 1363, 1288, 1207, 1145, 1102, 1074 cm^{-1} ; HRMS (DART)

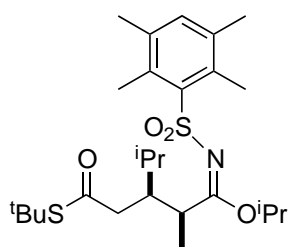
Exact mass calcd for $\text{C}_{24}\text{H}_{40}\text{NO}_4\text{S}_2$ $[\text{M}+\text{H}]^+$, 470.2399. Found 470.2368.

Isopropyl 2,5-dimethyl-3-(2-*tert*-butylthio-2-oxoethyl)-*N*-(2,3,5,6-tetramethylbenzenesulfonyl)-hexanimidate (19dd)



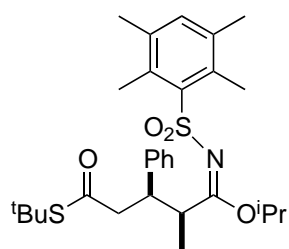
Obtained as diastereomer mixture; Colorless oil; ^1H NMR (CDCl_3) δ = 7.13 (s, 1H), 5.07 (septet, 1H, J = 6.2 Hz), 3.35 (septet, 1H, J = 7.4 Hz), 2.56 (s, 6H), 2.38 (dd, 1H, J = 14.5, 2.6 Hz), 2.26-2.19 (m, 8H), 1.59-1.56 (m, 1H), 1.44 (s, 9H), 1.271.24 (m, 6H), 1.21-1.14 (m, 4H), 1.14-1.05 (m, 1H), 0.84 (d, 3H, J = 6.8 Hz); ^{13}C NMR (CDCl_3) δ = 199.2, 177.3, 140.3, 135.6, 134.5, 71.4, 48.1, 47.7, 32.9, 41.9, 36.3, 29.6, 25.5, 23.4, 22.2, 21.3, 20.7, 17.9, 16.0; IR (neat) 2957, 2927, 2870, 1739, 1720, 1684, 1590, 1461, 1364, 1302, 1228, 1207, 1145, 1101, 1014 cm^{-1} ; HRMS (DART) Exact mass calcd for $\text{C}_{27}\text{H}_{46}\text{NO}_4\text{S}_2$ $[\text{M}+\text{H}]^+$, 512.2868. Found 512.2843.

Isopropyl 3-isopropyl-2-methyl-5-*tert*-butylthio-5-oxo-*N*-(2,3,5,6-tetramethylbenzenesulfonyl)-pentanimidate (19de)



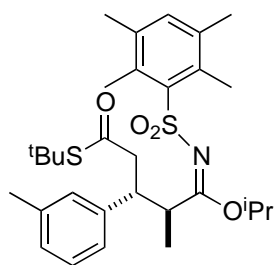
Colorless oil; ^1H NMR (CDCl_3) δ = 7.16 (s, 1H), 5.13-5.11 (m, 1H), 3.15-3.10 (m, 1H), 2.58 (s, 6H), 2.37-2.32 (m, 1H), 2.27 (s, 6H), 2.16-2.12 (m, 1H), 1.89-1.80 (m, 2H), 1.42 (s, 9H), 1.26-1.23 (m, 7H), 1.11 (d, 3H, J = 6.2 Hz), 0.82 (d, 3H, J = 6.9 Hz), 0.66 (d, 3H, J = 6.9 Hz); ^{13}C NMR (CDCl_3) δ = 199.1, 178.1, 140.4, 135.9, 135.3, 134.6, 71.6, 47.7, 42.8, 41.3, 29.7, 27.3, 21.2(2), 21.1(8), 20.8, 18.1, 17.9, 16.3, 15.6; IR (neat) 2963, 2876, 1737, 1686, 1586, 1462, 1383, 1363, 1308, 1240, 1206, 1146, 1100, 1016 cm^{-1} ; HRMS (DART) Exact mass calcd for $\text{C}_{26}\text{H}_{44}\text{NO}_4\text{S}_2$ $[\text{M}+\text{H}]^+$, 498.2712. Found 498.2720.

Isopropyl 2-methyl-3-phenyl-5-*tert*-butylthio-5-oxo-*N*-(2,3,5,6-tetramethylbenzenesulfonyl)-pentanimidate (19df)



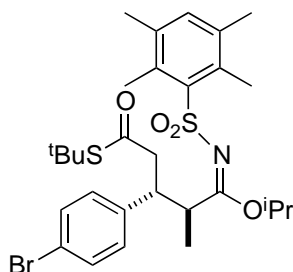
Obtained as diastereomer mixture; White solid; ^1H NMR (CDCl_3) δ = 7.27-7.17 (m, 4H), 7.02 (d, 2H, J = 6.8 Hz), 5.20 (septet, 2H, J = 6.2 Hz), 3.47-3.43 (m, 1H), 3.22 (td, 1H, J = 11.1, 4.2 Hz), 2.61 (s, 6H), 2.38-2.33 (m, 1H), 2.31 (s, 6H), 1.34 (d, 3H, J = 6.2 Hz), 1.31 (d, 3H, J = 6.2 Hz), 1.23 (s, 9H), 0.90 (d, 3H, J = 6.8 Hz); ^{13}C NMR (CDCl_3) δ = 197.8, 177.1, 140.3, 139.8, 135.9, 135.5, 134.6, 128.3, 127.9, 126.9, 71.7, 48.5, 47.6, 46.0, 43.7, 29.4, 21.3, 20.8, 18.0, 16.4; IR (neat) 3030, 2968, 2931, 2878, 178, 1716, 1682, 1590, 1494, 1457, 1376, 1364, 1301, 1229, 1206, 1146, 1102, 1039 cm^{-1} ; HRMS (DART) Exact mass calcd for $\text{C}_{29}\text{H}_{42}\text{NO}_4\text{S}_2$ $[\text{M}+\text{H}]^+$, 532.2555. Found 532.2531.

Isopropyl 2-methyl-3-(3-methylphenyl)-5-tert-butylthio-5-oxo-N-(2,3,5,6-tetramethylbenzenesulfonyl)-pentanimidate (19dg)



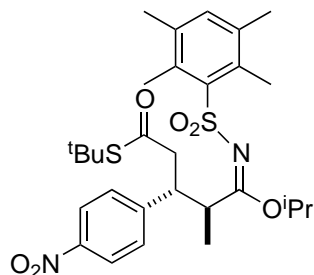
Obtained as diastereomer mixture; Colorless oil; ^1H NMR (CDCl_3) δ = 7.19 (s, 1H), 7.14 (t, 1H, J = 7.6 Hz), 6.99 (d, 1H, J = 7.6 Hz), 6.86 (s, 1H), 6.81 (d, 1H, J = 7.6 Hz), 5.19 (septet, 1H, J = 6.2 Hz), 3.48-3.43 (m, 1H), 3.20 (td, 1H, J = 11.0, 3.4 Hz), 2.62 (s, 6H), 2.38-2.28 (m, 11H), 1.35-1.30 (m, 6H), 1.25 (s, 9H), 0.90 (d, 3H, J = 6.9 Hz); ^{13}C NMR (CDCl_3) δ = 197.9, 177.2, 140.3, 139.7, 137.7, 135.8, 135.4, 134.5, 129.0, 128.2, 127.7, 125.1, 71.6, 48.7, 47.6, 46.0, 43.6, 29.4, 21.3, 21.2, 20.6, 18.0, 16.4; IR (neat) 2969, 2929, 2873, 1739, 1682, 1590, 1458, 1376, 1363, 1295, 1228, 1207, 1146, 1101, 1039 cm^{-1} ; HRMS (DART) Exact mass calcd for $\text{C}_{30}\text{H}_{44}\text{NO}_4\text{S}_2$ $[\text{M}+\text{H}]^+$, 546.2712. Found 546.2713.

Isopropyl 2-methyl-3-(4-bromophenyl)-5-tert-butylthio-5-oxo-N-(2,3,5,6-tetramethylbenzenesulfonyl)-pentanimidate (19dh)



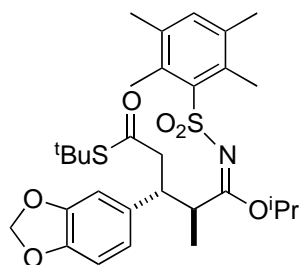
Obtained as diastereomer mixture; Pale yellow solid; ^1H NMR (CDCl_3) δ = 7.39 (d, 2H, J = 8.5 Hz), 7.19 (s, 1H), 6.94 (d, 2H, J = 8.5 Hz), 5.17 (septet, 1H, J = 6.2 Hz), 3.49-3.43 (m, 1H), 3.22 (td, 1H, J = 10.5, 4.5 Hz), 2.60 (s, 6H), 2.43-2.37 (m, 2H), 2.30 (s, 6H), 1.34-1.29 (m, 6H), 1.26 (s, 9H), 0.91 (d, 3H, J = 6.8 Hz); ^{13}C NMR (CDCl_3) δ = 197.5, 176.5, 140.2, 139.0, 135.9, 135.5, 134.5, 131.4, 129.9, 120.8, 71.7, 48.3, 47.8, 45.5, 43.5, 29.4, 21.2(2), 21.1(7), 20.7, 18.0, 17.7, 16.3; IR (neat) 2969, 2931, 2873, 1738, 1717, 1682, 1591, 1489, 1459, 1376, 136, 1301, 1228, 1206, 1146, 1099, 1074, 1038, 1011 cm^{-1} ; HRMS (DART) Exact mass calcd for $\text{C}_{29}\text{H}_{41}\text{BrNO}_4\text{S}_2$ $[\text{M}+\text{H}]^+$, 610.1660. Found 610.1618.

Isopropyl 2-methyl-3-(4-nitrophenyl)-5-tert-butylthio-5-oxo-N-(2,3,5,6-tetramethylbenzenesulfonyl)-pentanimidate (19di)



Obtained as diastereomer mixture; Yellow solid; ^1H NMR (CDCl_3) δ = 8.16 (d, 2H, J = 8.5 Hz), 7.30 (d, 2H, J = 8.5 Hz), 7.21 (s, 1H), 5.18 (septet, 1H, J = 6.0 Hz), 3.65-3.58 (m, 1H), 3.41 (td, 1H, J = 11.1, 3.6 Hz), 2.61 (s, 6H), 2.50-2.42 (m, 2H), 2.32 (s, 6H), 1.35-1.31 (m, 6H), 1.25 (s, 9H), 0.93 (d, 3H, J = 7.9 Hz); ^{13}C NMR (CDCl_3) δ = 197.3, 175.7, 147.9, 147.0, 140.0, 135.9, 135.6, 134.6, 129.2, 123.6, 72.0, 48.2, 45.9, 43.4, 29.4, 21.3, 21.2, 20.8, 18.0, 17.7, 16.3; IR (neat) 2969, 2931, 2873, 1738, 1717, 1681, 1593, 1524, 1459, 1347, 1299, 1280, 1230, 1206, 1146, 1100, 1039, 1014 cm^{-1} ; HRMS (DART) Exact mass calcd for $\text{C}_{29}\text{H}_{41}\text{N}_2\text{O}_6\text{S}_2$ $[\text{M}+\text{H}]^+$, 577.2406. Found 577.2440.

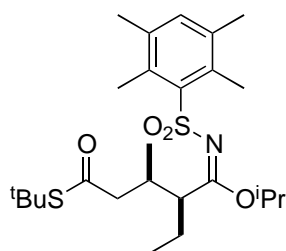
Isopropyl 2-methyl-3-(benzo-[d][1,3]-dioxol-5-yl)-5-*tert*-butylthio-5-oxo-*N*-(2,3,5,6-tetramethylbenzenesulfonyl)-pentanimidate (19dj)



Obtained as diastereomer mixture; Colorless oil; ^1H NMR (CDCl_3) δ = 7.20 (s, 1H), 6.68 (d, 1H, J = 8.2 Hz), 6.50 (d, 1H, J = 8.2 Hz), 6.42 (s, 1H), 5.92 (s, 2H), 5.20 (septet, 1H, J = 6.2 Hz), 3.34-3.29 (m, 1H), 3.13 (td, 1H, J = 11.0, 3.4 Hz), 2.61 (s, 6H), 2.31 (s, 6H), 2.27-2.19 (m, 2H), 1.34-1.30 (m, 6H), 1.28 (s, 9H), 0.92 (d, 3H, J = 6.9 Hz); ^{13}C NMR (CDCl_3) δ = 197.9, 177.1, 147.7, 146.4, 140.4, 136.1, 135.6, 134.7, 133.7, 121.9, 108.0, 71.7, 48.7, 47.8, 45.8, 43.9, 29.6, 21.3(3), 21.2(7), 20.8, 20.7, 18.1, 17.7, 16.4;

IR (neat) 2969, 2927, 1738, 1715, 1682, 1589, 1505, 1488, 1456, 1363, 1315, 1284, 1248, 1206, 1147, 1100, 1039 cm^{-1} ; HRMS (DART) Exact mass calcd for $\text{C}_{30}\text{H}_{42}\text{NO}_6\text{S}_2$ $[\text{M}+\text{H}]^+$, 576.2454. Found 576.2418.

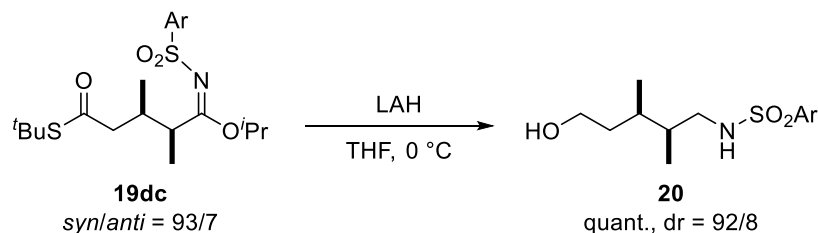
Isopropyl 2-ethyl-3-methyl-5-*tert*-butylthio-5-oxo-*N*-(2,3,5,6-tetramethylbenzenesulfonyl)-pentanimidate (19gc)



Obtained as diastereomer mixture; Colorless oil; ^1H NMR (CDCl_3) δ = 7.13 (s, 1H), 5.08 (septet, 1H, J = 6.2 Hz), 3.24-3.20 (m, 1H), 2.57 (s, 6H), 2.37-2.25 (m, 9H), 1.74-1.67 (m, 1H), 1.60-1.54 (m, 1H), 1.45 (s, 9H), 1.28-1.25 (m, 6H), 0.98 (d, 3H, J = 6.2 Hz), 0.91 (t, 3H, J = 7.4 Hz); ^{13}C NMR (CDCl_3) δ = 199.5, 176.2, 140.3, 135.6, 135.2, 134.6, 71.3, 50.6, 49.3, 47.8, 33.5, 29.7, 23.5, 21.4, 21.3, 20.8, 18.0, 16.9, 11.3; IR (neat) 2968, 2934, 2876, 1738, 1718, 1683, 1591, 1463, 1365, 1307, 1257, 1207, 1145, 1101 cm^{-1} ; HRMS (DART) Exact mass calcd for $\text{C}_{25}\text{H}_{42}\text{NO}_4\text{S}_2$ $[\text{M}+\text{H}]^+$, 484.2555. Found 484.2551.

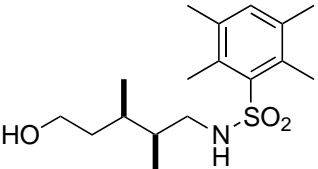
Further conversions of 1,4-adduct. Procedures and compound information

1-1. LAH reduction

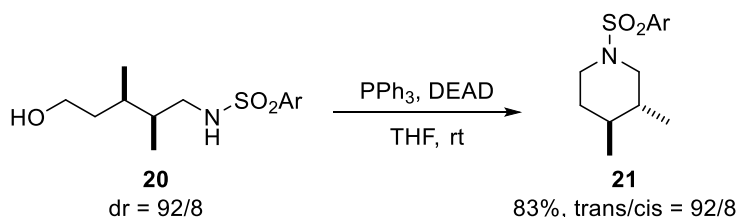


Compound **19dc** (140.9 mg, 0.3 mmol) in THF (1 mL) was added to a suspension of LAH (34 mg, 0.9 mmol) in THF (2 mL) at 0 °C. The mixture was stirred for 30 min and then water was added. The mixture was extracted with DCM and the organic layer was dried over anhydrous Na_2SO_4 . After removal of the solvents under reduced pressure, the product was purified by pTLC (DCM/MeOH = 19/1) to afford quantitative yield of the desired product **20** (99.4 mg, dr = 92/8).

N-(2,3,5,6-tetramethylbenzensulfonyl)-2,3-dimethyl-5-hydroxypentylamine (**20**)

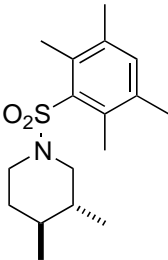
 Colorless oil; ^1H NMR (CDCl_3) δ = 7.14 (s, 1H), 5.25 (t, 1H, J = 6.8 Hz), 3.66-3.56 (m, 2H), 2.82-2.72 (m, 2H), 2.55 (s, 6H), 2.43 (br s, 1H), 2.27 (s, 6H), 1.77-1.75 (m, 1H), 1.66-1.62 (m, 1H), 1.52-1.48 (m, 1H), 1.41-1.36 (m, 1H), 0.74 (d, 3H, J = 6.8 Hz), 0.70 (d, 3H, J = 6.8 Hz); ^{13}C NMR (CDCl_3) δ = 137.6, 135.7, 135.5, 134.9, 60.5, 46.6, 37.4, 36.5, 29.7, 20.9, 17.8, 13.6, 12.2; IR (neat) 3501, 3311, 2960, 2932, 2878, 1463, 1386, 1362, 1315, 1255, 1205, 1144, 1060, 1014 cm^{-1} ; HRMS (DART) Exact mass calcd for $\text{C}_{17}\text{H}_{30}\text{NO}_3\text{S}$ $[\text{M}+\text{H}]^+$, 328.1946. Found 328.1934.

1-2. Cyclization reaction of aminoalcohol **20**

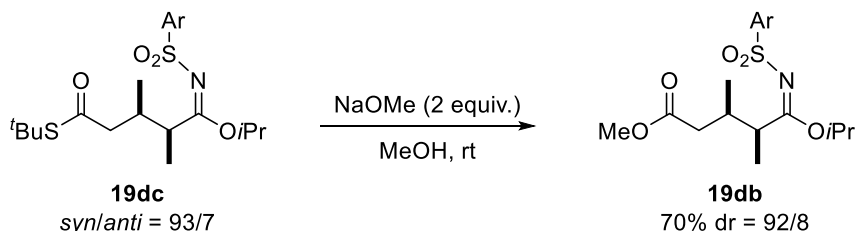


To a solution of reduced product **20** (121.2 mg, 0.37 mmol) and triphenylphosphine (194 mg, 0.74 mmol) in 3.7 mL of THF, 252 μL of diethyl azodicarboxylate solution (DEAD, ca. 2.2 M in toluene; 0.74 mmol) was added slowly at rt. The mixture was stirred overnight and then solvent was removed under reduced pressure. The product was purified by pTLC (hexane/EtOAc = 5/1) to afford the desired piperidine derivative (94.6 mg, 83%, trans/cis = 92/8). ^1H - ^1H COSY NMR and several ^1H -decoupling experiments determined stereo configuration of final product **21** ($J_{\text{H-H}} = 11.0$ for major, 4.1 for minor; details are shown below).

N-(2,3,5,6-tetramethylbenzensulfonyl)-3,4-dimethylpiperidine (**21**)

 White solid; ^1H NMR (CDCl_3) δ = 7.12 (s, 1H), 3.51-3.43 (m, 2H), 2.71 (ddd, 1H, J = 12.5, 12.4, 2.7), 2.69 (s, 6H), 2.51 (dd, 1H, J = 11.7, 11.7), 2.24 (s, 6H), 1.60 (m, 1H), 1.20 (m, 2H), 1.07 (m, 1H), 0.90 (d, 3H, J = 6.6), 0.85 (d, 3H, J = 6.7); ^{13}C NMR (CDCl_3) δ = 136.5, 135.9, 135.6(2), 135.5(7), 50.6, 44.6, 37.2, 33.5, 20.9, 19.4, 17.7, 17.6, 16.6; IR (neat) 2953, 2926, 2873, 2849, 1458, 1390, 1310, 1256, 1205, 1181, 1143, 1029; HRMS (DART) Exact mass calcd for $\text{C}_{17}\text{H}_{28}\text{NO}_2\text{S}$ $[\text{M}+\text{H}]^+$, 310.1841. Found 310.1846.

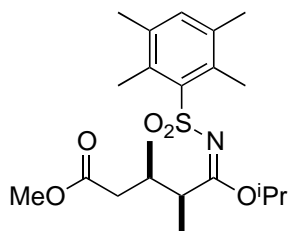
2. Methanolysis



Product **19dc** (58.7 mg, 0.123 mmol) was added at rt to a solution of sodium methoxide as a solution in MeOH (0.25 mL) (6.8 mg, 0.123 mmol in 0.25 mL MeOH). The mixture was stirred for 2 d and then poured into saturated aq. NH_4Cl solution. The mixture was extracted with DCM and the organic layers were dried over anhydrous

Na₂SO₄. On the crude NMR analysis ~20% of the remaining starting material **19dc** was observed (dr ~ 7/3). Purification by pTLC (Hexane/EtOAc = 9/1) afforded the desired sulfonylimidate **19db** (35.3 mg, 70%, *syn/anti* = 98/2).

Isopropyl 2,3-dimethyl-5-methoxy-5-oxo-*N*-(2,3,5,6-tetramethylbenzenesulfonyl)-pentanimidate (19db**)**



Obtained as diastereomer mixture; White crystal; ¹H NMR (CDCl₃) δ = 7.05 (s, 1H), 4.99 (septet, 1H, *J* = 5.7 Hz), 3.58 (s, 3H), 3.24-3.14 (m, 1H), 2.48 (s, 6H), 2.20-2.13 (m, 8H), 1.98-1.93 (m, 1H), 1.18-1.07 (m, 9H), 0.88 (d, 3H, *J* = 6.8 Hz); ¹³C NMR (CDCl₃) δ = 177.7, 173.3, 140.6, 135.6, 135.5, 134.8, 71.6, 51.9, 44.3, 39.7, 33.6, 21.6, 21.1, 18.4, 17.2, 15.8; IR (neat) 2979, 2949, 2881, 1740, 1590, 1460, 1382, 1357, 1303, 1258, 1177, 1144, 1100 cm⁻¹; HRMS (DART) Exact mass calcd for C₂₁H₃₄NO₅S [M+H]⁺, 412.2158.

Found 412.2157.

Determination of stereochemistry

Relative stereoconfiguration of piperidine **21** was assigned from coupling constants of ^1H -NMR spectroscopy. From ^1H - ^1H COSY experiment (Figure 8-1), each proton was determined as described in Figure 8-2. To determine the coupling constant between H_3 and H_4 , several irradiation experiments were performed (Figure 8-3). For major isomer, rf was irradiated to 5-H(b) and 4-Me then 4-H was successfully decoupled into dd ($J = 11.0, 11.0$, Figure 8-3 left). For minor isomer, rf was irradiated to 2-H(a) and 2-H(b) then 3-H was decoupled into dq ($J_{3\text{H}-4\text{H}} = 4.1$, $J_{3\text{H}-3\text{Me}} = 6.9$, Figure 8-3 right).

Figure 8-1. ^1H - ^1H COSY spectrum of **21**

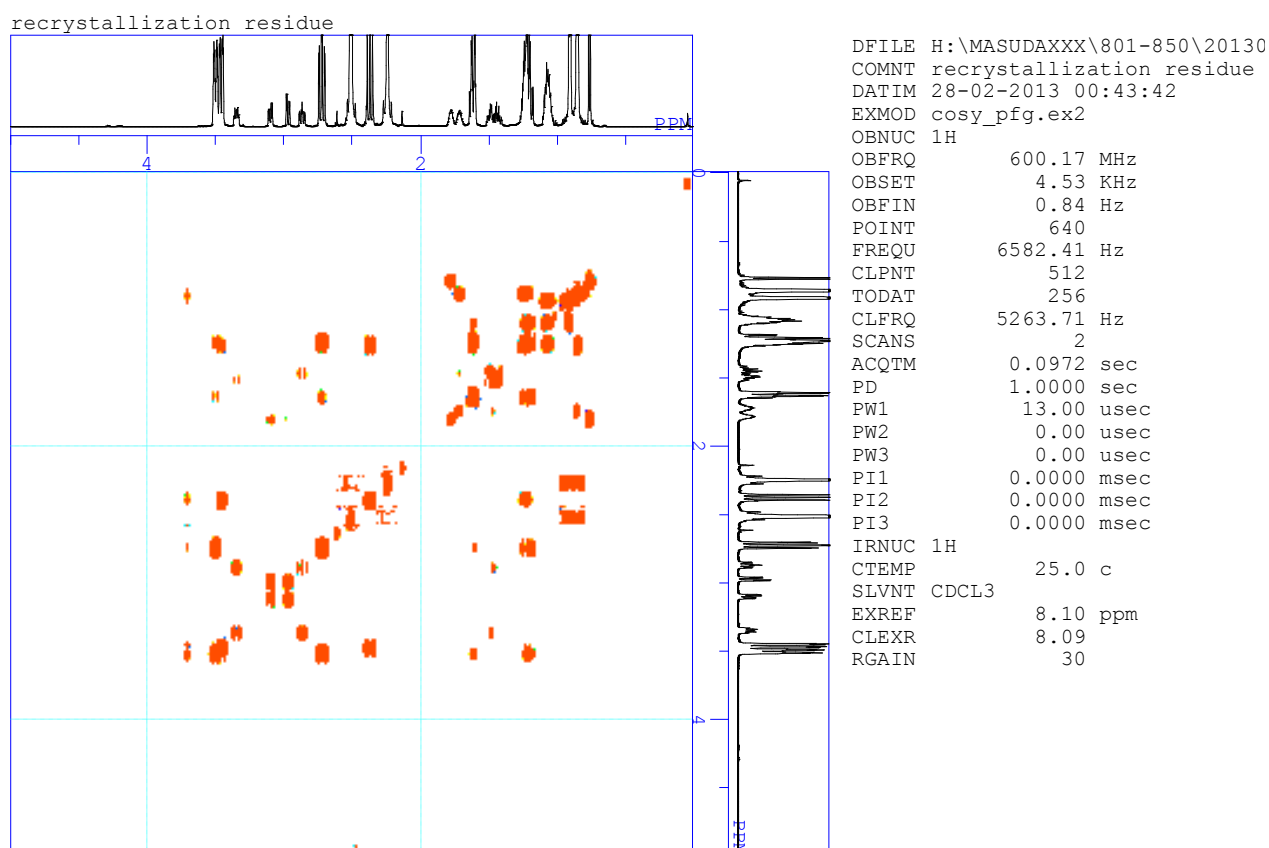


Figure 8-2. Assignment of the peaks of 21 on ^1H -NMR

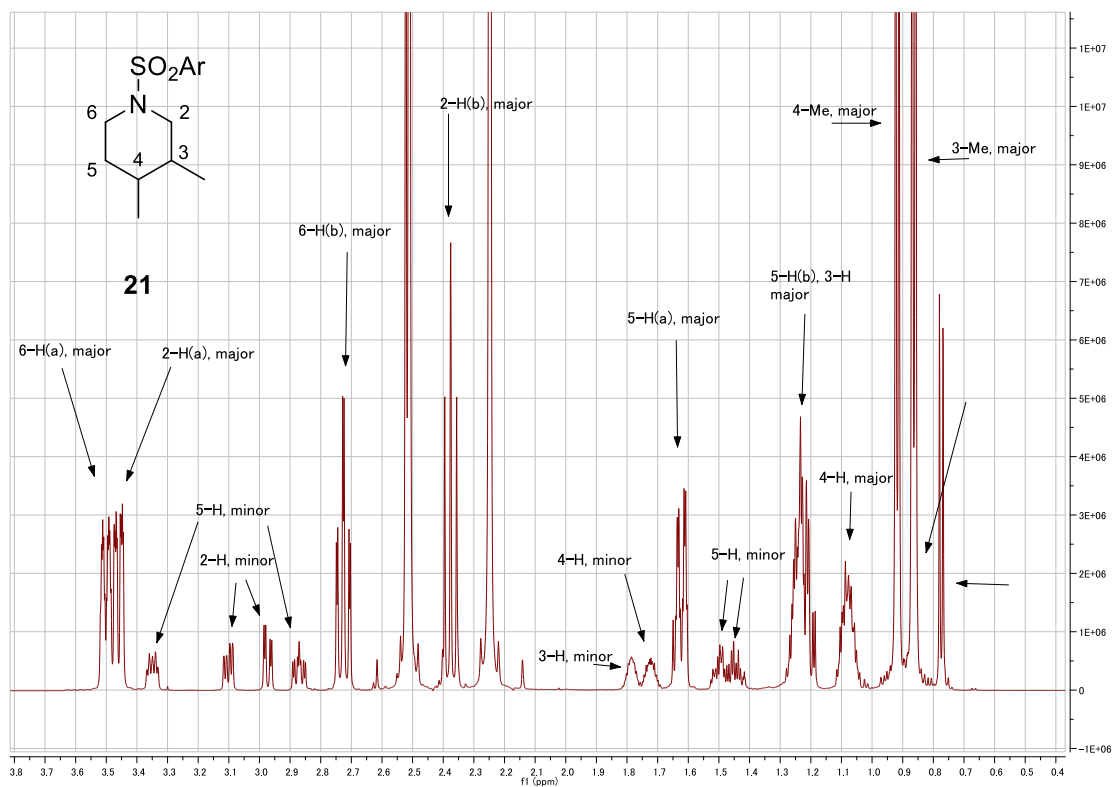
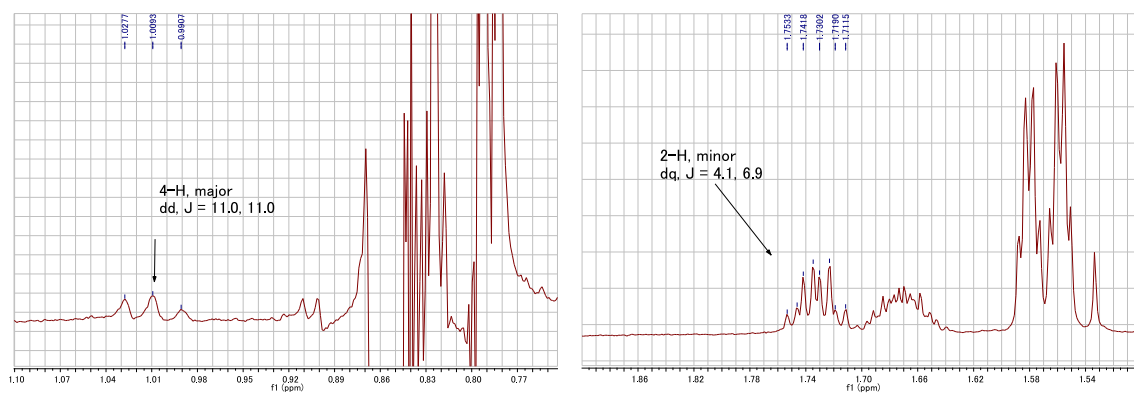


Figure 8-3. Irradiation experiments



9. References

- (1) Wilhelmy, L. *Ann. der Phys. und Chemie* **1850**, 157, 499–526.
- (2) Berthelot, P. M.; Saint-Gilles, L. P. *Ann. Chim. Physique* **1862**, 63, 385–422.
- (3) Guldberg, C. M.; Waage, P. *Etudes sur les affinités chimiques*; Imprimerie de Brøgger & Christie: Christiania, 1867.
- (4) Harcourt, A. V.; Esson, W. *Proc. R. Soc. London* **1865**, 14, 470–474.
- (5) Harcourt, A. V.; Esson, W. *Philos. Trans. R. Soc. London* **1866**, 156, 193–221.
- (6) Arrhenius, S. *Zeitschrift für Phys. Chemie* **1889**, 4, 226.
- (7) Hoff, J. H. van't *Etudes de dynamique chimique*; Frederik Muller: Amsterdam, 1884.
- (8) Ostwald, W. *Grundriss der allgemeinen Chemie*; W. Engelmann: Leipzig, 1909.
- (9) Polanyi, M.; Wigner, E. *Zeitschrift für Phys. Chemie--Stoichiometrie und Verwandtschaftslehre* **1928**, 139, 439–452.
- (10) Pelzer, H.; Wigner, E. *Zeitschrift für Phys. chemie-Abteilung B-Chemie der Elem. aufbau der Mater.* **1932**, 15, 445–471.
- (11) Eyring, H.; Polanyi, M. *Zeitschrift für Phys. chemie-Abteilung B-Chemie der Elem. aufbau der Mater.* **1931**, 12, 279–311.
- (12) Laidler, K. J. *Chemical kinetics*; Harper & Row: New York, 1987.
- (13) Berzelius, J. *Jahres-Bericht über die Fortschritte der Phys. Wiss.* **1836**, 243.
- (14) Roberts, M. W. *Catal. Letters* **2000**, 67, 1–4.
- (15) Ertl, G.; Gloyna, T. *Zeitschrift für Phys. Chemie* **2003**, 217, 1207–1220.
- (16) Lindemann, F. A.; Arrhenius, S.; Langmuir, I.; Dhar, N. R.; Perrin, J.; McC. Lewis, W. C. *Trans. Faraday Soc.* **1922**, 17, 598–606.
- (17) Hinshelwood, C. N. *Proc. R. Soc. London Ser. A-Containing Pap. a Math. Phys. Character* **1926**, 113, 230–233.
- (18) Rice, O. K.; Ramsperger, H. C. *J. Am. Chem. Soc.* **1927**, 49, 1617–1629.
- (19) Weinberg, W. H. *Acc. Chem. Res.* **1996**, 29, 479–487.
- (20) Ramsden, J. H.; Drago, R. S.; Riley, R. *J. Am. Chem. Soc.* **1989**, 111, 3958–3961.
- (21) Wang, M.-L.; Wu, H.-S. *Chem. Eng. Sci.* **1991**, 46, 509–517.
- (22) Enami, S.; Sakamoto, Y.; Colussi, A. J. *Proc. Natl. Acad. Sci. U. S. A.* **2014**, 111, 623–628.
- (23) Fita, P. *J. Phys. Chem. C* **2014**, 118, 23147–23153.
- (24) Audi, G. *Int. J. Mass Spectrom.* **2006**, 251, 85–94.
- (25) Thomson, J. J. *Proc. R. Soc. A Math. Phys. Eng. Sci.* **1913**, 89, 1–20.
- (26) Dempster, A. J. *Phys. Rev.* **1916**, 8, 651–662.
- (27) Dempster, A. J. *Phys. Rev.* **1918**, 11, 316–325.
- (28) Aston, F. W. *Philos. Mag.* **1919**, 38, 707–714.
- (29) Aston, F. W. *Nature* **1920**, 104, 334.
- (30) Klemm, A. *Zeitschrift Naturforsch. Tl. A* **1946**, 1, 137.
- (31) Stephens, W. E. *Phys. Rev.* **1946**, 69, 691–691.
- (32) Paul, W. Von; Steinwedel, H. *Zeitschrift für Naturforsch. A* **1953**, 8a, 448–451.
- (33) Brown, L.; Gabrielse, G. *Rev. Mod. Phys.* **1986**, 58, 233–311.
- (34) Knight, R. D. *Appl. Phys. Lett.* **1981**, 38, 221–223.
- (35) Comisarow, M. B.; Marshall, A. G. *Chem. Phys. Lett.* **1974**, 25, 282–283.
- (36) Crookes, W. *Philos. Trans. R. Soc. London* **1879**, 170, 135–164.
- (37) Silverstein, R. M.; Bassler, G. C. *J. Chem. Educ.* **1962**, 39, 546–553.
- (38) Silverstein, R. M.; Webster, F. X.; Kiemle, D. J. *Spectrometric identification of organic compounds*; John Wiley & Sons: Hoboken, NJ, 2005.
- (39) Yamashita, M.; Fenn, J. B. *J. Phys. Chem.* **1984**, 88, 4451–4459.
- (40) Fenn, J. B.; Mann, M.; Meng, C. K.; Wong, S. F.; Whitehouse, C. M. *Science* **1989**, 246, 64–71.
- (41) Karas, M.; Bachmann, D.; Hillenkamp, F. *Anal. Chem.* **1985**, 57, 2935–2939.
- (42) Tanaka, K.; Waki, H.; Ido, Y.; Akita, S.; Yoshida, Y.; Yoshida, T.; Matsuo, T. *Rapid Commun. Mass Spectrom.* **1988**, 2, 151–153.
- (43) Cooks, R. G.; Ouyang, Z.; Takats, Z.; Wiseman, J. M. *Science* **2006**, 311, 1566–70.
- (44) Venter, A.; Nefliu, M.; Graham Cooks, R. *TrAC - Trends Anal. Chem.* **2008**, 27, 284–290.
- (45) Chen, H.; Venter, A.; Cooks, R. G. *Chem. Commun.* **2006**, 2042–2044.
- (46) Haddad, R.; Milagre, H. M. S.; Catharino, R. R.; Eberlin, M. N. *Anal. Chem.* **2008**, 80, 2744–2750.
- (47) Shiea, J.; Huang, M. Z.; Hsu, H. J.; Lee, C. Y.; Yuan, C. H.; Beech, I.; Sunner, J. *Rapid Commun. Mass Spectrom.* **2005**, 19, 3701–3704.
- (48) McEwen, C. N.; McKay, R. G.; Larsen, B. S. *Anal. Chem.* **2005**, 77, 7826–7831.
- (49) Na, N.; Zhao, M.; Zhang, S.; Yang, C.; Zhang, X. *J. Am. Soc. Mass Spectrom.* **2007**, 18, 1859–1862.

- (50) Harper, J. D.; Charipar, N. a; Mulligan, C. C.; Zhang, X.; Cooks, R. G.; Ouyang, Z. *Anal. Chem.* **2008**, *80*, 9097–9104.
- (51) Cody, R. B.; Laramée, J. a; Durst, H. D. *Anal. Chem.* **2005**, *77*, 2297–2302.
- (52) Fernández-Peralbo, M. a; Ferreiro Vera, C.; Priego-Capote, F.; Luque De Castro, M. D. *Talanta* **2014**, *126*, 170–176.
- (53) Stöcklin, R.; Vu, L.; Vadas, L.; Cerini, F.; Kippen, a D.; Offord, R. E.; Rose, K. *Diabetes* **1997**, *46*, 44–50.
- (54) Nilles, J. M.; Connell, T. R.; Durst, H. D. *Anal. Chem.* **2009**, *81*, 6744–6749.
- (55) Brun, V.; Masselon, C.; Garin, J.; Dupuis, A. *J. Proteomics* **2009**, *72*, 740–9.
- (56) Danhelova, H.; Hradecky, J.; Prinosilova, S.; Cajka, T.; Riddellova, K.; Vaclavik, L.; Hajslava, J. *Anal. Bioanal. Chem.* **2012**, *403*, 2883–2889.
- (57) Urey, H.; Brickwedde, F.; Murphy, G. *Phys. Rev.* **1932**, *39*, 164–165.
- (58) Dean, D. C.; Filer, C. N.; McCarthy, K. E. *Synthesis and applications of isotopically labelled compounds : proceedings of the eighth International Symposium, Boston, USA, 1-5 June 2003*; Wiley: Chichester, 2004.
- (59) Voges, R.; Heys, J. R.; Moenius, T. *Preparation of compounds labeled with tritium and carbon-14*; Wiley: Chichester, U.K., 2009.
- (60) Journal of Labelled Compounds and Radiopharmaceuticals - Wiley Online Library
[http://onlinelibrary.wiley.com/journal/10.1002/\(ISSN\)1099-1344](http://onlinelibrary.wiley.com/journal/10.1002/(ISSN)1099-1344) (accessed Jan 11, 2015).
- (61) Yu, S.; Crawford, E.; Tice, J.; Musselman, B.; Wu, J.-T. *Anal. Chem.* **2009**, *81*, 193–202.
- (62) Kubec, R.; Cody, R. B.; Dane, a J.; Musah, R. a; Schraml, J.; Vattekkatte, A.; Block, E. *J. Agric. Food Chem.* **2010**, *58*, 1121–1128.
- (63) Ackerman, L. K.; Noonan, G. O.; Begley, T. H. *Food Addit. Contam. Part A. Chem. Anal. Control. Expo. Risk Assess.* **2009**, *26*, 1611–1618.
- (64) Grange, A. H. *Environ. Forensics* **2008**, *9*, 127–136.
- (65) Grange, A. H. *Environ. Forensics* **2008**, *9*, 137–143.
- (66) Grange, A. H. *Environ. Forensics* **2009**, *10*, 183–195.
- (67) Grange, A. H. *Rapid Commun. Mass Spectrom.* **2013**, *27*, 305–318.
- (68) Cho, D. S.; Gibson, S. C.; Bhandari, D.; McNally, M. E.; Hoffman, R. M.; Cook, K. D.; Song, L. *Rapid Commun. Mass Spectrom.* **2011**, *25*, 3575–3580.
- (69) Sonneveld, E. J.; Visser, J. W. *J. Appl. Crystallogr.* **1975**, *8*, 1–7.
- (70) 化学便覧 基礎編 改訂5版; 丸善出版.
- (71) Manabe, K.; Mori, Y.; Kobayashi, S. *Tetrahedron* **1999**, *55*, 11203–11208.
- (72) Manabe, K.; Kobayashi, S. *Synlett* **1999**, *1999*, 547–548.
- (73) Manabe, K.; Mori, Y.; Wakabayashi, T.; Nagayama, S.; Kobayashi, S. *J. Am. Chem. Soc.* **2000**, *122*, 7202–7207.
- (74) Lipshutz, B. H.; Isley, N. a; Fennewald, J. C.; Slack, E. D. *Angew. Chem. Int. Ed.* **2013**, *52*, 10952–10958.
- (75) Lipshutz, B. H.; Ghorai, S. *Green Chem.* **2014**, *16*, 3660–3679.
- (76) Notz, W.; Tanaka, F.; Barbas, C. F. *Acc. Chem. Res.* **2004**, *37*, 580–591.
- (77) Machajewski, T.; Wong, C. *Angew. Chem. Int. Ed.* **2000**, *39*, 1352–1375.
- (78) Palomo, C.; Oiarbide, M.; García, J. M. *Chem. Soc. Rev.* **2004**, *33*, 65–75.
- (79) Guillena, G.; Nájera, C.; Ramón, D. J. *Tetrahedron: Asymmetry* **2007**, *18*, 2249–2293.
- (80) Mukaiyama, T. *Org. React.* **1982**, *28*, 203–331.
- (81) Arya, P.; Qin, H. *Tetrahedron* **2000**, *56*, 917–947.
- (82) Kitanosono, T.; Kobayashi, S. *Adv. Synth. Catal.* **2013**, *355*, 3095–3118.
- (83) Braun, M.; Sacha, H. *J. für Prakt. Chemie/Chemiker-Zeitung* **1993**, *335*, 653–668.
- (84) Mukaiyama, T.; Shiina, I.; Iwadare, H.; Saitoh, M.; Nishimura, T.; Ohkawa, N.; Sakoh, H.; Nishimura, K.; Tani, Y.; Hasegawa, M.; Yamada, K.; Saitoh, K. *Chem. - A Eur. J.* **1999**, *5*, 121–161.
- (85) Evans, D. A.; Takacs, J. M.; McGee, L. R.; Ennis, M. D.; Mathre, D. J.; Bartroli, J. Chiral enolate design. *Pure Appl. Chem.* **1981**, *53*, 1109–1127.
- (86) Hoveyda, A. H.; Evans, D. A.; Fu, G. C. *Chem. Rev.* **1993**, *93*, 1307–1370.
- (87) Saito, S.; Yamamoto, H. *Chem. - A Eur. J.* **1999**, *5*, 1959–1962.
- (88) Lubineau, A. *J. Org. Chem.* **1986**, *51*, 2142–2144.
- (89) Lubineau, A.; Meyer, E. *Tetrahedron* **1988**, *44*, 6065–6070.
- (90) Kobayashi, S. *Chem. Lett.* **1991**, 2187–2190.
- (91) Kobayashi, S.; Wakabayashi, T.; Nagayama, S.; Oyamada, H. *Tetrahedron Lett.* **1997**, *38*, 4559–4562.
- (92) Kobayashi, S.; Wakabayashi, T. *Tetrahedron Lett.* **1998**, *39*, 5389–5392.
- (93) Manabe, K.; Kobayashi, S. *Org. Lett.* **1999**, *1*, 1965–1967.
- (94) Mori, Y.; Kakumoto, K.; Manabe, K.; Kobayashi, S. *Tetrahedron Lett.* **2000**, *41*, 3107–3111.
- (95) Kokubo, M.; Ogawa, C.; Kobayashi, S. *Angew. Chem. Int. Ed.* **2008**, *47*, 6909–6911.
- (96) Kobayashi, S.; Kokubo, M.; Kawasumi, K.; Nagano, T. *Chem. - An Asian J.* **2010**, *5*, 490–492.
- (97) Bolm, C.; Ewald, M.; Felder, M.; Schlingloff, G. *Chem. Ber.* **1992**, *125*, 1169–1190.

- (98) Bolm, C.; Zehnder, M.; Bur, D. *Angew. Chem.* **1990**, *102*, 206–208.
- (99) Prakash, G. K. S.; Paknia, F.; Vaghoo, H.; Rasul, G.; Mathew, T.; Olah, G. a *J. Org. Chem.* **2010**, *75*, 2219–2226.
- (100) Student *Biometrika* **1908**, *6*, 1–25.
- (101) Wang, L.; Wah Wong, M. *Tetrahedron Lett.* **2008**, *49*, 3916–3920.
- (102) Sai, M.; Akakura, M.; Yamamoto, H. *Chem. Commun.* **2014**, *50*, 15206–8.
- (103) Wong, C. T.; Wong, M. W. *J. Org. Chem.* **2007**, *72*, 1425–30.
- (104) Lee, J. M.; Helquist, P.; Wiest, O. *J. Am. Chem. Soc.* **2012**, *134*, 14973–14981.
- (105) Wuts, P. G. M.; Greene, T. W. *Greene's Protective Groups in Organic Synthesis*; John Wiley & Sons, Inc.: Hoboken, NJ, USA, 2006.
- (106) Mukherjee, C.; Kitanosono, T.; Kobayashi, S. *Chem. - An Asian J.* **2011**, *6*, 2308–2311.
- (107) Hatanaka, M.; Morokuma, K. *J. Am. Chem. Soc.* **2013**, *135*, 13972–13979.
- (108) Kitanosono, T.; Ollevier, T.; Kobayashi, S. *Chem. - An Asian J.* **2013**, *8*, 3051–3062.
- (109) Ishikawa, S.; Hamada, T.; Manabe, K.; Kobayashi, S. *J. Am. Chem. Soc.* **2004**, *126*, 12236–12237.
- (110) Starks, C. M.; Liotta, C. L.; Halpern, M. *Phase-transfer catalysis : fundamentals, applications, and industrial perspectives*; Chapman & Hall: New York, 1994.
- (111) Sasson, Y.; Neumann, R. *Handbook of phase transfer catalysis*; Blackie Academic & Professional: London, 1997.
- (112) Maruoka, K. *Asymmetric phase transfer catalysis*; Wiley-VCH: Weinheim; [Chichester], 2008.
- (113) Kitanosono, T.; Sakai, M.; Ueno, M.; Kobayashi, S. *Org. Biomol. Chem.* **2012**, *10*, 7134–7147.
- (114) Sibi, M. P.; Manyem, S. *Tetrahedron* **2000**, *56*, 8033–8061.
- (115) Krause, N.; Hoffmann-Röder, A. *Synthesis* **2001**, *2001*, 0171–0196.
- (116) Tsogoeva, S. B. *Eur. - J. Org. Chem.* **2007**, *2007*, 1701–1716.
- (117) Oudeyer, S.; Brière, J.-F.; Levacher, V. *Eur. - J. Org. Chem.* **2014**, *2014*, 6103–6119.
- (118) Bhattacharya, A.; Segmüller, B.; Ybarra, A. *Synth. Commun.* **1996**, *26*, 1775–1784.
- (119) Cody, R. B.; Laramée, J. A.; Nilles, J. M.; Durst, H. D. *JEOL News* **2005**, *40*, 8–12.
- (120) Sartori, G.; Maggi, R. *Chem. Rev.* **2006**, *106*, 1077–104.
- (121) Minakata, S.; Komatsu, M. *Chem. Rev.* **2009**, *109*, 711–24.
- (122) Schneider, U.; Ueno, M.; Kobayashi, S. *J. Am. Chem. Soc.* **2008**, *130*, 13824–13825.
- (123) Brown, H. C.; Racherla, U. S.; Pellechia, P. J. *J. Org. Chem.* **1990**, *55*, 1868–1874.
- (124) Kobayashi, S.; Endo, T.; Yoshino, T.; Schneider, U.; Ueno, M. *Chem. - An Asian J.* **2013**, *8*, 2033–2045.
- (125) Taylor, M. S.; Jacobsen, E. N. *Angew. Chem. Int. Ed.* **2006**, *45*, 1520–1543.
- (126) Alcaide, B.; Almendros, P. *Eur. - J. Org. Chem.* **2002**, *2002*, 1595–1601.
- (127) Córdova, A. *Acc. Chem. Res.* **2004**, *37*, 102–112.
- (128) Dondoni, A.; Massi, A. *Angew. Chem. Int. Ed.* **2008**, *47*, 4638–4660.
- (129) List, B. *Acc. Chem. Res.* **2004**, *37*, 548–557.
- (130) Marques, M. M. B. *Angew. Chem. Int. Ed.* **2006**, *45*, 348–352.
- (131) Notz, W.; Tanaka, F.; Watanabe, S. I.; Chowdari, N. S.; Turner, J. M.; Thayumanavan, R.; Barbas, C. F. *J. Org. Chem.* **2003**, *68*, 9624–9634.
- (132) Saito, S.; Yamamoto, H. *Acc. Chem. Res.* **2004**, *37*, 570–579.
- (133) Yamashita, Y.; Suzuki, H.; Kobayashi, S. *Org. Biomol. Chem.* **2012**, *10*, 5750.
- (134) Morimoto, H.; Wiedemann, S. H.; Yamaguchi, A.; Harada, S.; Chen, Z.; Matsunaga, S.; Shibasaki, M. *Angew. Chem. Int. Ed.* **2006**, *45*, 3146–3150.
- (135) Morimoto, H.; Lu, G.; Aoyama, N.; Matsunaga, S.; Shibasaki, M. *J. Am. Chem. Soc.* **2007**, *129*, 9588–9589.
- (136) Iwata, M.; Yazaki, R.; Suzuki, Y.; Kumagai, N.; Shibasaki, M. *J. Am. Chem. Soc.* **2009**, *131*, 18244–18245.
- (137) Saito, S.; Kobayashi, S. *J. Am. Chem. Soc.* **2006**, *128*, 8704–8705.
- (138) Matsubara, R.; Berthiol, F.; Kobayashi, S. *J. Am. Chem. Soc.* **2008**, *130*, 1804–1805.
- (139) Matsubara, R.; Kobayashi, S. *Synthesis* **2008**, *2008*, 3009–3011.
- (140) Kan, S. B. J.; Matsubara, R.; Berthiol, F.; Kobayashi, S. *Chem. Commun.* **2008**, 6354–6356.
- (141) Matsubara, R.; Berthiol, F.; Nguyen, H. V.; Kobayashi, S. *Bull. Chem. Soc. Jpn.* **2009**, *82*, 1083–1102.
- (142) Van Nguyen, H.; Matsuhara, R.; Kobayashi, S. *Angew. Chem. Int. Ed.* **2009**, *48*, 5927–5929.
- (143) Matsubara, R.; Masuda, K.; Nakano, J.; Kobayashi, S. *Chem. Commun.* **2010**, *46*, 8662–8664.
- (144) Nakano, J.; Masuda, K.; Yamashita, Y.; Kobayashi, S. *Angew. Chem. Int. Ed.* **2012**, *51*, 9525–9529.
- (145) *Superbases for Organic Synthesis*; Ishikawa, T., Ed.; John Wiley & Sons, Ltd: Chichester, UK, 2009.
- (146) Schwesinger, R.; Willaredt, J.; Schlemper, H.; Keller, M.; Schmitt, D.; Fritz, H. *Chem. Ber.* **1994**, *127*, 2435–2454.
- (147) Schwesinger, R.; Schlemper, H.; Hasenfratz, C.; Willaredt, J.; Dambacher, T.; Breuer, T.; Ottaway, C.; Fletschinger, M.; Boele, J.; Fritz, H.; Putzas, D.; Rotter, H. W.; Bordwell, F. G.; Satish, A. V.; Ji, G.; Peters, E.-M.; Peters, K.; von Schnering, H. G.; Walz, L. *Liebigs Ann.* **1996**, 1055–1081.
- (148) Schwesinger, R.; Dambacher, T. *Zeitschrift für Naturforsch. B- A J. Chem. Sci.* **2006**, *61B*, 1229–1233.

- (149) Verkade, J. G.; Kisanga, P. B. *Tetrahedron* **2003**, *59*, 7819–7858.
- (150) Kisanga, P. B.; Ilankumaran, P.; Fetterly, B. M.; Verkade, J. G. *J. Org. Chem.* **2002**, *67*, 3555–3560.
- (151) Kisanga, P. B.; Verkade, J. G.; Schwesinger, R. *J. Org. Chem.* **2000**, *65*, 5431–5432.
- (152) Kisanga, P. B.; Verkade, J. G. *Tetrahedron* **2001**, *57*, 467–475.
- (153) Yasuda, M.; Chiba, K.; Ohigashi, N.; Katoh, Y.; Baba, A. *J. Am. Chem. Soc.* **2003**, *125*, 7291–7300.
- (154) Saito, S.; Tsubogo, T.; Kobayashi, S. *J. Am. Chem. Soc.* **2007**, *129*, 5364–5365.
- (155) Ooi, T.; Doda, K.; Takada, S.; Maruoka, K. *Tetrahedron Lett.* **2006**, *47*, 145–148.
- (156) Ooi, T.; Doda, K.; Maruoka, K. *J. Am. Chem. Soc.* **2003**, *125*, 9022–9023.
- (157) Utsumi, N.; Kitagaki, S.; Barbas, C. F. *Org. Lett.* **2008**, *10*, 3405–3408.
- (158) Suzuki, Y.; Yazaki, R.; Kumagai, N.; Shibasaki, M. *Chemistry* **2011**, *17*, 11998–2001.
- (159) Massa, A.; Utsumi, N.; Barbas, C. F. *Tetrahedron Lett.* **2009**, *50*, 145–147.
- (160) Su, W.; McLeod, D.; Verkade, J. G. *J. Org. Chem.* **2003**, *68*, 9499–9501.
- (161) Crystallographic data reported in this manuscript have been deposited with Cambridge Crystallographic Data Centre as supplementary publication no. CCDC 924129. Copies of the data can be obtained free of charge via www.ccdc.cam.ac.uk/conts/retrieving.html.
- (162) Tang, J.; Dopke, J.; Verkade, J. G. *J. Am. Chem. Soc.* **1993**, *115*, 5015–5020.
- (163) Ishikawa, S.; Hamada, T.; Manabe, K.; Kobayashi, S. *Synthesis* **2005**, 2176–2182.
- (164) Poisson, T.; Dalla, V.; Marsais, F.; Dupas, G.; Oudeyer, S.; Levacher, V. *Angew. Chem. Int. Ed.* **2007**, *46*, 7090–7093.
- (165) Chantrapromma, K.; Ollis, W. D.; Sutherland, I. O. *J. Chem. Soc. Perkin Trans. 1* **1983**, 1049.
- (166) Ruan, J.; Saidi, O.; Iggo, J. A.; Xiao, J. *J. Am. Chem. Soc.* **2008**, *130*, 10510–10511.
- (167) Hillier, I. H.; Smith, S.; Mason, S. C.; Whittleton, S. N.; Watt, C. I. F.; Willis, J. *J. Chem. Soc. Perkin Trans. 2* **1988**, 1345.
- (168) Kobayashi, S.; Endo, T.; Schneider, U.; Ueno, M. *Chem. Commun.* **2010**, *46*, 1260–1262.
- (169) Hoffmann, R. W.; Landmann, B. *Chem. Ber.* **1986**, *119*, 1039–1053.
- (170) Hoffmann, R. W.; Jens Wolff, J. *Chem. Ber.* **1991**, *124*, 563–569.
- (171) Liu, H.-J.; Rose, P. a.; Sasaki, D. J. *Can. J. Chem.* **1991**, *69*, 934–936.
- (172) Mohrig, J. R.; Schultz, S. C.; Morin, G. *J. Am. Chem. Soc.* **1983**, *105*, 5150–5151.
- (173) Lucast, D. H.; Wemple, J. *Tetrahedron Lett.* **1977**, *18*, 1103–1106.

Acknowledgement

I would like to express my greatest appreciation to my supervisor Prof. Dr. Shū Kobayashi for his generous and continuous encouragement throughout my Ph.D course. Although this work is a bit far from his major, he never gave up and provided me a great guidance to conduct a study in analytical chemistry.

Dr. Miyuki Yamaguchi (Univ. of Shizuoka) and Mr. Jun Tamura (JEOL Ltd.) are gratefully acknowledged for their fruitful advices and discussions especially about mass spectrometry and their help on the development of an auto-sampler. Without their kind helps and technical advices, I could have not established this thesis.

I thank Dr. Yasuhiro Yamashita, Dr. Yuichiro Mori, Dr. Masaharu Ueno, Dr. Hiroyuki Miyamura, Dr. Woo-Jin Yoo, and Dr. Tetsu Tsubogo for their discussions on my research. Especially I am very grateful to Dr. Yamashita for his daily discussions over miscellaneous things and his good organization of Lab 1.

I express my special thanks and pay my respects to my colleagues, Taku Kitanosono and Tomohiro Yasukawa. They are my best friends as well as good rivals for 6 years from our undergraduate courses.

I thank Dr. Kenji Takasugi and Mr. yasuharu Morii for their daily support in Lab 10, Dr. Junya Nakano, Dr. Masatoshi Matsumoto, Dr. Mark Honey, Dr. Mark J. Dutton, Mr. Susumu Yoshimoto, Mr. Hirotsugu Suzuki, Mr. Masashi Harada, Mr. Nam Liang Cheng, Mr. Yuuki Saito, Mr. Io Sato, Mr. Seiya Fushimi and Mr. Kodai Minami for their daily support and our joyful lab life in Lab 1.

I also thank all the former and current members in Kobayashi Lab. for discussions, encouragement, and other helps for me.

Finally, I express my appreciation to Dr. Masataka Masuda and Ms. Nobuyo Masuda for their great education on me. Financial supports by University of Tokyo and Japan Society for the Promotion of Science are also acknowledged.